AN EXPERIMENTAL DETERMINATION OF THE RESPONSE TIME OF DIVIDERS FOR HIGH VOLTAGE IMPULSE MEASUREMENTS

A Thesis

Presented to

The Faculty of Graduate Studies and Research

The University of Manitoba

In partial Fulfillment of the

Requirements for the Degree

Master of Science in Electrical Engineering

by

John Kenneth Holland

May 1968

ABSTRACT

An experimental study of the factors involved in the determination of the response time of voltage dividers for H.V. impulse generators is presented, with particular emphasis on those factors essential to the development of a circuit for producing linear rates of rise.

PREFACE

The behaviour of power transformers when subjected to impulse waves is presently one of the major study areas in power transformer research programs. The stresses produced in a transformer winding are completely dependent on the wave shape and amplitude of the applied impulse wave. It is therefore essential that an accurate measuring system be used to measure the applied impulse voltage. Since no measuring system can be perfectly accurate, it is essential that some measure of the degree of accuracy be developed.

This thesis describes methods of determining the accuracy of a measuring system with particular emphasis on a practical approach using a volt-time curve for linearly rising voltage waves.

When a particular measuring system is thoroughly understood it can be used to study the shape of the impulse waves applied to power transformers, in particular the shape and duration of the voltage collapse across a rod gap which is the most severe rate

of change of voltage that a power transformer winding undergoes.

The author wishes to thank Prof. J.P.C McMath, Head of the Electrical Engineering Department, University of Manitoba for his guidance and continued interest throughout this study.

The support of Pioneer Electric, and in particular, Mr. E.A. Dillon, Director of the Research and Development Department of Pioneer Electric, is gratefully acknowledged.

Thanks are due also to Mr. J.R. Elliot, technician of the High Voltage laboratory of the University of Manitoba, for his assistance in preparing circuits and in obtaining photographic results for this study.

Finally, sincere appreciation is extended to Mrs. F. Dojack for the typing of this thesis.

TABLE OF CONTENTS

LIST OF FIGURES

FIGURE PAGE

LIST OF TABLES

CHAPTER I

INTRODUCTION

The impulse test which has been widely used for many years as a standard dielectric test for much of the high voltage electrical equipment manufactured is in many ways an unknown quantity.

Although the techniques for measuring the standard impulse wave * are fairly well developed, the measurement of fast changing impulse waves is far from satisfactory.

Typical of the fast changing impulse wave is that of a chopped wave applied to the terminals of a power transformer by means of chopping the full wave voltage with a rod gap. Although this test is often used, few people, if any, understand thoroughly what happens during the chop. It is mainly a measurement problem and there are very few measuring circuits which can adequately measure the time taken for the voltage to collapse and accurately record the waveform during the chop.

---

* The standard impulse wave has now been accepted by the IEC in Europe as 1.2 x 50 μs. This wave form will very likely be accepted in North America in the near future.

Since power transformer designers are faced with the problem of adequately insulating transformers to withstand the standard impulse wave it is essential that they know precisely the duration and shape of the applied wave.

Since the waveform applied to the unit is recorded by the voltage divider and associated components it is essential that the divider record the voltage as accurately as possible. If the divider does not record accurately, it is possible that the applied waveform may be much more severe than is indicated.

The I.E.C.* has adopted two parameters for controlling the accuracy of a measuring system. These are the "response time" and "the time taken for the response to settle down." They feel that limitations placed on these two parameters will control the accuracy of the measuring system. Creed has stated that the time taken for the response to settle down is meaningless and that another criterion should be adopted.[7†] In any event the determination of the response time of a measuring system is very important in defining the usefulness of the system.

---

† Superscripts refer to references listed at the end of this thesis.

* I.E.C. - International Electrotechnical Commission

The response time of the system can be determined by calculation or by measurement. The theoretical approach is quite complicated although it does result in adequate results. [5]

The experimental method which makes use of a sphere gap volt-time curve is a method recently developed by several authors in conjunction with CIGRE* It is not precisely clear, however, exactly how the volt-time curve is used to determine the response time of a divider. An attempt at clarification will be discussed in the text.

The volt-time curve for a sphere gap is determined by applying a linearly rising voltage and measuring the voltage and the time at which the sphere gap breaks down for various rates of rise. A linearly rising wave is required since the response time of a system is a measure of how much the output voltage lags behind the input voltage when the input is a linearly rising voltage wave.

The development of a circuit which results in a linear rate of rise of voltage is therefore essential in determining a volt-time curve or in calibrating a divider in conjunction with a standard volt-time curve.

---

* CIGRE: Conference Internationale des Grands Reseaux Electriques

Such a circuit is not immediately obvious especially if one is concerned with extremely fast rise times. A discussion of the essential steps found necessary in the development of the circuit will be presented.

The calibration of two different voltage dividers is discussed and the features of dividers essential to the accurate reproduction of an impulse voltage wave are dealt with.

CHAPTER II

THEORETICAL CONSIDERATIONS

Standard impulse voltage dividers are adequate for measuring standard impulse wave shapes but as stated in the introduction, measurements of chopped waves are much more difficult in that the divider has to respond very quickly. This deviation from the standard waveshape is the basis for a divider study.

Two terms used in conjunction with chopped waves are the time-to-chop and the time-of-chop. The time-to-chop is the time from the virtual time zero of the wave to the time where the voltage begins to collapse. The time-of-chop is the time taken from that point when the voltage begins to collapse until the voltage reaches zero. It is essential that the shape of the chop and the time-of-chop be accurately measured.

Another deviation from the standard waveshape occurs at the beginning of the voltage rise as shown in figure 2.1. The loop inductances which are inherent in any impulse generator circuit will cause oscillations

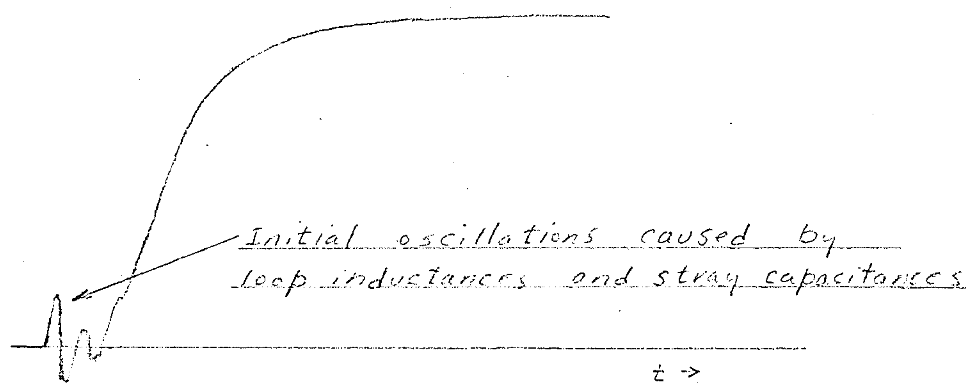

FIGURE 2-1

IMPULSE GENERATOR OUTPUT
SHOWING INITIAL OSCILLATIONS

with the loading and/or stray capacitances and give a 1 to 10 megahertz oscillation at the beginning of the voltage rise. These oscillations can become quite severe and may in theory reach twice the amplitude of the final peak voltage. This, however, is highly unlikely. Creed states that it is possible, due to this oscillation, for an operator to heavily overstress a test object.[7]

Measurement System Requirement

The response time and the time taken for the response to settle down are the two main measurement system requirements as adopted by the I.E.C.

The response time is the integral of the area between an applied unit step and the normalized response to the unit step. This is shown on figure 2-2 for both an oscillatory and non-oscillatory response. The response time has the dimension of time, and it indicates how much the output voltage from the measuring system lags behind the input when the input is a linearly rising voltage. Consequently the response time indicates both amplitude and time errors for a linearly rising voltage, whereas, for a voltage which rises to a peak value and then stays there, or else decays slowly, the response time essentially defines only the error in rise time because the output of the measuring system will still reach essentially the peak amplitude.[6]

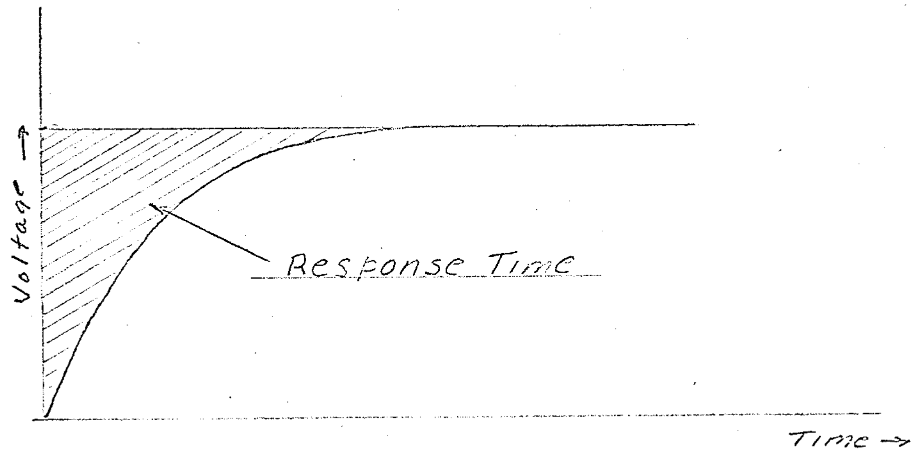

FIGURE 2-2-a

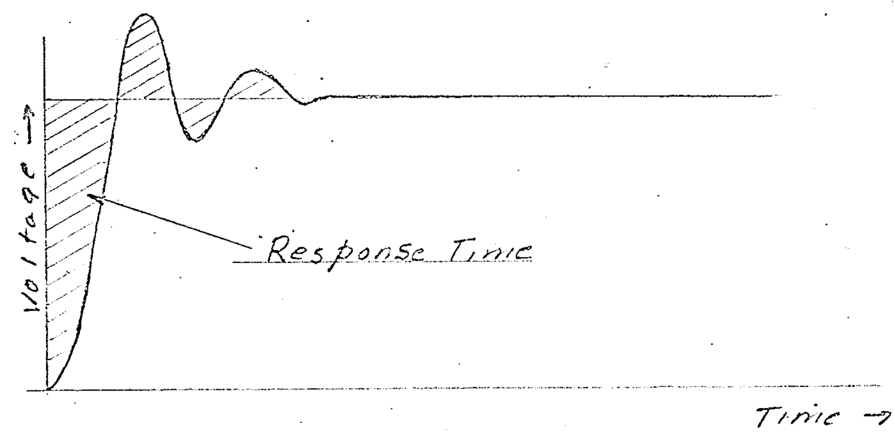

FIGURE 2-2-b

FIGURE 2-2

MEASUREMENT SYSTEM RESPONSE TIME
FOR a) NON-OSCILLATORY RESPONSE
AND b) OSCILLATORY RESPONSE

The I.E.C. has suggested that the response time be not greater than 200 nanoseconds.

Creed states that the second parameter, the time taken for the response to settle down is essentially meaningless in that in some cases a system which has a very long settling time will give excellent results for fast rising linear waves. This parameter would be useful only if full knowledge of the circuit were available.[6]

Faxo has suggested that a standard rise time be used as a criterion for specifying the measuring system. He defines the standard rise time as

$$T_S = \left(\int_0^{\infty} t^2 \, g'(t) \, dt - T_m^{\,2} \right)^{\frac{1}{2}}$$

Where $g^1(t)$ is the derivative of the step response, and Tm is the response time[6]. This suggestion certainly merits further investigation as it relates the requirement of the divider directly to the problem the divider is trying to measure (i.e. a fast changing voltage wave).

If the accuracy of the measurement is to be limited to recording the rise and the chop accurately, the response time or the standard rise time could be a sufficient criterion for controlling the measuring system. If the accuracy of the measurement of the preliminary oscillations is also to be controlled, additional criteria are required.

In transformer impulse testing it is felt that the duration of one cycle of the preliminary oscillation will normally be so short that chances of an insulation failure would be quite remote unless the oscillation reached twice the final applied voltage. Since this occurrence seems highly unlikely, it is believed that the measurement of these oscillations is unnecessary.

If it is necessary to measure these oscillations, Creed suggests that some criteria may be developed which would compare the shape of the step response to the accuracy of the oscillation measurements.[7]

There are several other divider requirements which, although not critical, are nevertheless essential to accurate measurements.

1. The divider must be non-reactive. The voltage and the current in the test circuit must not substantially vary when the measuring instrument is switched off.
2. It must be possible to calibrate the divider and its calibration must not change during operation.
3. The residual inductance in any resistance or capacitance element must be negligible.[13]
4. The impedance drop in the lead from the point at which the high voltage is to be measured to the high voltage end of the divider must be small.[13]

5. The impedance drop in the ground return lead from the divider, due to either extraneous ground current flowing in this lead or divider current, must be negligible.[13]

6. Oscillations set up in the divider circuit (caused by capacitance from the divider high voltage terminal to ground and lead and loop inductance) must be minimized.[13]

Techniques for Determining the Response Time

The response time of a measuring system can be determined by two different methods. The first method involves applying a unit step voltage measuring the resulting wave, and integrating to find the difference between the two. The second involves the use of the volt time curve for a linearly rising wave. Both methods give satisfactory results although the first is much more complicated and difficult to apply. When the response time of a measuring system is accurately known, correction of measured values for response time errors can be made.

Measurement of the Response Time of a Divider Using an Applied Unit Step Voltage.

As stated before, the response time is defined as the algebraic difference between the integral under a unit step and the integral of the divider response to the unit step. The response of the divider to a unit step (i.e. the step response of a measuring system) is normally obtained with a zero impedance step generator.

This measurement does not necessarily indicate what steepness of wave can be accurately recorded when multiple reflections in the divider lead are caused by a source impedance. This would indicate therefore that the effect of a series source impedance should also be investigated.

Creed[5] has developed several methods of measuring the response time with and without a zero impedance source. He accomplished this by means of chopping the voltage wave with a pressurized sphere gap thereby obtaining a unit step.

In order to make a direct determination of the response of a measuring system to a voltage from a zero impedance source it is necessary to inject between the two input terminals of the system a voltage step having zero rise time using a zero impedance generator. The oscillogram thus recorded provides all the information needed to determine the output of the system for any voltage-time function input.

There is no known method however of generating a voltage step of zero impedance between two points which are widely separated in space. It is therefore necessary to determine the step response indirectly.

Creed[5] has shown in detail the method of making this measurement. It includes a proposed standard modification which would place the step generator on the ground plane directly under the high voltage input terminal of the measuring system. The generator is connected to the input terminal of the system by a vertical lead.

Creed[5] also considers the effect of a damping resistor located at the input end of the lead to the top of the divider. If the damping resistor of the lead matches its surge impedance,[20] the response of the measuring system can reach its steady state value in a very short time providing a zero impedance source is used. If, on the other hand, the source has an impedance, an oscillation will be set up as the reflected wave from the divider will not see Z_o upon reaching the damping resistor.[1]

In effect, the divider and its lead can be looked upon as a variable impedance shunted across the test object. Initially the impedance is $2Z_o$ and it will reach a final value equal to the divider resistance. The time taken for the effective impedance of the divider to attain its steady state value is the determining factor in deciding what is the minimum rise time that can be measured, not the time taken for the unit step response to reach its steady state value. The time relating to the divider impedance is a function of the degree of mismatch in the divider lead damping and is therefore a function of the source impedance. On this basis Creed suggests that the time taken for the step response to settle down provides an unsatisfactory criterion for the quality of a measuring system.

From the above it can be seen that the determination of the response time from a unit step measurement is a tedious and difficult chore. It is therefore desirable to use some other method of measuring the response time.

Measurement of the Response Time Using the Volt-Time Curve

Park and Cones[13] suggested that a volt-time curve could be used to determine the response time of a system providing its shape could be accurately determined.

Creed discovered through extensive testing that the volt-time curve for a sphere gap obtained with a high impedance divider agrees very well with the same curve obtained with a low impedance divider.[1] Accordingly an accurate volt-time curve for any sphere gap could be used in calibrating any voltage divider of any impedance.

The use of the volt-time curve for determining the response time of a measuring system is based on the fact that any measuring system can accurately measure a steady rate of rise of voltage provided the voltage rise lasts long enough. If a system is used to determine the volt-time curve for the particular gap in question, the only error in the experimental curve should be the measurement of the time to breakdown and this error is by definition the response time of the measuring system. The experimental curve will therefore be shifted vertically from the volt-time curve by the response time of the system.

It is helpful to note that according to the U.S. Bureau of Standards if the rate of rise is constant between the 60 cycle breakdown voltage and the impulse breakdown voltage, the rate of rise of voltage below the 60 cycle breakdown voltage has negligible effect on the test.[11]

Members of CIGRE Study Committee #8 - Lightning and Surges - have conducted an intensive investigation to determine accurately the volt-time curve for a 60 mm gap between 25 cm spheres. This committee has submitted to the I.E.C. a volt-time curve for the gap which is reproduced in figure 2-3 - curve a.[7]

In order to determine the response time of a divider therefore a volt-time curve for the divider in question must be produced. The difference between this curve and the CIGRE volt-time curve for any rate of rise is the response time of the divider.

If the volt-time curve of a particular system as determined using the 60 mm gap between 25 cm spheres

FIGURE 2 - 3

SPHERE GAP VOLT-TIME CURVE

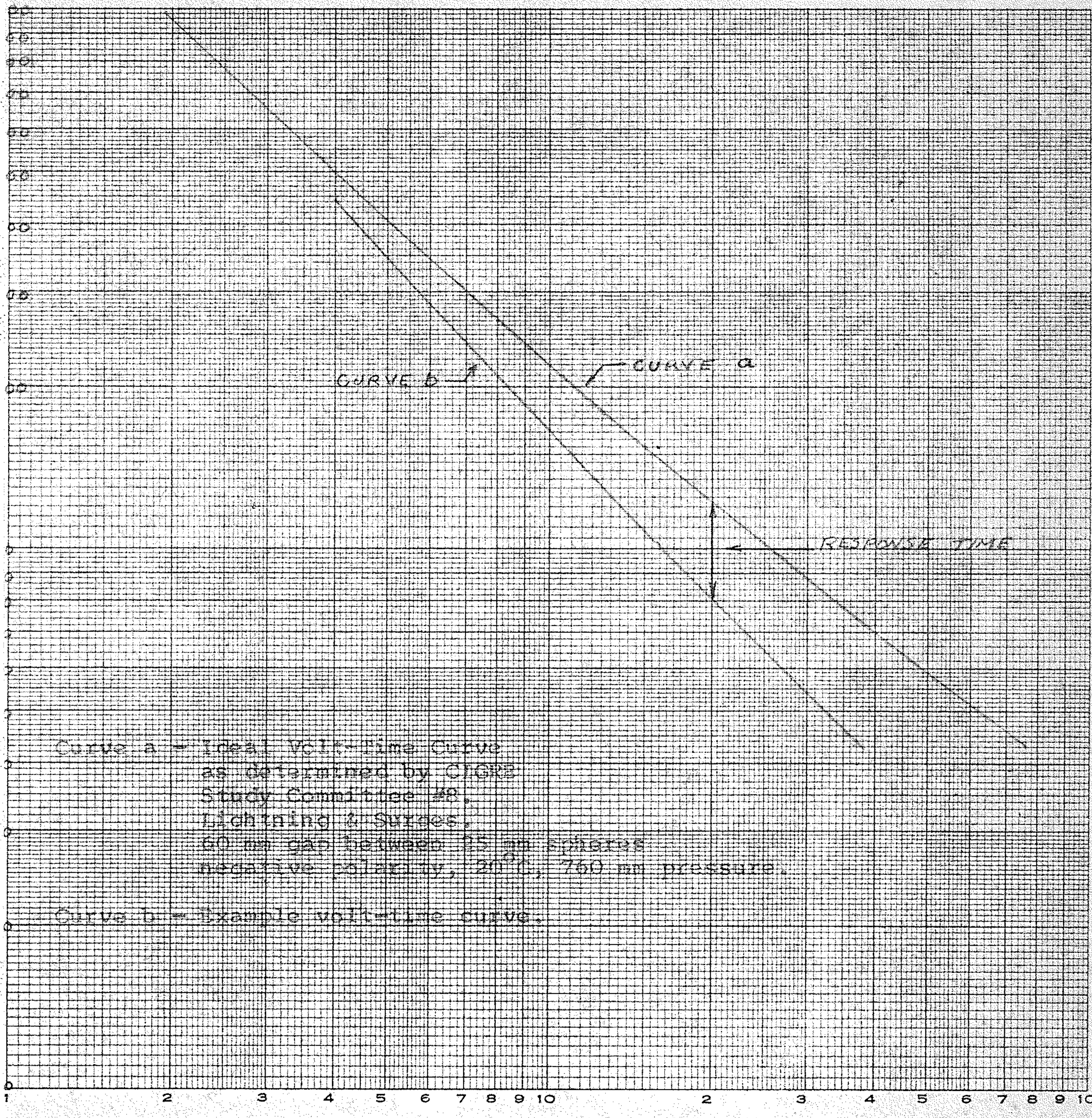

S - Rate of Rise (KV/Nanosecond)

is as shown on curve b of figure 2-3, the response time of the system would be equal to the vertical difference between curves a and b as shown. In the example shown the response time equals 50 nanoseconds.

Dividers and Their Characteristics

There are many different types of dividers now in use. Some are quite satisfactory while others are of no value other than for the measurement of relatively slowly rising waves.

An uncompensated resistance divider is satisfactory for measuring fast changing waveshapes only if its resistance is low (in the order of 500 ohms). If its resistance is high, (above 10 k) the impedance of the divider becomes too high in relation to that of the stray capacitances from the divider to ground. It can be seen that any stray capacitance to ground will bypass some of the high frequency voltage components entering the high voltage terminal of the divider. The recorded voltage may therefore be considerably in error.

If a suitable form of capacitive grading is used, the error can be minimized. The purpose of the grading is to ensure that the ground capacitance from any point on the divider is compensated by an equivalent capacitance to the high voltage terminal. In this way, all voltage components appearing at the divider high voltage terminal will be measured at the low voltage terminal.

Depending on the degree of capacitive grading this type of divider can have a very short response time. It is also possible as stated above to eliminate the effect of the stray ground capacitances by making the actual resistance of the divider low (in the order of 500 ohms). Dividers of this type have been successfully manufactured by several laboratories. If the physical size of such a divider is limited to reasonable dimensions however the divider will only withstand short duration pulses.

Chapter V will discuss the calibration of a capacitively graded resistance divider and a low resistance divider.

It is important to note that the high resistance divider has stray capacitance to ground due to its physical size, not its actual resistance. Creed verified this by making a small high impedance pressurized divider and found the response time very small.[1]

The pure capacitive divider has a ratio which is independent of frequency and consequently can be used for both fast and slow transients. A problem arises when it is necessary to use a length of coaxial cable from the low voltage portion of the divider to the oscilloscope since the termination of this cable presents considerable difficulty. Special techniques can be adopted which will give reasonable results. When possible, connecting the capacitance divider directly to the scope has proven very satisfactory.

The response of a standard resistance divider can be sometimes improved by adding a series of capacitors in parallel with the resistance. It is essential in this type of divider that the RC time constant of the high voltage arm be the same as the RC time constant of the low voltage arm. This type of divider behaves as a capacitance divider for fast pulses and a resistance divider for slow pulses.

Any inductance present in any divider will severely limit its usefulness in that its response time will be drastically increased.

CHAPTER III

CIRCUIT PARAMETERS FOR LINEARLY RISING WAVES

Although many authors have shown results of tests on small gaps very little is published on the circuit problems encountered in acquiring a linearly rising waveform for such tests. Chapters III and IV discuss some of the problems that can be encountered in this type of testing.

According to the U.S. Bureau of Standards[13] it is not necessary to acquire a linear rate of rise below the 60 cycle breakdown voltage of the gap. Attempts were made in this study however to eliminate all oscillations on the rising portion of the wave. As a result of this study, many features essential to achieving a linear rate of rise have been discovered.

The discussion in this chapter and the next will frequently refer to various oscillograms. These oscillograms will be shown on the accompanying figures. In some cases several traces will appear on one oscillogram. This was done since some difficulty was experienced in achieving consistent firing, particularly when dealing with very fast rates of rise. These traces will be numbered consecutively from the top. For example, oscillogram 3-4-b-2 will be the second trace on oscillogram b shown on figure 4 in Chapter III.

The timing wave, the calibration voltages, the charge voltages and the oscilloscope attenuation used for each oscillogram are given beneath the oscillogram. It should also be mentioned that the frequency of the various oscillations mentioned in this and the next chapter were measured from the oscillograms by means of an accurate horizontal measurement device manufactured by Griffin and George Limited, London, England.

The generator used was a 24-stage 2400 KV generator with a total output energy of 30 KWS. A discussion of the measuring and recording systems will be given in Chapter V.

A study of the waveform obtained directly from the generator was the first step in the investigation. The divider used was a 46.2KΩ 600 KV haefly compensated resistance divider. The circuit used is shown in fugure 3-1-a.

Although the waveform of oscillogram 3-2-a appears fairly smooth, when it is recorded with a faster sweep as shown on oscillogram 3-2-b, definite oscillations are evident. These oscillations were

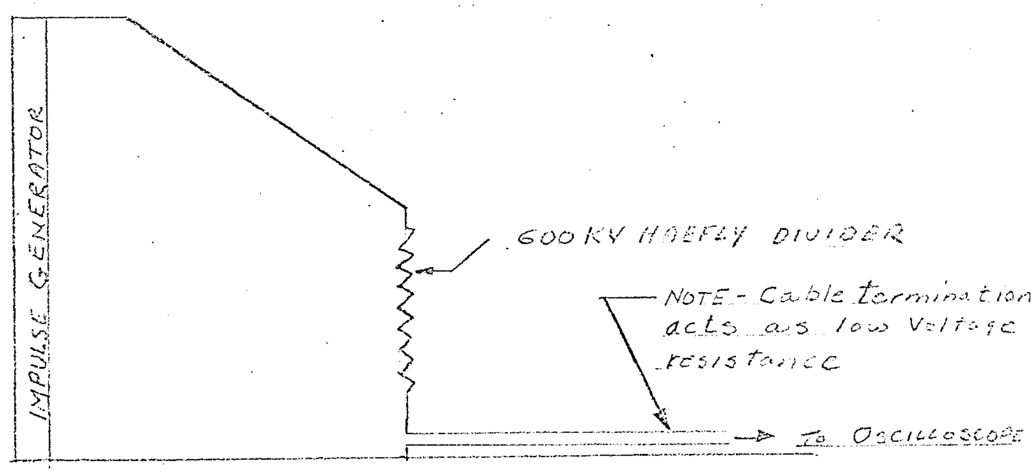

FIGURE 3-1-a

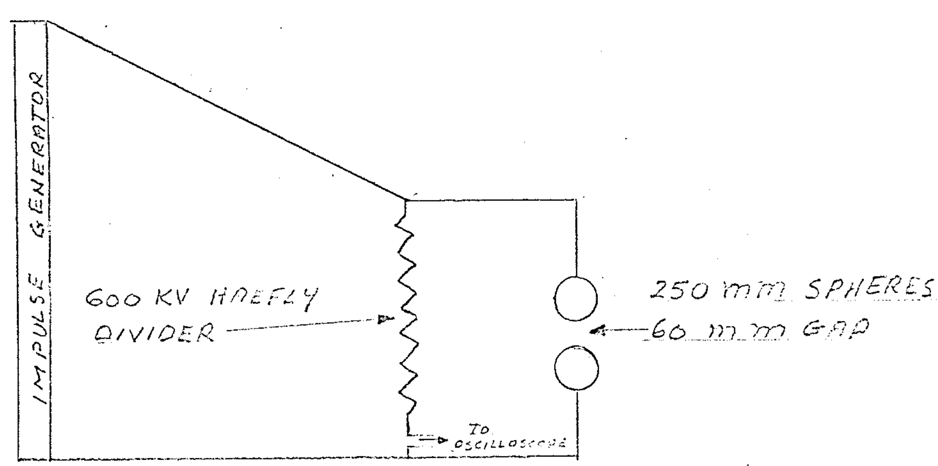

FIGURE 3-1-b

FIGURE 3-1

CIRCUITS FOR INVESTIGATING GENERATOR OUTPUT WITH AND WITHOUT A SPHERE GAP

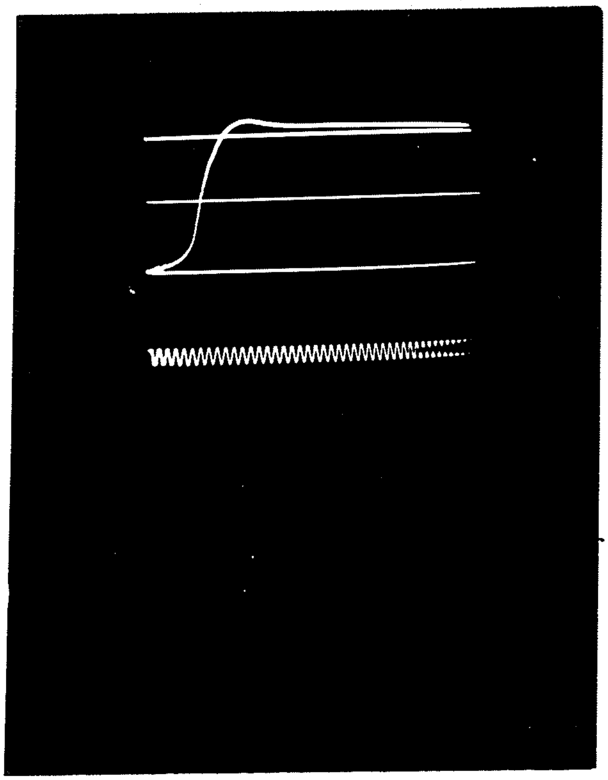

FIG 3-2-a
TIMING WAVE 10 MHz
CAL. 150, 300 V
CHARGE 17.5 KV
ATTENUATION 50%

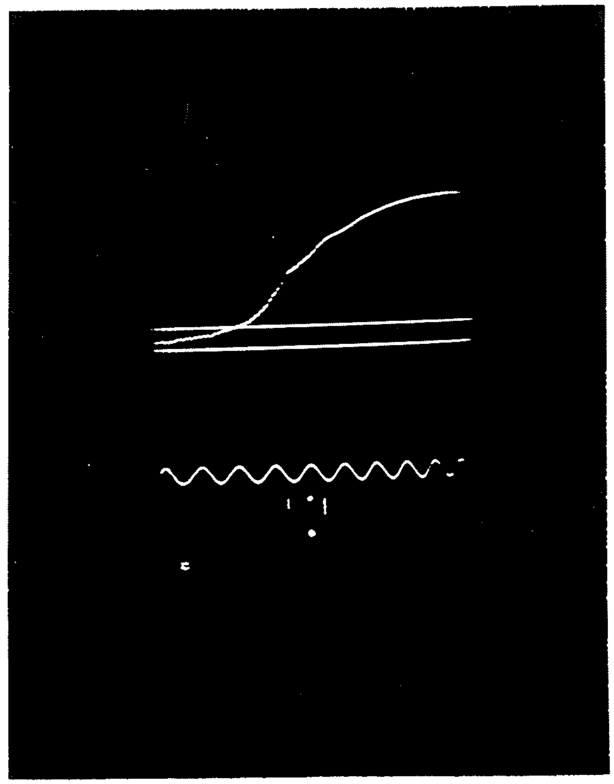

FIG 3-2-b
TIMING WAVE 10 MHz
CAL. 50 V
CHARGE 17.5 KV
ATTENUATION 50%

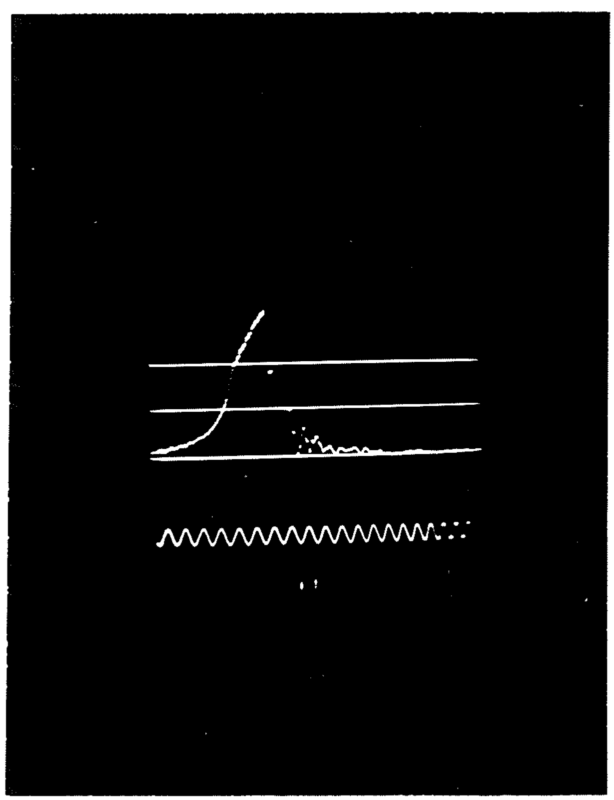

FIG 3-2-c
TIMING WAVE 10 MHz
CAL. 100, 200 V
CHARGE 11.0 KV
ATTENUATION 100%

FIGURE 3-2 VOLT-TIME OSCILLOGRAMS

measured to be approximately 10 MHz. A 10 MHz timing pulse and a 17.5 KV charging voltage was used for oscillograms 3-2-a and 3-2-b.

When the 60 mm gap used to determine the CIGRE curve is placed across the divider as shown in figure 3-1-b, the resulting waveform is as shown on oscillogram 3-2-c. Note that a 12 MHz oscillation occurs. A high frequency oscillation and a definite bend are quite pronounced on the rise. Any attempt at calibrating the divider using the waveform of oscillogram 3-2-c would only result in an unacceptable error due to the serious nonlinearity of the rise.

The bend in the waveform disappears for greater charging voltages. Since the generator energy is proportional to the charge voltage squared, a higher charge voltage increases the available energy which in turn affects the rise of the wave. This will be discussed in greater detail later.

Pre-breakdown corona discharges at various highly stressed points in the circuitry and consequent energy loss across the 60 mm gap before the gap breaks down cause sufficient loss in energy to result in a bend in the waveform. A higher energy would reduce the probability of an output voltage dip.

The frequency of the oscillation after the chop is fairly high (20 MHz) for several hundred nanoseconds after which it decreases to 12 MHz. The high frequency oscillation on the wavefront is about 45 MHz.

In Appendices I and II loop inductances, sphere gap capacitances, resonant frequencies and damping resistances are calculated for a circuit which will be discussed in detail later. The calculations given do apply however to the present situation since circuit dimensions are somewhat similar to certain sections of the circuit studied.

From these calculations which are approximate only, some idea of the frequencies which can result from the circuit parameters can be achieved.

The inductance of any of loop B, C or D on figure A1, page 106, combined with either of the gap capacitances could result in a 12 MHz oscillation. It would be very difficult to decide exactly which combination caused the 12 MHz oscillation without in some way determining the parameters more accurately.

The circuit shown in figure 3-1 used to record oscillogram 3-2-c consists of the generator, the 600 KV divider and the 60 mm gap. The resonant frequency of the divider-gap loop combined with the 60 mm gap capacitance would be in the range of 10-12 MHz. This is most likely the source of the 12 MHz oscillation measured on oscillogram 3-2-c.

The 45 MHz oscillation is much more difficult to explain in that the parameters would have to be very small to account for such an oscillation. It possibly is due to either some corona source or more likely to the capacitance of one of the lines to ground resonating with a loop inductance. For example, if the capacitance to ground was about 1 pf and the loop inductance about 10 μh the resulting resonant frequency would be approximately 50 MHz.

The rise shown on oscillogram 3-3-a taken using the circuit of figure 3-1-b is actually quite linear except for the 45 MHz oscillation. The charge voltage for oscillogram 3-3-a was 15 KV while that for oscillogram 3-2-c was 11 KV. This explains why oscillogram 3-3-a is more linear than oscillogram 3-2-c. This oscillation, however, would cause significant errors in any calibration data taken with this circuit. When the charge voltage was raised to 20 KV the rise as shown in oscillogram 3-3-b appears to be somewhat steeper although the high frequency oscillation would as before cause an unacceptable error in any calibration attempt.

Some data were taken at this point, however, to permit a calibration curve to be determined and in this way determine the effect of the oscillations. This is especially important in view of the fact that some measuring systems (i.e. oscilloscopes) may not be able

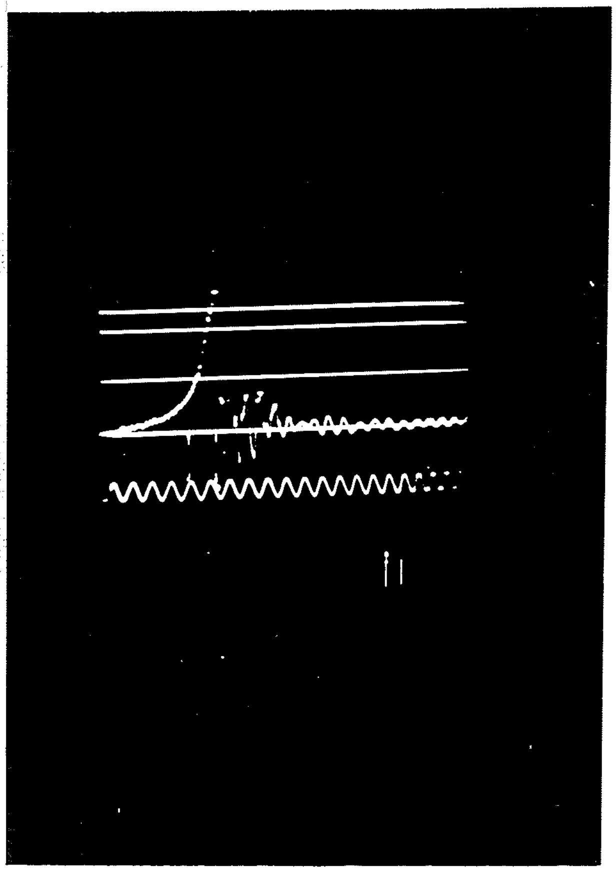

FIG 3-3-a
TIMING WAVE 10 MHz
CAL. 100, 200, 242 V
CHARGE 15 KV
ATTENUATION 100%

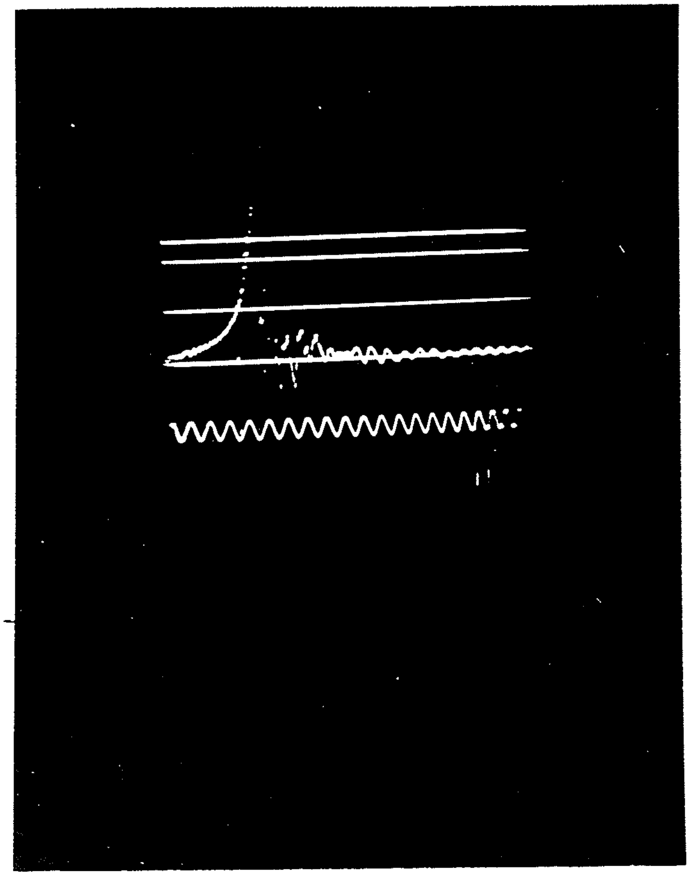

FIG 3-3-b
TIMING WAVE 10 MHz
CAL. 100, 200, 242 V
CHARGE 20 KV
ATTENUATION 100%

FIGURE 3-3 VOLT-TIME OSCILLOGRAMS

to record these oscillations. The results of the data obtained will be discussed in Chapter V.

It should be noted that the effect of the increased charging voltage is two-fold. Not only does it eliminate the bend on the rise but it also causes a faster rise. This results in a different point on the volt-time curve.

A study of the oscillations on the waveforms of oscillograms 3-4-a and 3-4-b proves helpful in obtaining a better understanding of some of the oscillations present in this type of circuit. The circuits used in this case are shown in figures 3-5-a and 3-5-b. A loading capacitor which was in fact the capacitive portion of a 2400 KV resistance-capacitance divider was placed in parallel with the generator in an attempt to slow down the rise. The waveform of oscillogram 3-4-a was taken using a 1200 pf loading capacitance as shown in figure 3-5-a, while that of oscillogram 3-4-b was taken using a 2400 pf loading capacitance as shown in figure 3-5-b. Notice that the rise of oscillogram 3-4-b has been appreciably slowed down due to the increased loading capacitance.

The oscillations measured on oscillogram 3-4-a are a 5.5 MHz oscillation on the rise with a 1.5 MHz major oscillation after the firing of the gap with a superimposed 12 MHz minor oscillation. On oscillogram 3-4-b the oscillation on the rise reduces to 3.0 MHz with the major oscillation after the chop decreasing to 1.0 MHz and the superimposed oscillation decreasing to 10 MHz.

The approximate circuit dimensions and associated resonant frequencies are shown in figures 3-5-a and 3-5-b.

Notice that the 1.5 MHz oscillation and the 1.0 MHz oscillations can be accounted for by the combination of the loading capacitor with the capacitor divider loop, the resultant calculated frequencies being 1.20 MHz and 1.00 MHz. The inductances and capacitances are estimated from the data derived in the appendices.

The combination of the divider gap loop inductance with the 60 mm gap capacitance results in an estimated 13 MHz ocsillation. This accounts for the measured oscillations of 12 and 10 MHz.

The cause of the 5.5 MHz and 3.0 MHz oscillation is not immediately obvious but from the relationship between the two it appears that they depend somewhat on the loading capacitances. The loading capacitances combined with some small stray inductance, possibly the internal inductance of the resistance portion of the RC divider used for the loading capacitor could cause these oscillations.

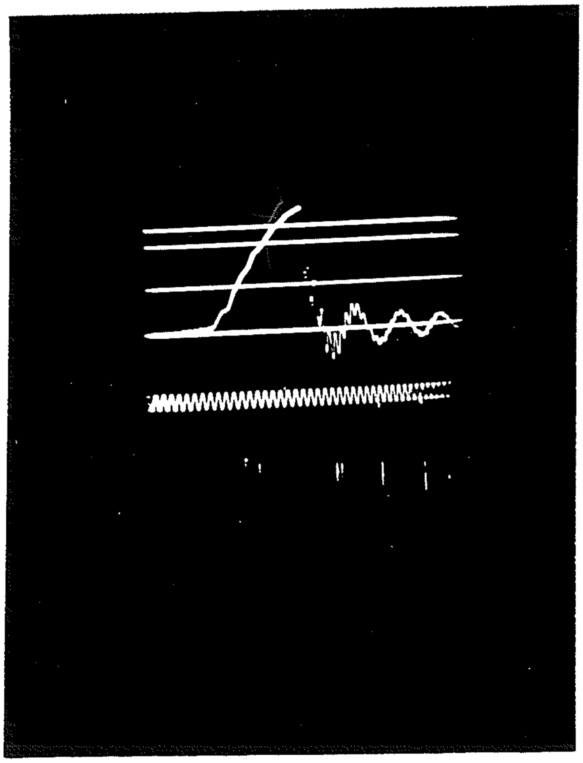

FIG 3-4-a
TIMING WAVE 10 MHz
CAL. 100, 200, 242
CHARGE 10 KV
ATTENUATION 100%

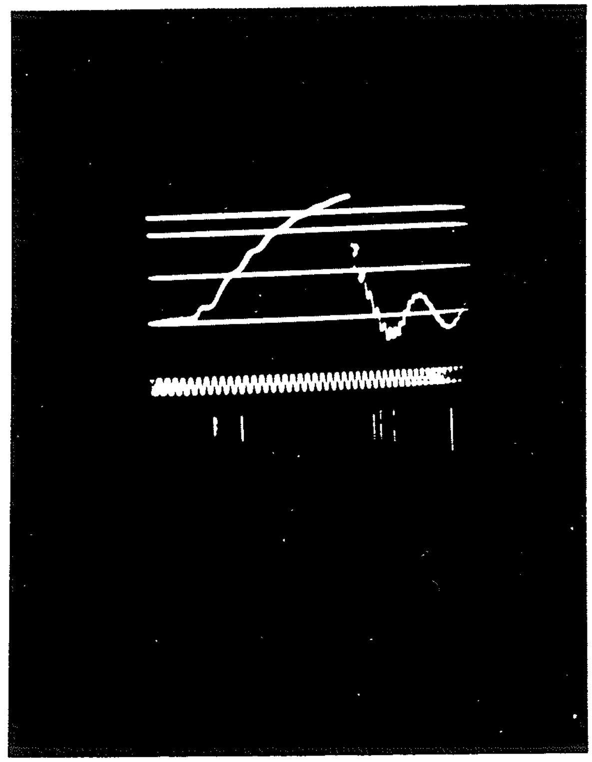

FIG 3-4-b
TIMING WAVE 10 MHz
CAL. 100, 200, 242 V
CHARGE 10 KV
ATTENUATION 100%

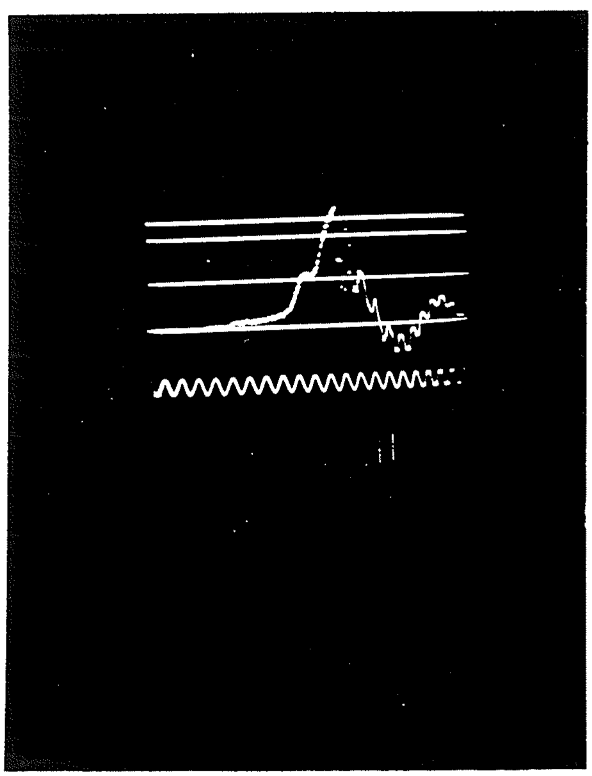

FIG 3-4-c
TIMING WAVE 10 MHz
CAL. 100, 200, 242
CHARGE 25 KV
ATTENUATION 100%

FIGURE 3-4 VOLT-TIME OSCILLOGRAMS

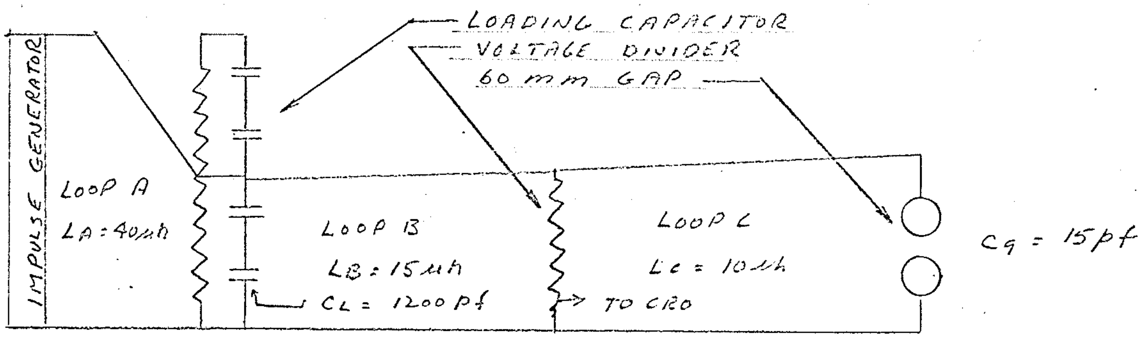

NOTE: CAPACITANCE AND INDUCTANCE VALUES ARE ESTIMATES

RESONANT FREQUENCIES: f_{LaCL} = .75 MHZ, f_{CLLB} = 1.20 MHZ, f_{LcCg} = 13.0 MHZ

FIGURE 3-5-a

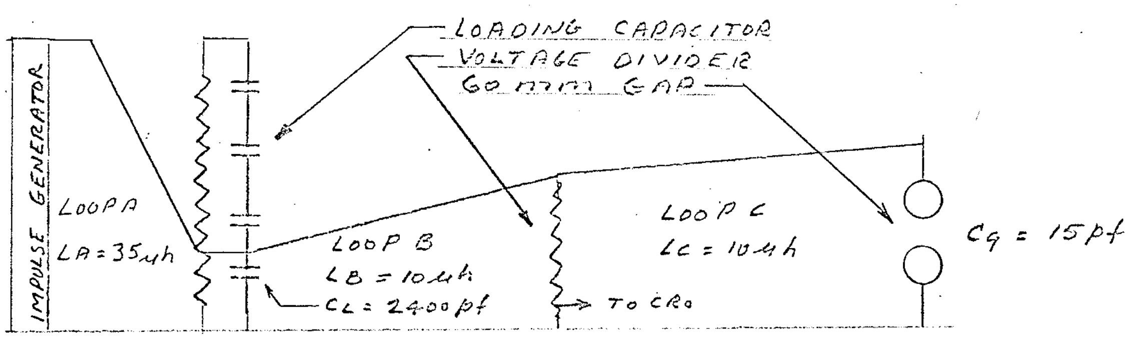

NOTE: CAPACITANCE AND INDUCTANCE VALUES ARE ESTIMATES

RESONANT FREQUENCIES: f_{LaCL} = .55 MHZ f_{CBLB} = 1.00 MHZ, f_{LcCg} = 13.0 MHZ

FIGURE 3-5-b

FIGURE 3-5

CIRCUITS FOR OBTAINING LINEARLY RISING WAVES UTILIZING EXTERNAL LOADING CAPACITANCE

The charge voltage was then increased to increase the rate of rise and perhaps eliminate the end evident on oscillograms 3-4-a and 3-4-b. The result is as shown on oscillogram 3-4-c. The rise was indeed steepened but a severe oscillation appeared on the rise. It is apparent from oscillograms 3-4-a, 3-4-b and 3-4-c that any attempt at calibration would be futile due to the severe nonlinearity of the rise.

It was decided at this point that a more elaborate circuit would have to be used. It was decided to utilize an auxiliary sphere gap as suggested by Creed[1] to try and acquire a linear rate of rise and at the same time acquire a fast rising waveform. This is therefore the subject of the next chapter.

CHAPTER IV

THE DEVELOPMENT OF A CIRCUIT FOR LINEAR FAST RISING IMPULSE WAVES

The initial circuit used in this study was as shown in figure 4-1.

The principles of operation of this circuit are as follows. The impulse generator charges the 150 pf loading capacitor and simultaneously raises the voltage across the series gap. When the breakdown level of the series gap is reached, the gap breaks down and the voltage begins to rise across the 50 KΩ resistor. This voltage rises very rapidly since the RC time constant of the loading capacitor and the resistance of the circuit is very low. The rate of rise can be increased by decreasing the series resistance in the circuit after the loading capacitor. When the voltage across the 60 mm gap reaches the breakdown level the gap breaks down. The voltage divider should theoretically record everything that occurs after the series gap breaks down.

A series resistor must be placed between the impulse generator and the loading capacitor. If its

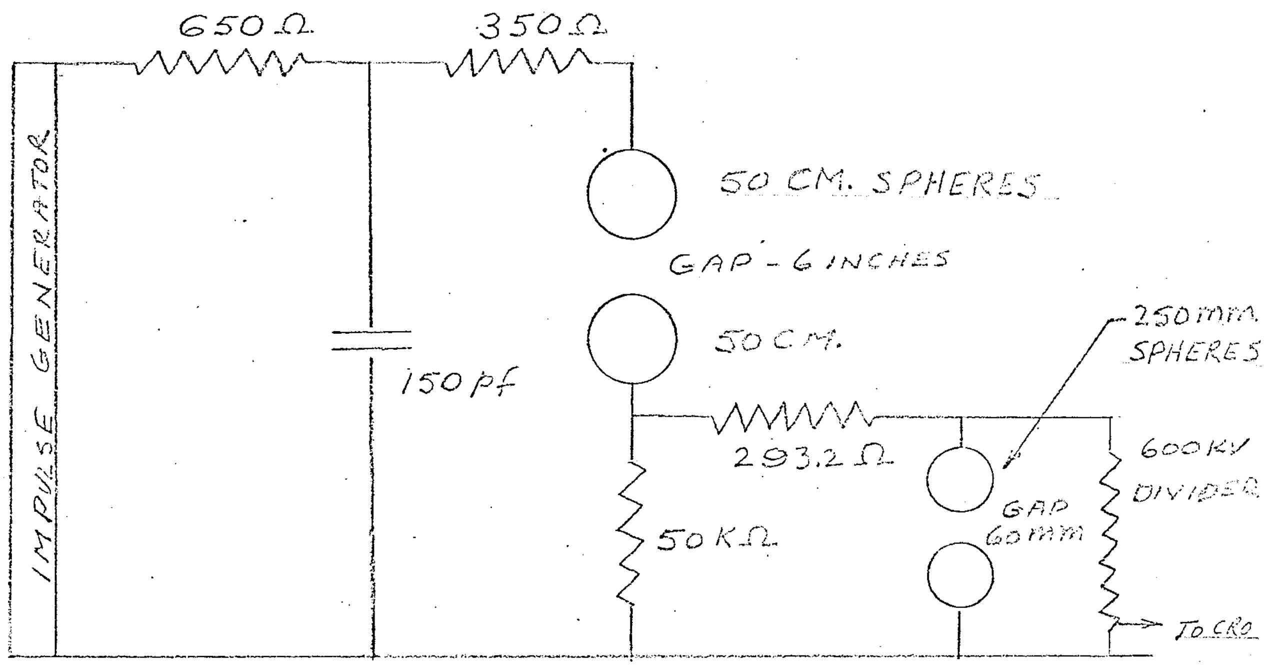

FIGURE 4-1

INITIAL CIRCUIT FOR THE STUDY OF LINEAR FAST RISING VOLTAGE WAVES resistance is too low, the generator output will affect the voltage across the 60 mm gap before the series gap breaks down. This is because if a low resistance series resistor is used the time constant of the circuit is low. The resulting waveform therefore will have high frequencies. The impedance of the series gap to these high frequencies is relatively low compared to the 50 KΩ resistor and as a result, significant voltage can appear across the 60 mm gap prior to the breakdown of the series gap. Conversely, if the series resistance in question is high it will essentially isolate the generator from the rest of the circuit by providing a high output time constant for the generator-resistor network and thus a high series gap impedance. In this case the loading capacitor will be the only significant source of voltage after the series gap breaks down in the time range being considered.

In fact, the series resistor can have any large value, the only limiting factor being the voltage drop across it. An excessively high value of resistor will result in too low a voltage across the series gap. In other words, for a fixed charging voltage, the higher the series resistor, the lower the available series gap voltage. The solution for this is naturally a higher charging voltage if it is available, otherwise, the series resistance would have to be reduced. It is important also to ensure that the series gap is large enough to supply sufficient over-voltage across the 60 mm gap and thus ensure consistent results.

The resistor between the bottom of the series gap and ground minimizes the voltage appearing across the divider before the series gap breaks down. Since the series gap has a capacitance of approximately 25 pf its impedance in series with the divider impedance will cause a voltage division such that a significant voltage will appear across the divider before the series gap breaks down. An appropriate choice of resistor will eliminate this problem. Too small a resistor will result in insufficient voltage across the 60 mm gap.

The problem is not critical for a large series gap since the gap capacitance is low and its gap impedance is high. Any fairly high value of resistance will then be adequate.

The resistors shown in figure 4-1 were not chosen from calculated data but were rather those resistors that were available.

The series resistor between the generator and the loading capacitance was initially chosen as 650 ohms while the resistor between the bottom of the series gap and ground was initially chosen as 50 K ohms.

The 350 ohm resistor and the 293 ohm resistor were intended to be used for damping but subsequently were found to be ineffective. The 650 and 350 ohm resistors were water resistors while the 293 ohm resistor was a non-inductive wirewound resistor.

The 150 pf loading capacitor consisted of a 115 KV class bushing mounted in a fairly small (4'x5'x6½') steel tank. The capacitance of the centre conductor and bottom conducting plate to the flange and the tank measured 150 pf.

The results of the measurements made with this circuit and the improvements that were made to obtain a linear rate of rise will now be discussed.

Referring to oscillogram 4-2-a which was taken using the circuit of figure 4-1 it can be seen that the rise is fairly linear although there is a 10 MHz oscillation superimposed on the rise and after the chop. From Appendices I and II it is obvious that the 10 MHz oscillation is most likely caused by the inductance of one of the smaller loops and the capacitance of one of the sphere gaps. It is interesting to note that the 10 MHz oscillation appears throughout the waveform. It occurs both before and after the series gap fires and before and after the 60 mm gap fires. It is therefore not caused by the capacitance of the gap itself but more likely by the capacitance of one of the spheres of the series gap to ground.

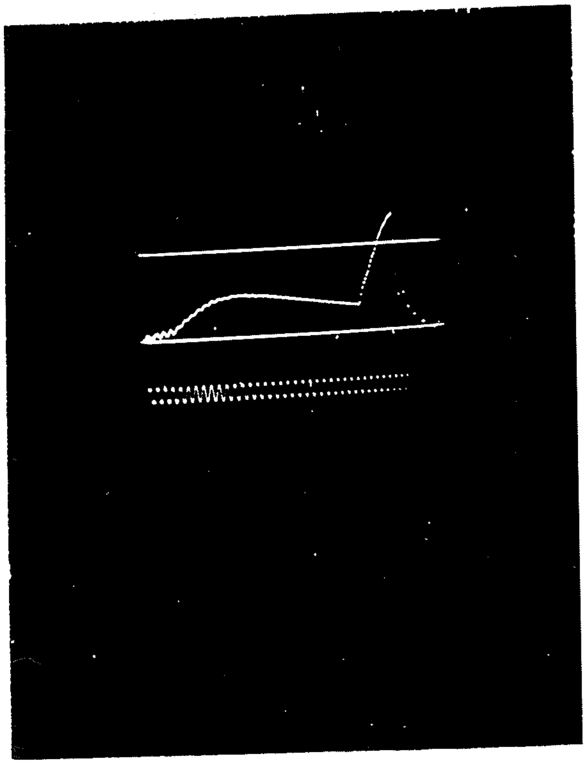

IG 4-2-a
IMING WAVE 10 MHz
AL. 200 V
HARGE 24 KV
TTENUATION 100%

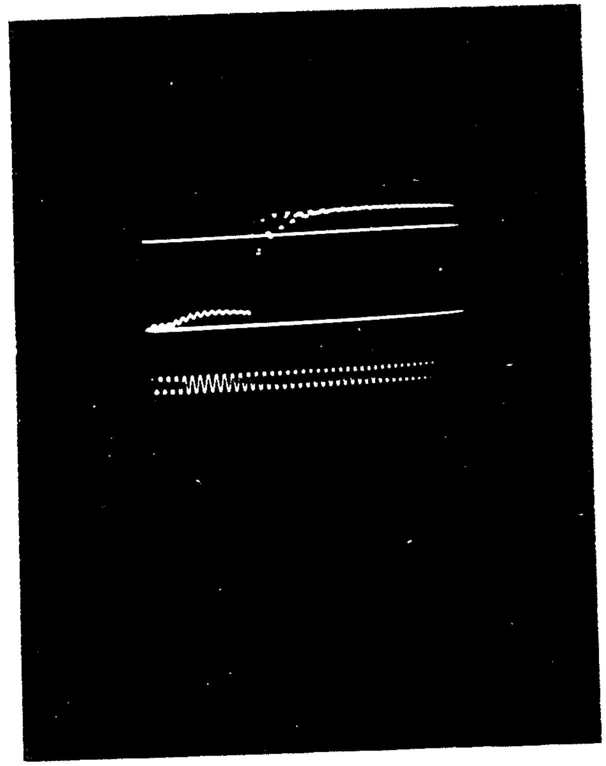

FIG 4-2-b
TIMING WAVE 10 MHz
CAL. 200 V
CHARGE 19 KV
ATTENUATION 100%

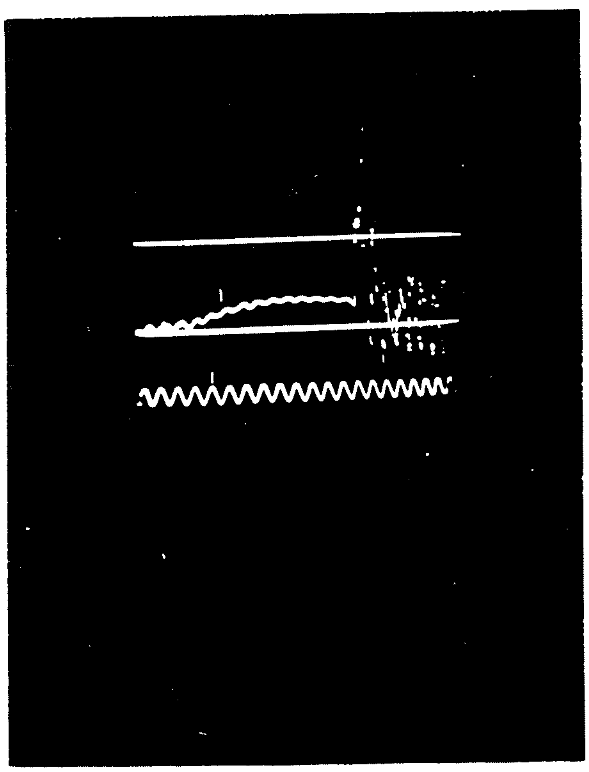

FIG 4-2-c
TIMING WAVE 10 MHz
CAL. 200 V
CHARGE 19 KV
ATTENUATION 100%

FIGURE 4-2 VOLT-TIME OSCILLOGRAMS

The voltage rise before the series gap breaks down is due to the high value of resistance between the series gap and ground. This resistance should be reduced to approximately 10 KΩ. This was done later in the development.

The series gap was set at 10 inches which means that a linearly rising voltage of about 500 KV would be necessary to break it down. Since the impulse generator is a 24-stage 100 KV/stage generator, a charge voltage of 24 KV would result in an ideal output of $\frac{24}{100}$ x 2.4 MV or 576 KV which is close to the critical breakdown level of the 10 inch gap. This is further shown by the fact that the voltage rise on oscillogram 4-2-a dips before the series gap breaks down. The series gap does not break down on the crest of the applied wave but rather fairly far out on the tail. The phenomenon will not be as apparent when the 50 KΩ resistor is reduced since the voltage rise should not be as pronounced.

A problem associated with a breakdown on the tail of the wave involves synchronization of the recording system with the series gap breakdown. If a higher voltage is applied to the series gap, it will break down on the rising portion of the voltage at approximately the same time each shot. If a lower voltage is applied to the series gap, it may break down on the tail of the applied wave. This results in very inconsistent firing and presents considerable difficulty in recording the 60 mm gap voltage. Once again the bend in the crest of the wave is evident. This bend which disappears for higher charging voltages and thus higher circuit energy, is also dependent on the 60 mm gap. This can be seen by comparing oscillogram 4-2-a, taken using the circuit of figure 4-1, and oscillogram 4-2-b, taken using the circuit of figure 4-3 but with the 60 mm gap removed. Apparently when the 60 mm gap is placed in the circuit it introduces oscillation which, combined with insufficient energy and insufficient loading capacitance, causes a bend in the wave. The bend can therefore be eliminated by increasing the loading capacitance, increasing the series gap and correspondingly the charging voltage, eliminating the oscillation due to the 60 mm gap or removing any one of the series resistors which would dissipate some of the available energy.

The following therefore will be an attempt to eliminate the bend by studying the effect of various parameters on the general waveform.

As a result of the foregoing, the circuit of figure 4-3 was further investigated. It should be noted that in this circuit all the damping resistors were removed excluding the 1250 ohm resistor to allow

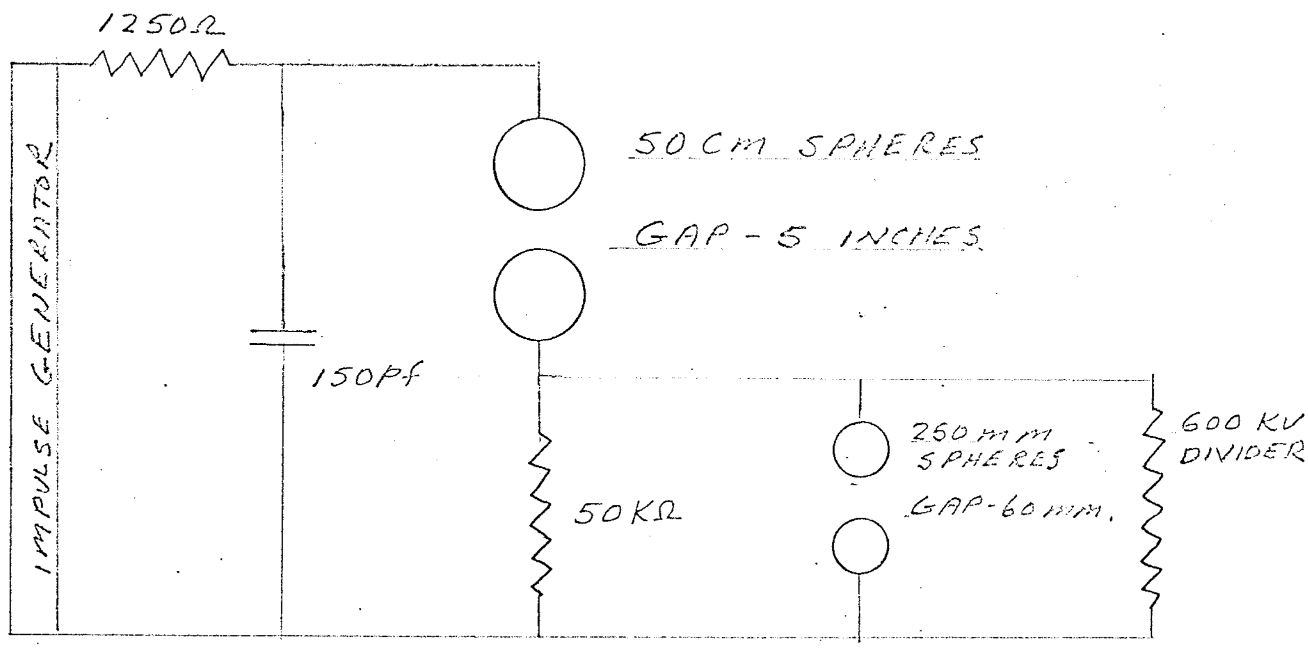

FIG 4-3

CIRCUIT FOR THE STUDY OF LINEAR FAST RISING WAVES WITH NO DAMPING for the greatest possible rate of rise. It should also be mentioned at this time that grounding of the various components of all the circuits described in the text was by means of a copper-ground plane made of 4 ft.x 8 ft. copper sheets attached to wooden frames and clamped together. This ground plane is shown in figure 4-4. . The resultant wave is shown on oscillogram 4-2-c. Notice that there is a 10 MHz oscillation before and after the breakdown of the 60 mm gap. This 10 MHz oscillation coupled with the 60 mm gap oscillation are the two main problems to be solved here. If the 60 mm gap is removed, the resulting waveform is as shown on oscillogram 4-2-b. Notice that the 10 MHz oscillation is still evident. This eliminates the 60 mm gap as the main source of the 10 MHz oscillation, although it does cause the oscillations responsible for the bend. It is highly unlikely that the oscillation is caused by reflections since a total distance between components of 50 ft. would be necessary to result in a 10 MHz oscillation assuming a travel time of 1 ft. per nanosecond.

As stated previously, it was felt that the capacitance of the series gap or of the spheres of the series gap to ground combined with one of the loop inductances was the major source of the 10 MHz oscillation.

An attempt was made to damp out the oscillations by placing a 500 ohm resistor between the loading capacitor

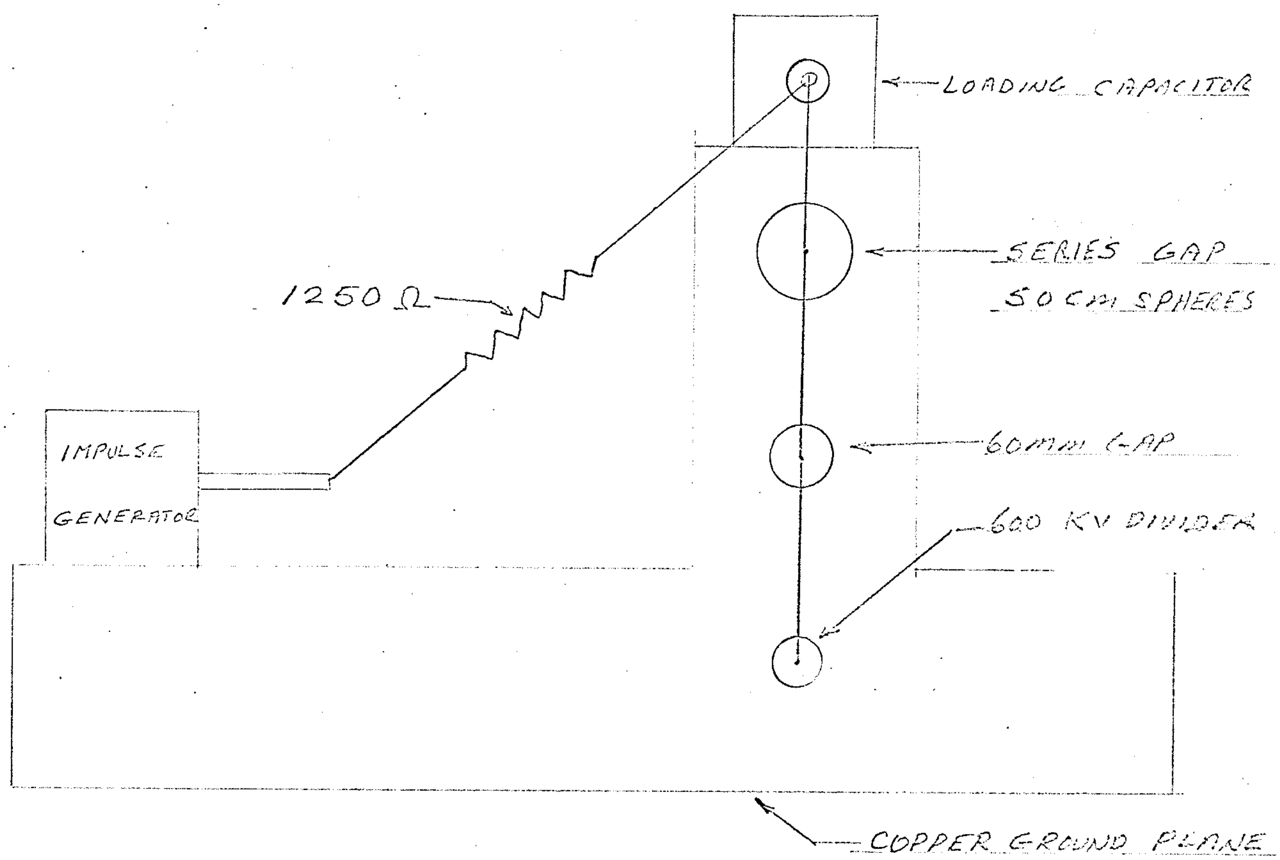

FIGURE 4-4
EQUIPMENT LAYOUT FOR THE STUDY OF LINEAR FAST RISING WAVES

and the series gap. Notice from oscillogram 4-5-a that the 500 ohm resistor appears to effectively reduce the pre-breakdown oscillations although they are still just barely evident. After the series gap breaks down, however, an oscillation is very prominent. The oscillation was measured as 15.4 MHz decreasing to 13.1 MHz nearer the peak.

The 500 ohm resistor reduced the rate of rise such that the oscillation appeared on the front. To critically damp the oscillations originating from the capacitance and inductance of the circuit it can be seen from Appendix II that a resistor of approximately 2000 ohms would be required. This would reduce the rate of rise to an unacceptable level. The reason that the pre-breakdown oscillation seems to have disappeared on 4-5-a when compared to 4-2-b is mainly due to the faster sweep speed used for 4-5-a. Notice on 4-2-b that the oscillations before the breakdown of the series gap are very small. Upon close inspection of 4-5-a these oscillations are still evident although reduced in amplitude slightly by the 500 ohm resistor.

Notice from 4-5-b that when the 60 mm gap is again placed in the circuit it once again introduces another oscillation and causes a rougher waveshape.

An attempt at damping the oscillation by means of a filter was made. This is shown in figure 4-6. The

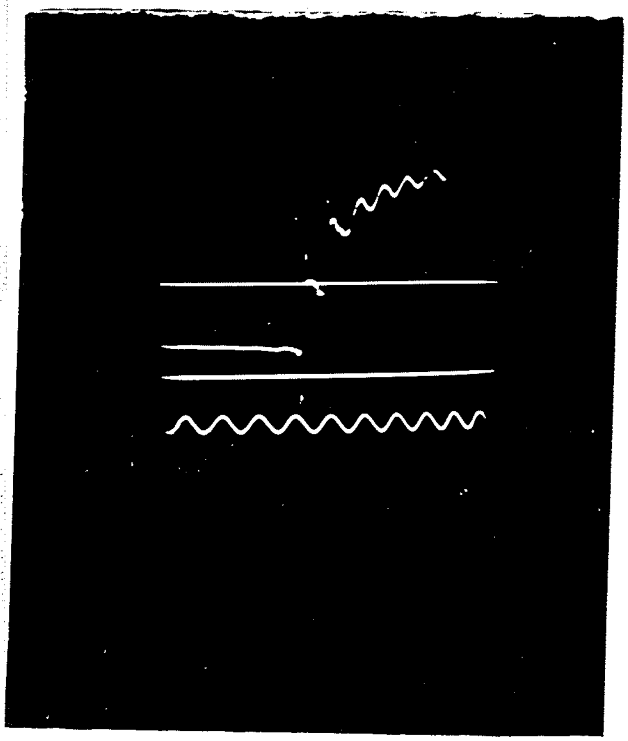

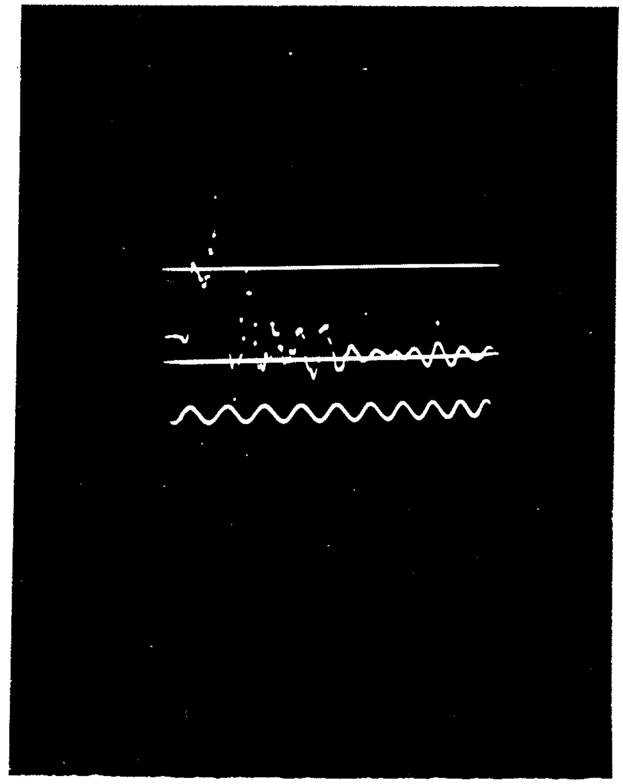

G 4-5-a
MING WAVE 10 MHz
L. 200 V
ARGE 19 KV
TENUATION 100%

FIG 4-5-b
TIMING WAVE 10 MHz
CAL. 200 V
CHARGE 19 KV
ATTENUATION 100%

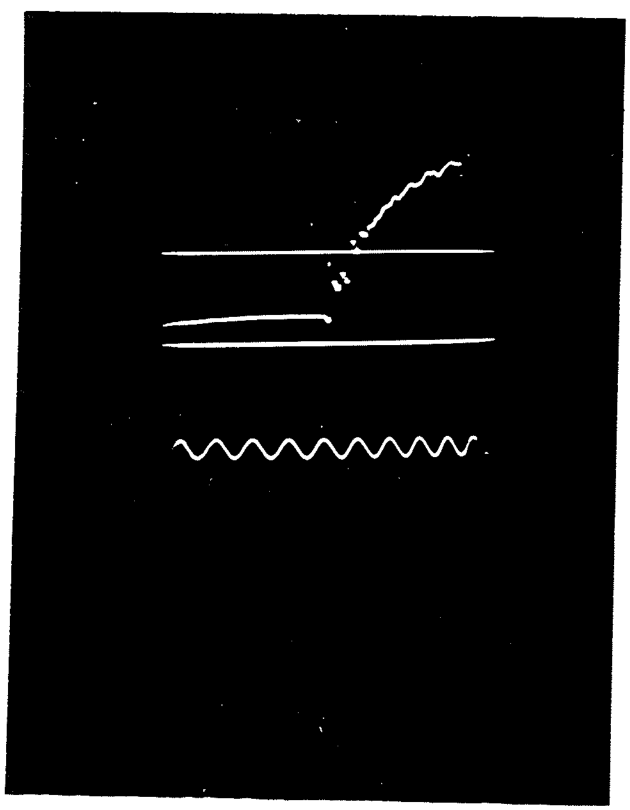

G 4-5-c
MING WAVE 10 MHz
L. 200 V
ARGE 20 KV
TENUATION 100%

FIGURE 4-5 VOLT-TIME OSCILLOGRAMS

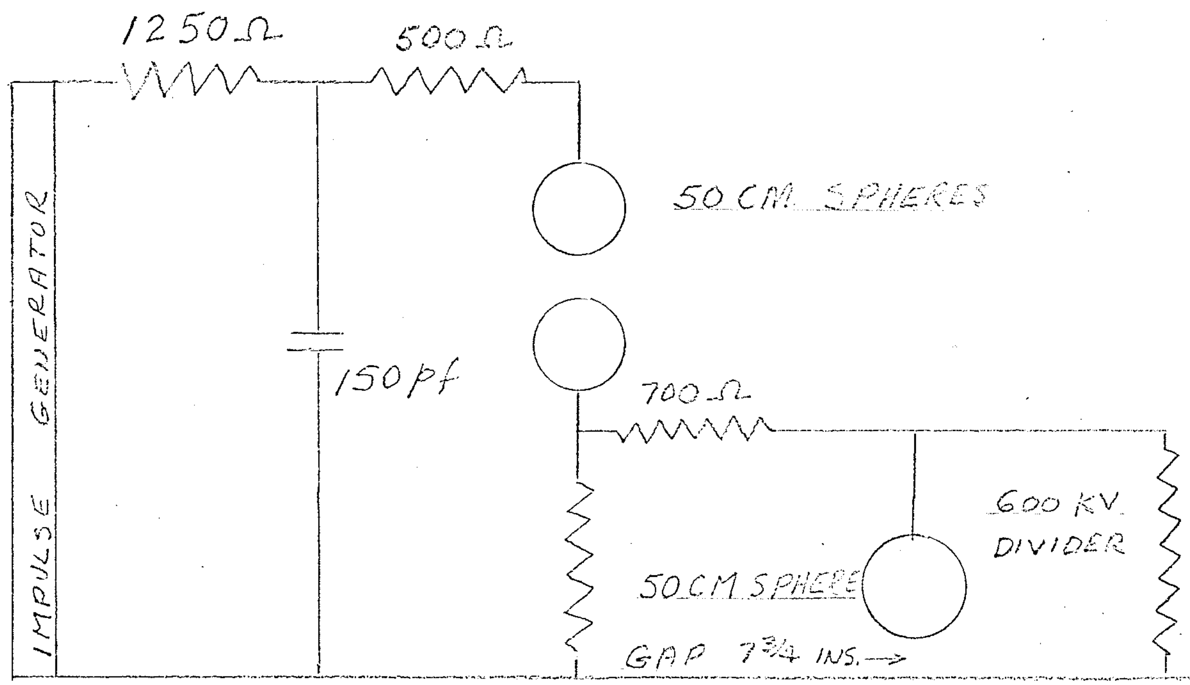

FIGURE 4-6

CIRCUIT FOR THE STUDY OF THE EFFECT OF A FILTER CIRCUIT ON LINEAR FAST RISING WAVES result is shown in 4-5-c. The 700 ohm resistor drastically reduced the rate of rise and the filter circuit seemed to introduce more oscillations. Due to our energy limitations it was decided that a filter circuit would not be possible. If more loading capacitance were available, utilization of this method would probably be possible.

The components for the preceding series of tests were arranged as shown in figure 4-4. There is little doubt that the loop inductances in this case are somewhat higher than they would be if the components extended continuously outward from the generator. It was therefore decided to rearrange the components in a straight line as shown in figure 4-7 and thereby reduce the loop inductances of the circuit. All damping was removed except the 1250 ohm resistor from the generator to the loading capacitor.

Oscillogram 4-8-a shows the results with the 60 mm gap not included. The rise is very satisfactory, only a slight deviation occurring half way up. This deviation is the first oscillation of a series that is evident after the crest. This series is the same 10 MHz oscillation previously discussed.

The results with the 60 mm gap included in the circuit are quite satisfactory as shown on oscillogram 4-8-b although as above the oscillation on the rise is still quite pronounced. Notice also the small oscillation

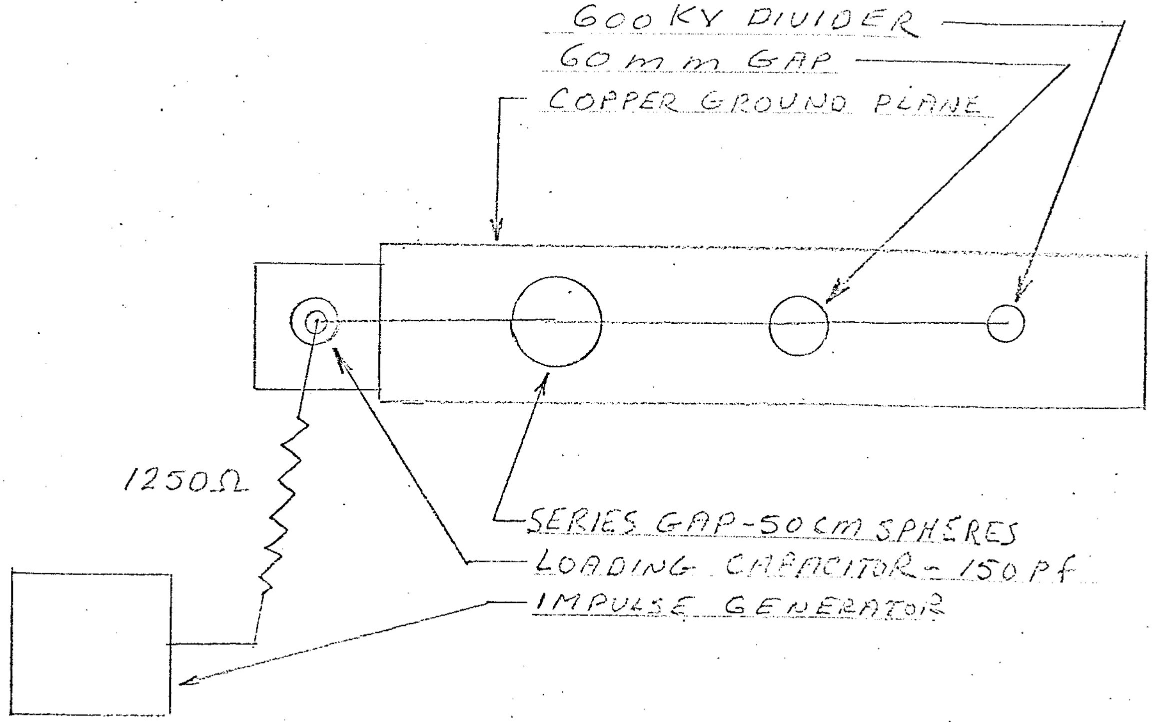

FIGURE 4-7

ARRANGEMENT OF CIRCUIT COMPONENTS TO MINIMIZE LOOP INDUCTANCES

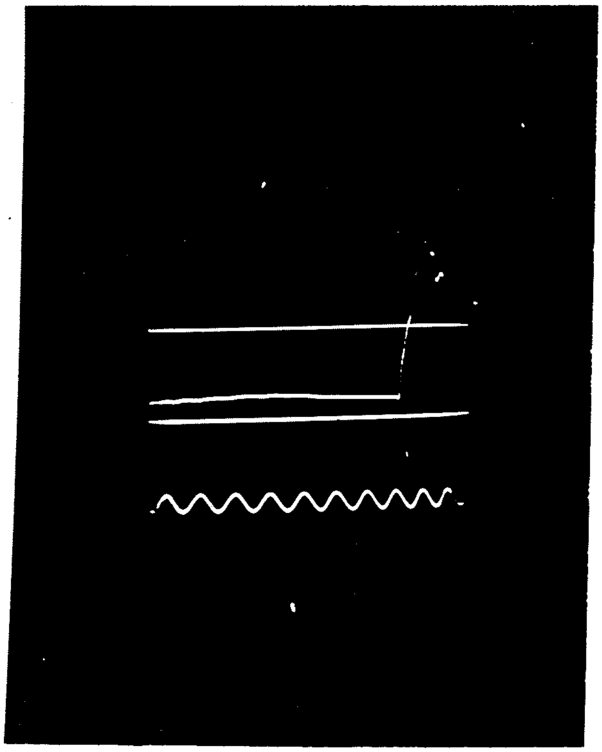

FIG 4-8-a
TIMING WAVE 10 MHz
CAL. 200 V
CHARGE 20 KV
ATTENUATION 100%

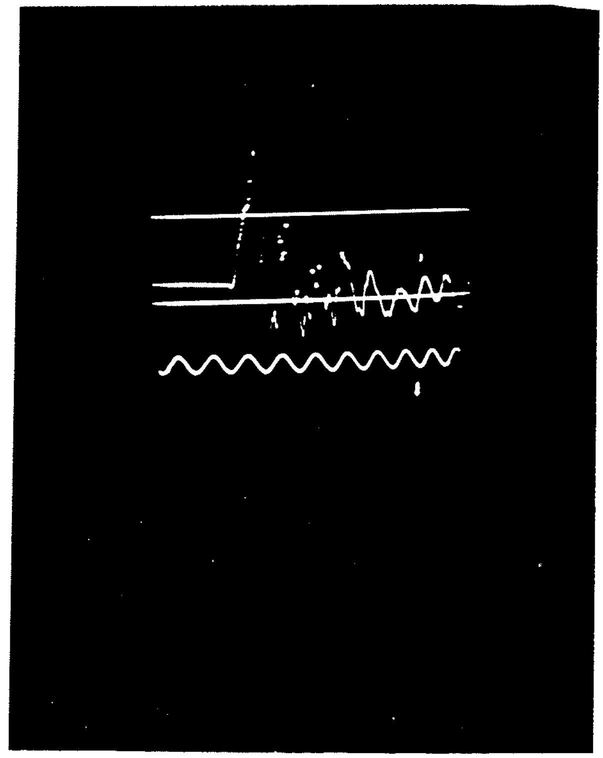

FIG 4-8-b
TIMING WAVE 10 MHz
CAL 200 V
CHARGE 20 KV
ATTENUATION 100%

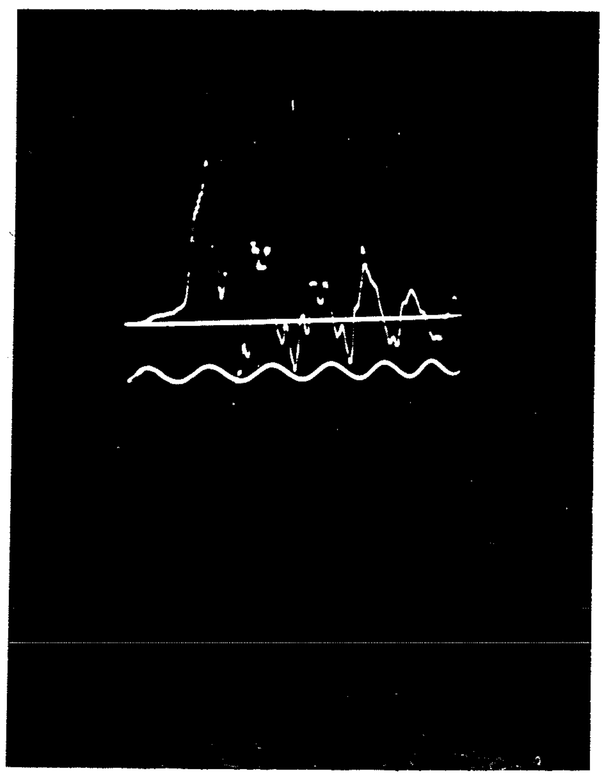

FIG 4-8-c
TIMING WAVE 10 MHz
CHARGE 20 KV
ATTENUATION 100%

FIGURE 4-8 VOLT-TIME OSCILLOGRAMS

introduced due to the 60 mm gap capacitance.

Any attempt at damping the 10 MHz oscillation on the front proved hopeless since too high a resistor was required to damp the oscillation. The high resistor would only slow down the front.

It was decided at this point to find the effect of increasing the resistance from the generator to the loading capacitor to 85 KΩ. The resulting waveform was as shown on oscillogram 4-8-c. This should be compared directly to oscillogram 4-8-b. Notice that the only effect was to eliminate the initial voltage rise seen on oscillogram 4-8-b. For the same charging voltage the 85 KΩ resistor will reduce the available energy to the remainder of the circuit. This means that the problems caused by insufficient energy should be intensified. This is indeed the case as is evident from oscillogram 4-8-c. Notice that the bending caused by the 60 mm gap oscillation is worse in oscillogram 4-8-c than in oscillogram 4-8-b.

A 621 ohm wirewound resistor was placed between the 60 mm gap and the divider. It was realized of course that this would prevent the divider from recording the gap voltage but the effect of the resistor on the measuring system was nevertheless studied. The effect of the change is shown on oscillogram 4-9-a.

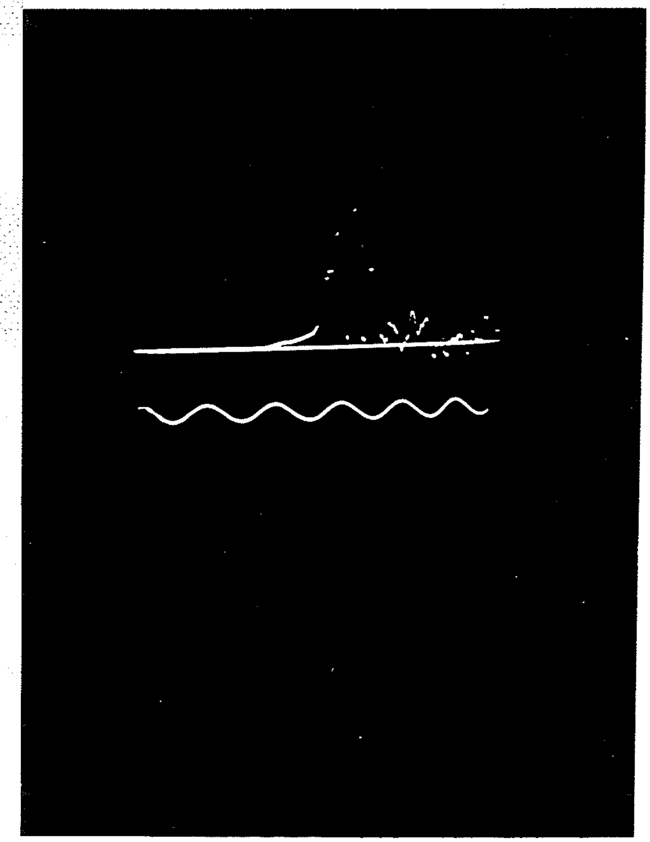

FIG 4-9-a
TIMING WAVE 10 MHz
CHARGE 20 KV
ATTENUATION 100%

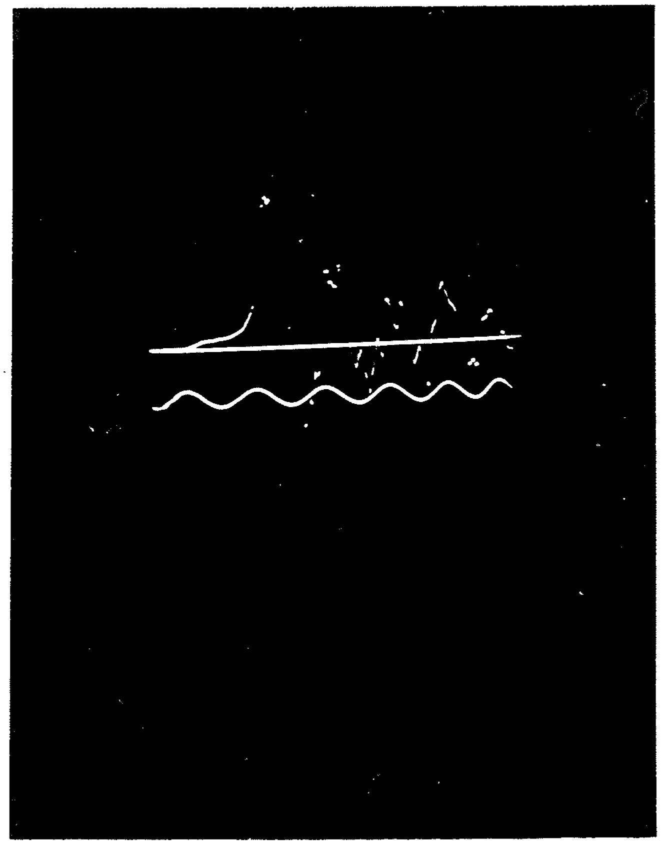

FIG 4-9-b
TIMING WAVE 10 MHz
CHARGE 20 KV
ATTENUATION 100%

FIGURE 4-9 VOLT-TIME OSCILLOGRAMS

Notice the very high first oscillation. It is apparent that the 621 ohm wirewound resistor affected the divider circuit in such a way as to give a serious reflection. The 60 mm gap circuit which was previously very near to a zero impedance circuit after the gap broke down was changed to a finite impedance after breakdown. Consequently, the reflection coefficients were changed and severe oscillations resulted.

Returning to 4-8-c, oscillations of 44.5 MHz and 10 MHz are measurable after the chop. Before the chop there is only a slight high frequency oscillation and a bend in the rise.

Oscillograms 4-8-c and 4-9-b were both obtained using the same circuit. Oscillogram 4-8-c shows a rise that bends slightly and oscillates to breakdown. Oscillogram 4-9-b rises to very near breakdown then shows a single oscillation just prior to breakdown. Once again the loading capacitance has not sufficient energy storage to produce a smooth rise to breakdown. The rise appears to reach a certain value then a deviation appears due to insufficient energy. This deviation may appear in the form of a bend or a single oscillation. The loading capacitor then apparently recovers and the rise continues until breakdown. A larger loading capacitor or a higher charging voltage would help remedy the situation. The charge voltage in this work was limited by the voltage rating of the loading capacitor.

It was finally decided that the only way to obtain satisfactory results with the 150 pf loading capacitor was to remove all damping and shorten the leads as much as possible, particularly the lead from the 60 mm gap to the divider which would reduce the energy loss to a minimum. This was done with the results shown in oscillogram 4-10-a.

The difficulty that arose in this case was that the results were not consistent. This is best illustrated by oscillogram 4-10-b which shows three consecutive shots using the same circuit.

The inconsistencies were caused by two problems. First, the hash at the top of all three waves and the bending which is particularly evident on the centre waveform, are due to the lack of stored energy. Second, the initial rise that is of much higher amplitude in the top waveform than in the other two is due to stray coupling between the series gap and the voltage divider. This stray coupling in the top waveform causes a significant preliminary voltage such that the additional voltage required for the gap to break down is less than it would have been if there were no preliminary voltage. The energy required to produce this smaller voltage is therefore also less. There is therefore sufficient energy in the loading capacitor to create a smooth rise

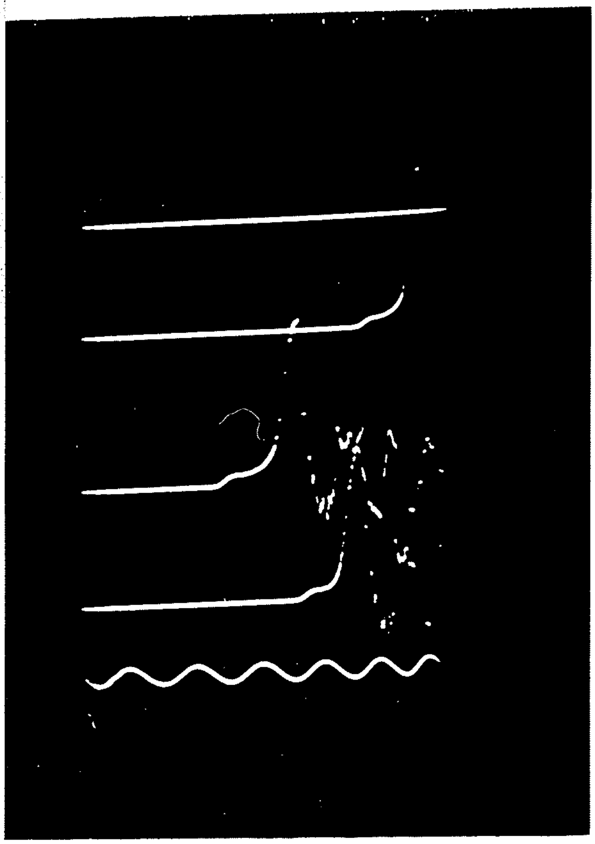

IG 4-10-a
IMING WAVE 10 MHz
IARGE 20 KV
TTENUATION 100%

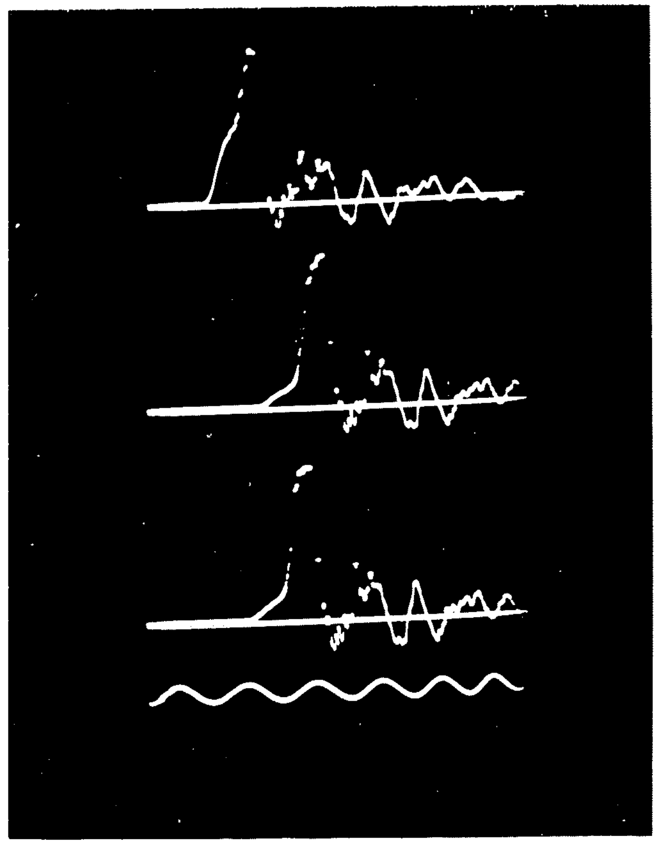

FIG 4-10-b
TIMING WAVE 10 MHz
CHARGE 20 KV
ATTENUATION 100%

FIGURE 4-10 VOLT-TIME OSCILLOGRAMS

to failure from the stray voltage. In the other two cases, however, the stray coupling is not sufficient to provide a smooth rise to breakdown.

Because of these two different effects it is obvious that the stray coupling is not consistent since on oscillogram 4-10-b it appears on the first oscillogram but does not affect the result in the second or third oscillograms appreciably. This inconsistency is dependent upon the breakdown of the series gap. It does not break down at exactly the same time and voltage each time, as is well known. The time and voltage of breakdown have a very pronounced effect on the coupling into the divider circuit.

The existence of the stray coupling between the two parts of the circuit is best illustrated by referring to oscillogram 4-11-a which is the waveform resulting from the circuit of figure 4-12. This circuit will be discussed in detail later. The 2400 pf capacitor is one section of the resistance capacitance divider mentioned in Chapter III and the 12.5 K water resistor is the original 85 KΩ water resistor which had deteriorated with time.

The oscillation on the rise of oscillogram 4-11-b-2 is obtained when the lead from the series gap to the divider is removed. It is obvious therefore that the oscillation is being capacitively coupled into

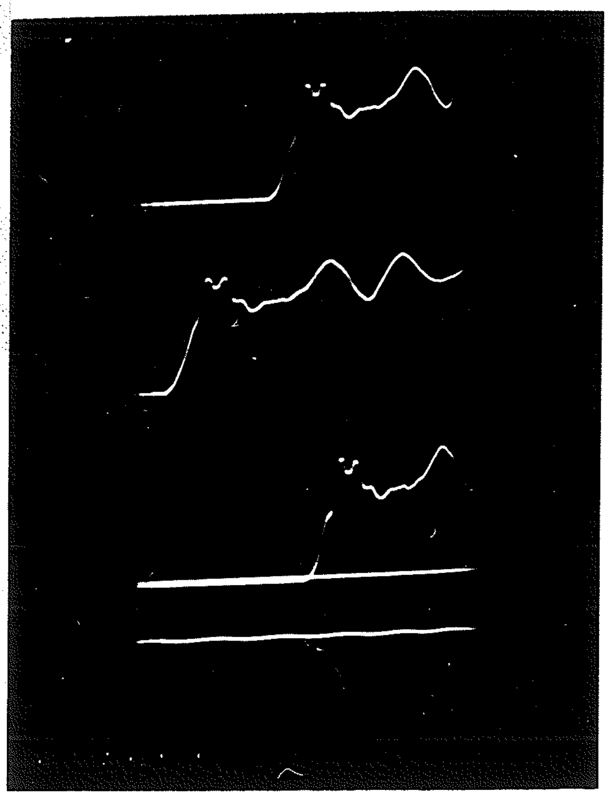

FIG 4-11-a
TIMING WAVE 10 MHz
CHARGE 25 KV
ATTENUATION 100%

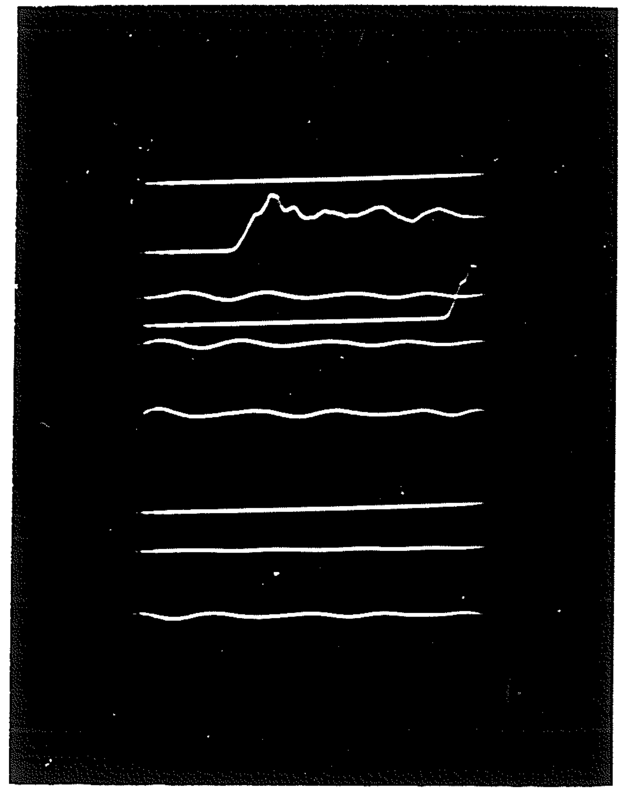

FIG 4-11-b
TIMING WAVE 10 MHz
CHARGE 25 KV
ATTENUATION 100%

FIGURE 4-11 VOLT-TIME OSCILLOGRAMS

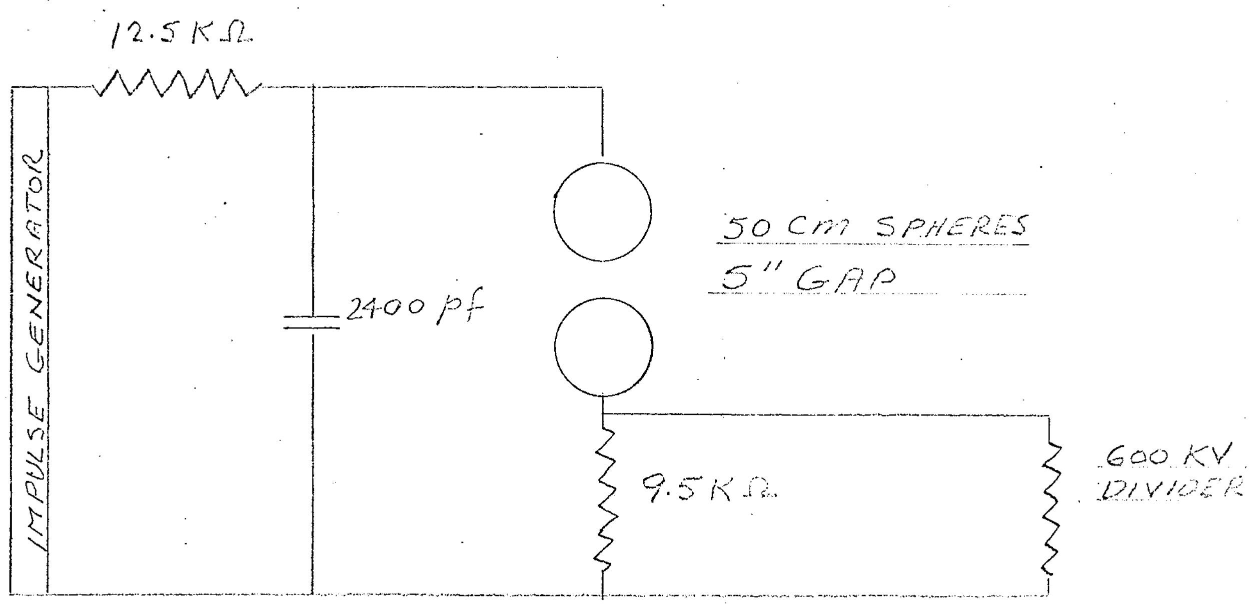

FIGURE 4-12

CIRCUIT FOR THE STUDY OF FAST RISING WAVES UTILIZING AN INCREASED AMOUNT OF LOADING CAPACITANCE the divider circuit. This oscillation is the same as that appearing on the rise of oscillogram 4-11-a. The oscillation has been measured to be approximately 10 MHz after the first few cycles. It is somewhat greater at the beginning of the wave. This stray coupling therefore introduces an initial voltage to the divider. This voltage has superimposed on it the 10 MHz oscillation resulting from the series gap. The stray capacitances are therefore the vehicle by which the 10 MHz oscillation appears at the divider. Later a method of shielding will be discussed which will effectively eliminate the stray coupling.

Oscillograms 4-13-a, 4-13-b, 4-14-a and 4-14-b illustrate this point very well. Notice that the oscillation on the rise of oscillograms 4-13-a and 4-13-b taken using the circuit of 4-12 appear on the rise of oscillograms 4-14-a and 4-14-b taken using the circuit of figure 4-12 with the 60 mm gap included. Notice here also that the small high frequency oscillation on the rising portion of the waveform caused by the 60 mm gap is again evident.

It is apparent from the following discussion that the resistor between the bottom series sphere gap and ground is not critical if the resistor from the generator to the loading capacitor is large. The reason for this is, as indicated before, that with a large resistor from the generator to the loading capacitor the

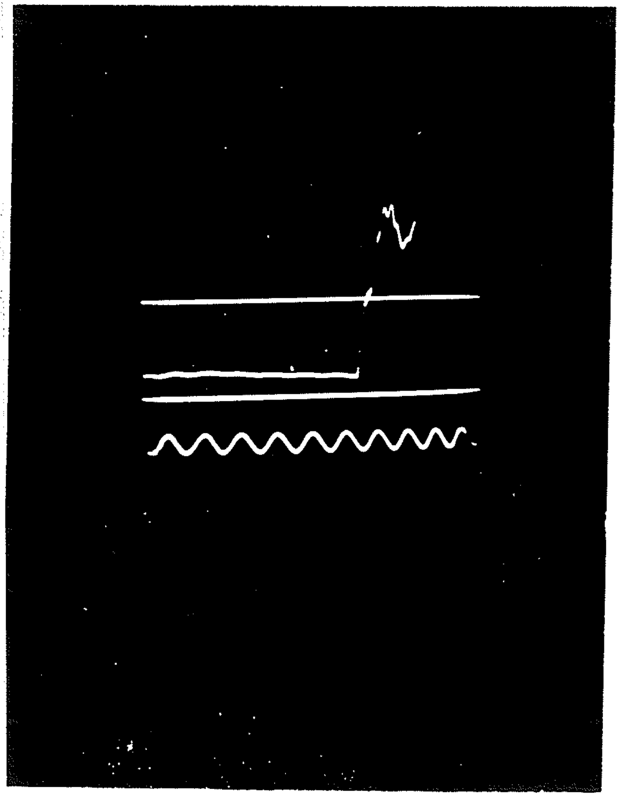

FIG 4-13-a
TIMING WAVE 10 MHz
CAL. 200 V
CHARGE 20 KV
ATTENUATION 100%

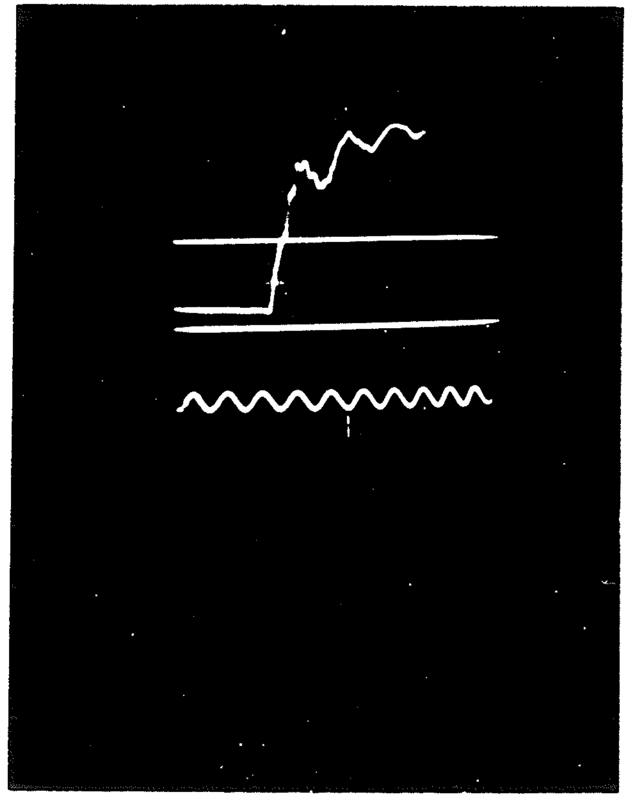

FIG 4-13-b
TIMING WAVE 10 MHz
CAL. 200 V
CHARGE 20 KV
ATTENUATION 100%

FIGURE 4-13 VOLT-TIME OSCILLOGRAMS

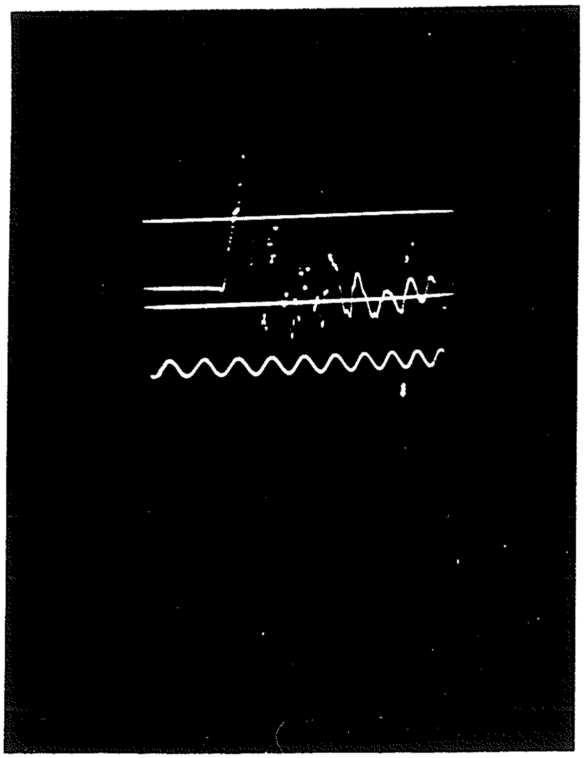

FIG 4-14-a
TIMING WAVE 10 MHz
CAL. 200 V
CHARGE 20 KV
ATTENUATION 100%

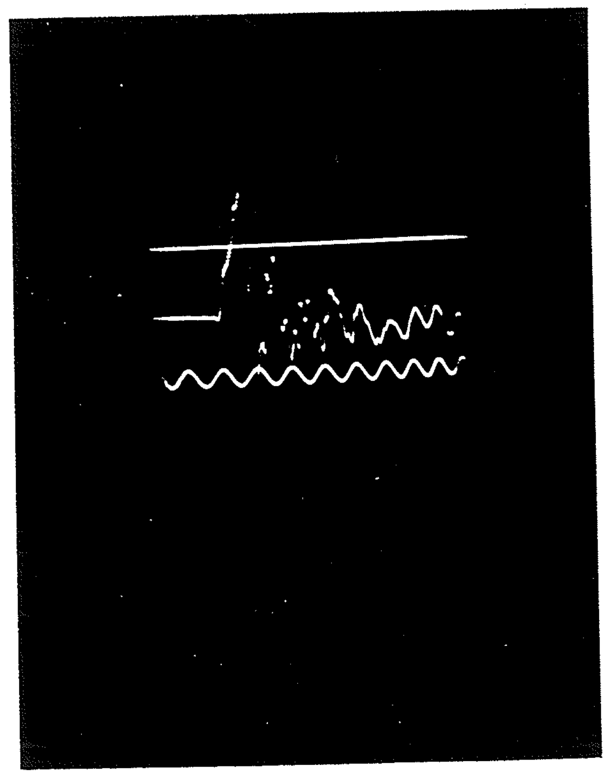

FIG 4-14-b
TIMING WAVE 10 MHz
CAL. 200 V
CHARGE 20 KV
ATTENUATION 100%

FIGURE 4-14 VOLT-TIME OSCILLOGRAMS

circuit time constant is such that the voltage across the loading capacitor increases relatively slowly. The impedance of the series gap to the resulting low frequency voltage is very high. Thus little voltage will be recorded at the divider. With a small resistance from the generator to the loading capacitor the circuit time constant is much lower, the accompanying frequencies are much higher and the impedance of the gap to these frequencies are lower. More voltage will therefore appear at the voltage divider.

The fact that the resistor from the series gap to ground is unimportant when the resistor from the generator to the loading capacitor is large is verified by the following oscillograms.

Oscillogram	Resistance from Series Gap to Ground
4-10-b	9.5 K
4-15-a	3.5 K
4-15-b	621 Ohms
4-16-a	100 K
4-16-b	Infinity

Each of the above oscillograms was taken with the series resistor equal to 12.5 $K\Omega$. Notice that on oscillograms 4-10-b, 4-15-a and 4-15-b no significant voltage occurs before the breakdown of the series gap other than the voltage due to stray coupling. A slight preliminary

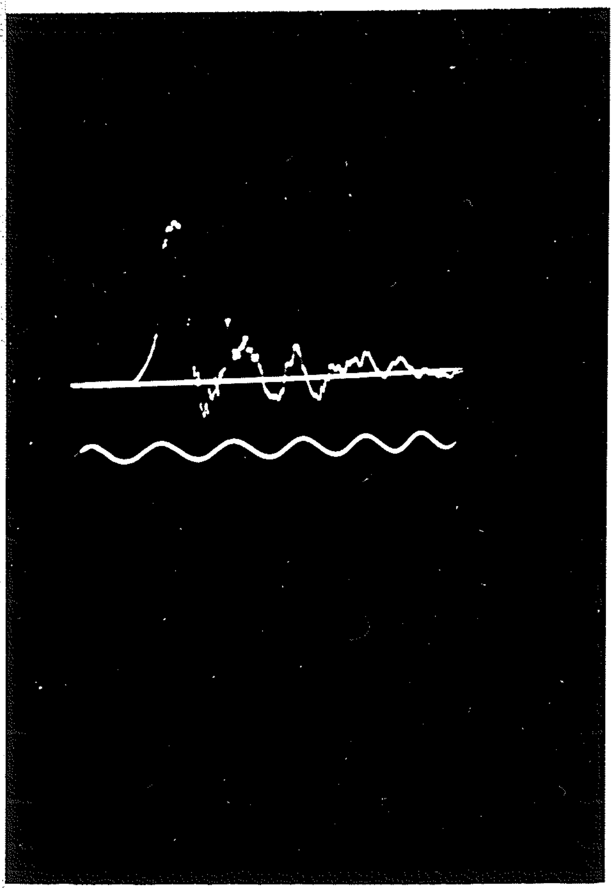

; 4-15-a
ING WAVE 10 MHz
RGE 20 KV
ENUATION 100%

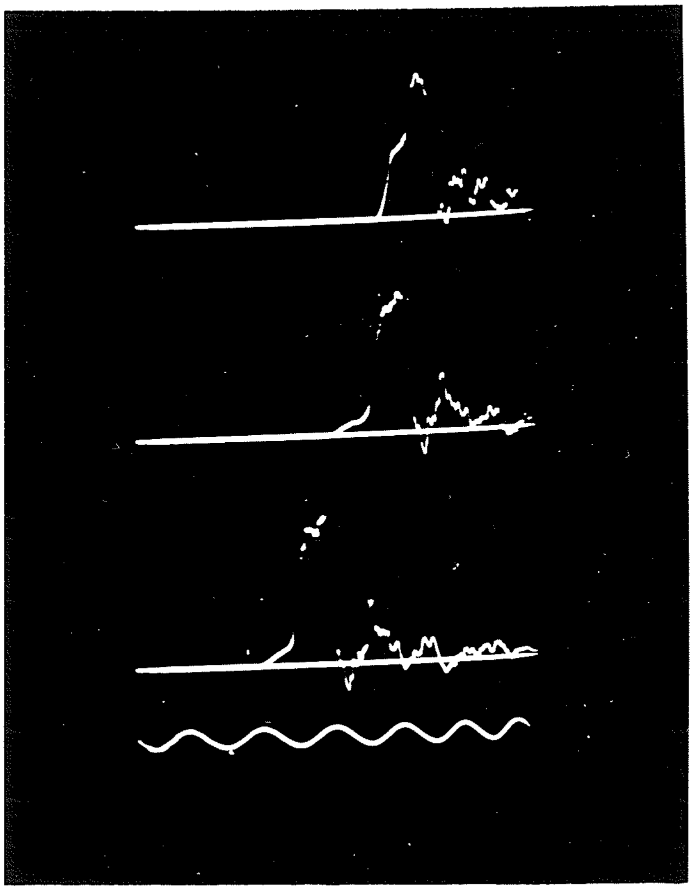

FIG 4-15-b
TIMING WAVE 10 MHz
CHARGE 20 KV
ATTENUATION 100%

FIGURE 4-15 VOLT-TIME OSCILLOGRAMS

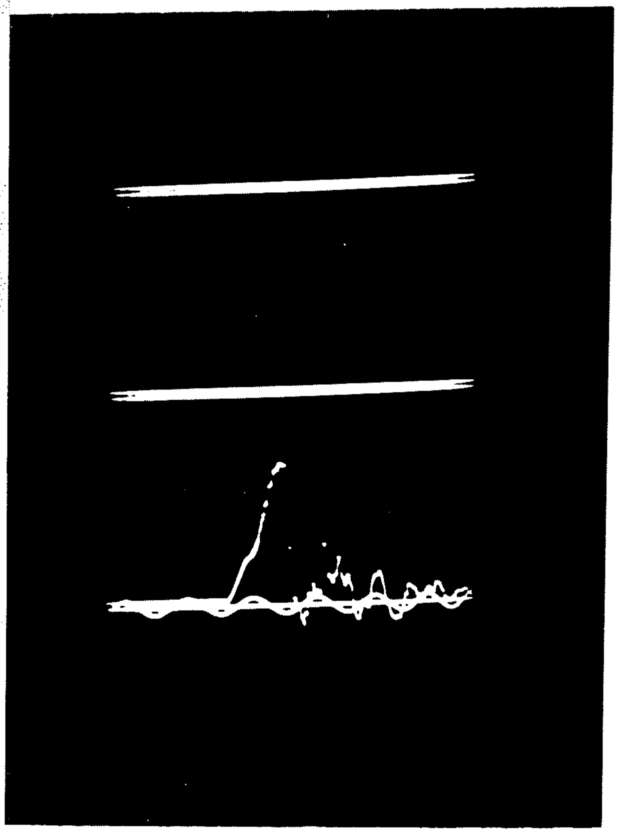

IG 4-16-a
IMING WAVE 10 MHz
HARGE 20 KV
TTENUATION 100%

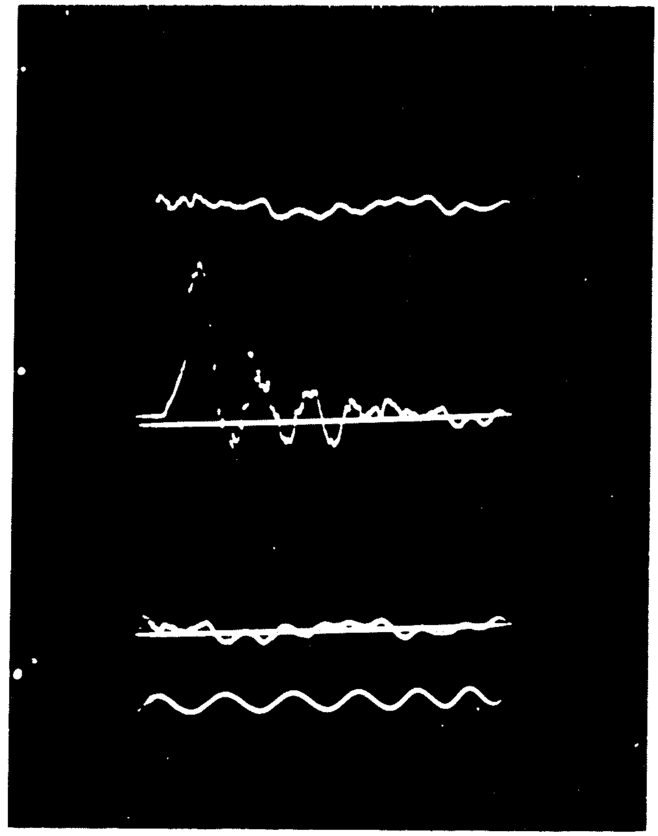

FIG 4-16-b
TIMING WAVE 10 MHz
CHARGE 20 KV
ATTENUATION 100%

FIGURE 4-16 VOLT-TIME OSCILLOGRAMS

voltage appears in oscillograms 4-16-a and 14-16-b however, due to the exceedingly high resistance used in this case. This can be identified as the low constant voltage component up to the beginning of the stray couplings on these two oscillograms. Oscillogram 4-2-a on the other hand which was taken with 650 ohm resistor from the generator to the loading capacitor shows a significant rise before the breakdown of the series gap. The circuit for oscillogram 4-2-a had a 50 K resistor from the series gap to ground. When this resistor was reduced to 9.5 K the initial voltage was reduced to that shown in oscillogram 4-2-c.

The discussion will now revert to the problem of the non-linear rise. On oscillograms 4-10-b-2 and 4-10-b-3 where the stray pickup does not significantly affect the rise, the wave does not quite rise to its peak smoothly. There is always the small deviation or oscillation near the peak. This deviation is known to be a result of the 60 mm gap and insufficient loading capacitance. This theory was confirmed by increasing the loading capacitor from 150 pf to 225 pf by placing a 50 cm sphere on the bottom of the bushing that was being used for a loading capacitor. The results are quite satisfactory. The resulting waveform is shown on oscillogram 4-17-a. The high frequency oscillation on the rise is due to the 60 mm gap.

Oscillograms 5-6-a and 5-6-b which were obtained using the increased capacitance were used to calibrate the divider. The details and measurements of the calibration will be presented in the next chapter.

An attempt was made to slow down the rise in order to get another point on the 600 KV divider volt-time curve for calibration purposes. Due to insufficient loading capacitance this was impossible. The wave would not rise linearly to breakdown with any resistance in the circuit.

With 350 ohms between the series and the 60 mm gaps, some calibration data were taken but since the data did not appear at all satisfactory, they were not included in this presentation.

At this point in the investigation it was felt that a higher loading capacitance would give even more satisfactory results. First an 1150 pf loading capacitor made of two 4 ft. x 8 ft. sheets of copper fastened to wood frames with four sheets of 1/2 inch plywood and two sheets of 1/4 inch pressboard between electrodes was used. This system was unsatisfactory due to corona discharges at the edges of the sheets.

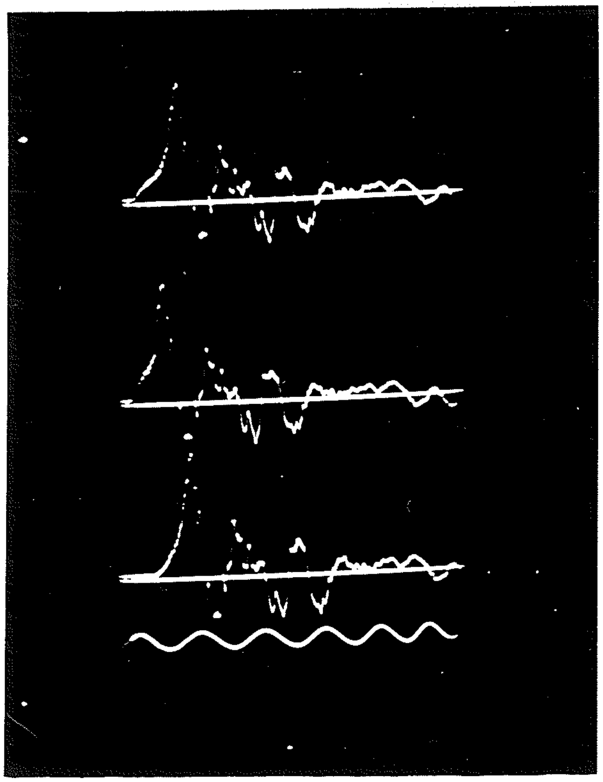

FIG 4-17-a
TIMING WAVE 10 MHz
CHARGE 20 KV
ATTENUATION 100%

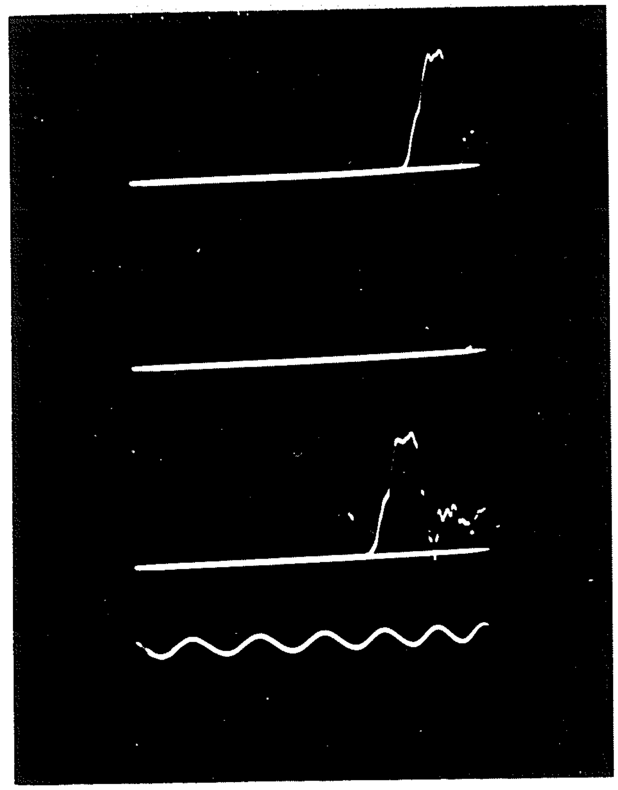

FIG 4-17-b
TIMING WAVE 10 MHz
CHARGE 26.5 KV
ATTENUATION 100%

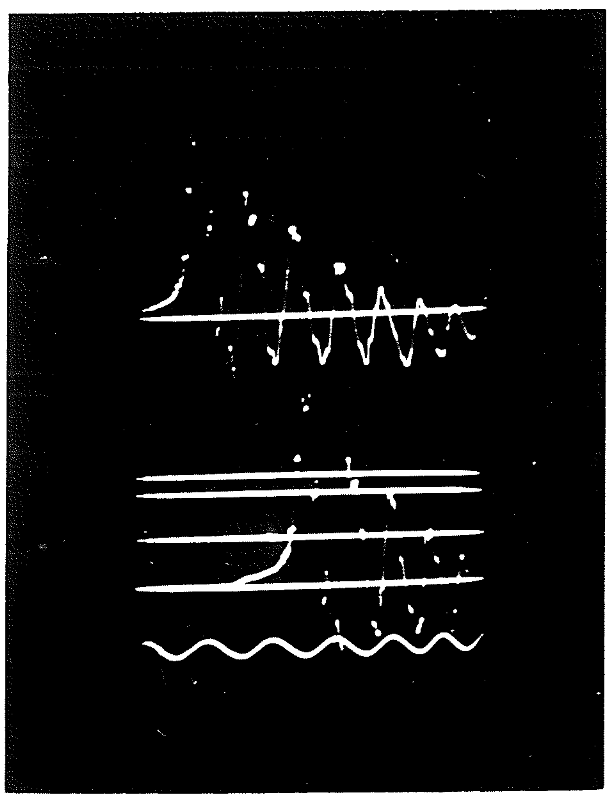

FIG 4-17-c
TIMING WAVE 10 MHz
CHARGE 41 KV
ATTENUATION 100%

FIGURE 4-17 VOLT-TIME OSCILLOGRAMS

A 2400 pf loading capacitor was then used. This capacitor was the bottom capacitance section of a four-stage 2400 KV resistance capacitance voltage divider. The resulting waveform is shown on oscillogram 4-17-b. The oscillation on the rise and at the peak of the wave is due to the stray capacitance pickup from the series gap discussed previously. The loading capacitor was then halved by two stages of the resistance capacitance voltage divider. This doubled the voltage ratingof the stack and consequently allowed a higher charge voltage. The resulting waveform obtained using a charge voltage of 40 KV is shown on oscillogram 4-17-c.

The oscillation or voltage rise due to stray pickup does not cause much of a problem in this case but a severe oscillation occurs on the rise. This oscillation was created due to the increased loop inductance caused by doubling the capacitance stack. It would therefore be best for calibration purposes to use the circuit with the smaller loop, thereby eliminating the stray coupling.

At this point a complete investigation of the stray coupling was carried out. The loading capacitor was again doubled to 2400 pf to give the maximum capacitance and thus the maximum energy availability. The resulting waveform is shown on oscillogram 4-18-a.

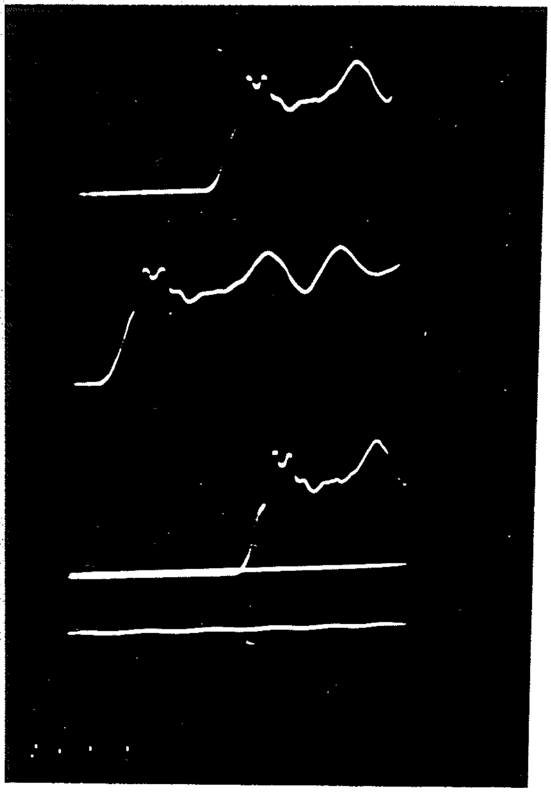

FIG 4-18-a
TIMING WAVE 10 MHz
CHARGE 25 KV
ATTENUATION 100%

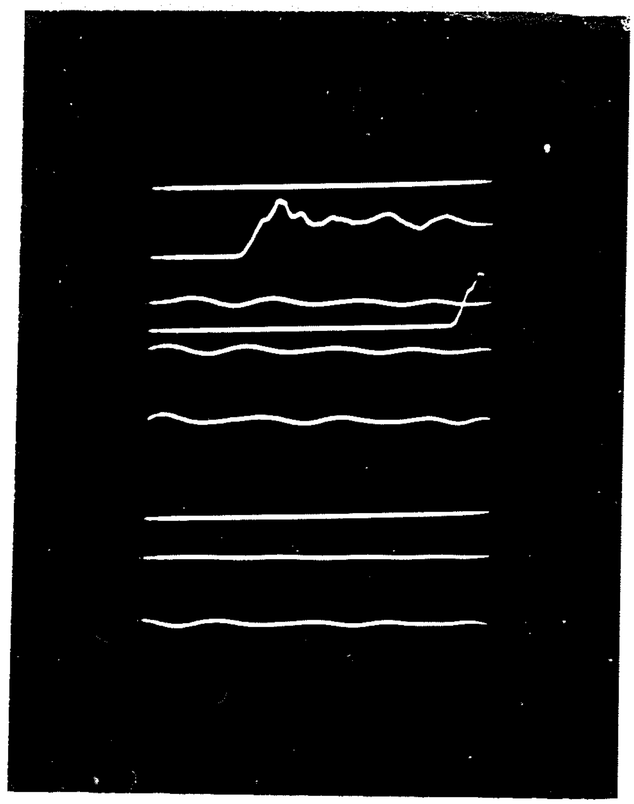

FIG 4-18-b
TIMING WAVE 10 MHz
CHARGE 25 KV
ATTENUATION 100%

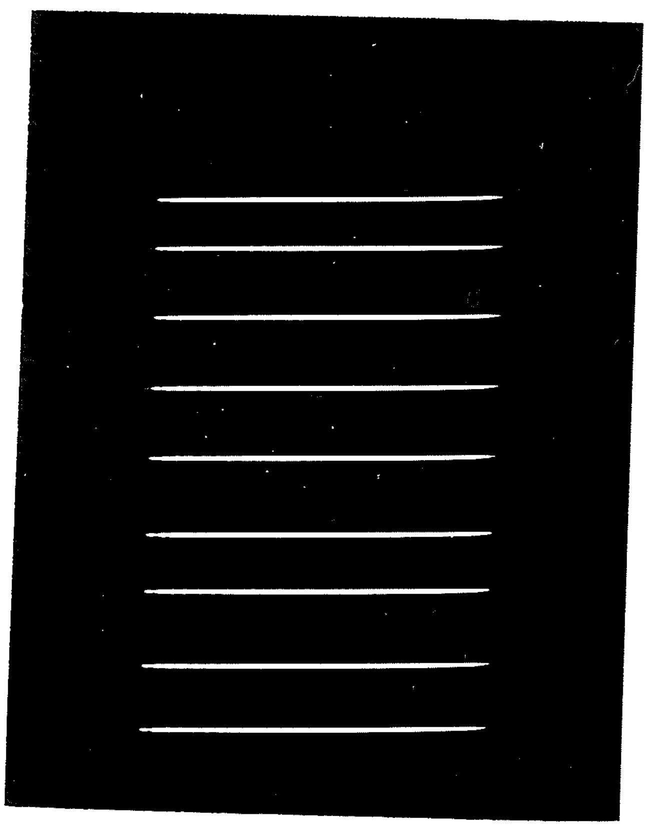

FIG 4-18-c
CHARGE 25 KV
ATTENUATION 100%

FIGURE 4-18 VOLT-TIME OSCILLOGRAMS

It was at this point in the investigation that the cause of the stray coupling was discovered. As stated previously, the lead from the series gap to the divider was removed. The resulting waveform is shown on oscillogram 4-18-b-2. Notice that the oscillations due to strays are of the same form as that on oscillogram 4-18-a. Oscillograms 4-18-a and 4-18-b are a repeat of 4-11-a and 4-11-b.

In order to verify that the coupling was not originating from the impulse generator, the lead from the series resistor on the generator to the loading capacitance was disconnected. Oscillogram 4-18-c shows a completely clean trace. The stray coupling was therefore originating from the series gap. The combination of the capacitance of the series gap and of the series gap to ground in conjunction with one of the loop inductances caused a 10 MHz oscillation which was coupled along with an initial component of voltage by stray capacitances into the divider circuit.

An 8 ft. x 8 ft. copper shield was built and was placed vertically between the 60 mm gap and the divider. With the 60 mm gap not in place and no lead from the series gap to the divider, a series of oscillograms were taken. These are shown on oscillogram 4-19-a. Notice that very little coupling is evident. The 60 mm

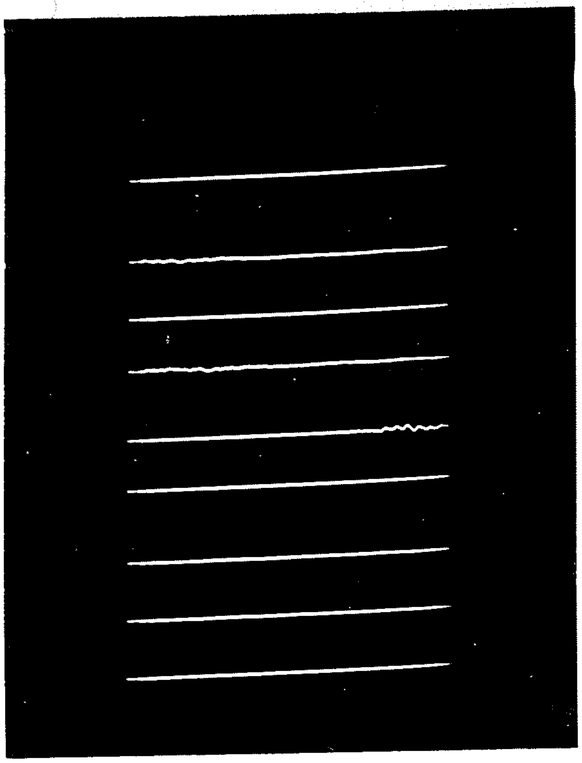

FIG 4-19-a
CHARGE 25 KV
ATTENUATION 100%

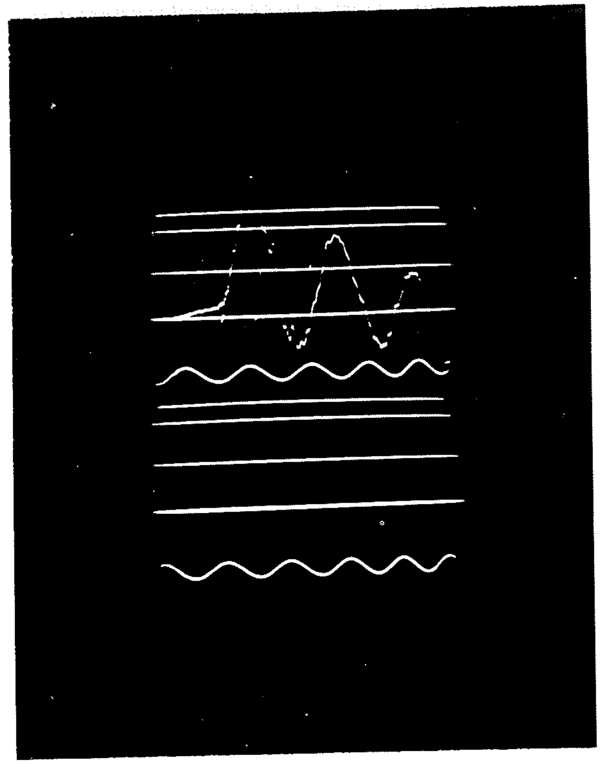

FIG 4-19-b
TIMING WAVE 10 MHz
CAL. 100, 200, 242 V
CHARGE 26 KV
ATTENUATION 100%

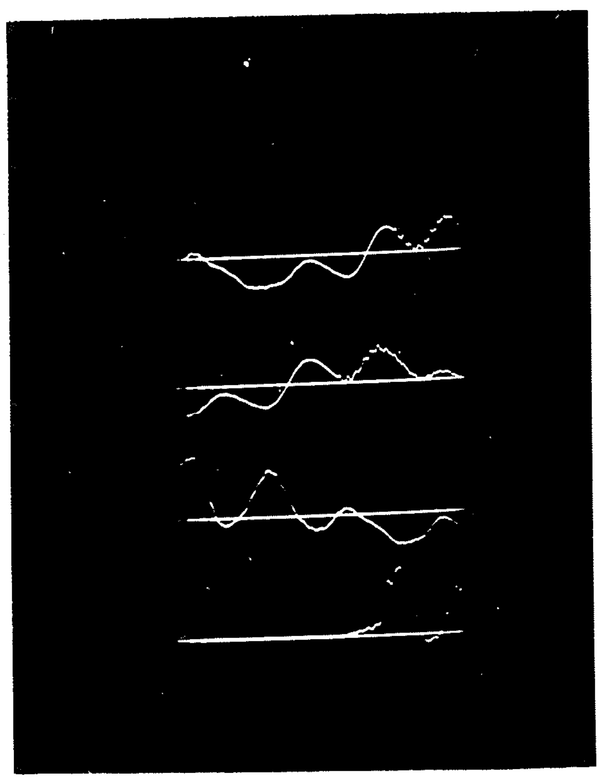

FIG 4-19-c
TIMING WAVE 10 MHz
CHARGE 31.5 KV
ATTENUATION 100%

FIGURE 4-19 VOLT-TIME OSCILLOGRAMS

gap was then placed in the circuit and all the leads attached. Oscillogram 4-19-b was obtained.

Notice that the rise is very fast and very linear. The 60 mm gap oscillation on the rise is still evident but does not seriously effect the linearity of the rise. It was felt that these oscillations would not significantly affect the calibration. A series of calibration oscillograms was then taken which will be shown and discussed in Chapter V.

Attempts were made to reduce the rate of rise by means of series resistors. Placing a series resistor in the circuit drastically increases the oscillations on the front. The wave in fact deteriorates to the point where it is of no value. The damping resistor required to dampen the oscillations would be so large that the wave front would be greatly lengthened and the resulting energy requirements for a linear rise would be greater than that available.

The oscillations on the front can be best shown to be caused by the 60 mm gap comparing oscillograms 4-13-a and 4-13-b with 4-14-a and 4-14-b. The oscillations do not appear on oscillogram 4-13-a and 4-13-b when the 60 mm gap is not included. They do however appear on oscillograms 4-14-a and 4-14-b when the gap is included. This argument is strengthened by the fact that if a rod gap is used to replace the

60 mm gap the waveform is clear of oscillations. This can be seen from oscillogram 4-19-c. The capacitance between rods and from the rods to ground is much less than for spheres and the oscillation on the rise would therefore not be developed.

As a result of the foregoing it was found that, with the loading capacitor available, the circuit as shown in figure 4-20 would be the most suitable for calibrating the divider. This circuit includes no series resistors but does include the shield to reduce the stray pickup. There appears to be no easy way to eliminate the high frequency oscillation caused by the 60 mm gap. In any event the oscillation will not cause an appreciable error in the calibration results. Figures 4-21 and 4-22 are photographs of the final circuit arrangement developed.

In conclusion it is felt that an adequate calibration of a voltage divider for the higher rates of rise can be achieved with the developed circuit but for calibration using much lower rates of rise, a much larger loading capacitor would have to be available.

Chapter V will discuss the calibration of two dividers using the circuit developed in this chapter.

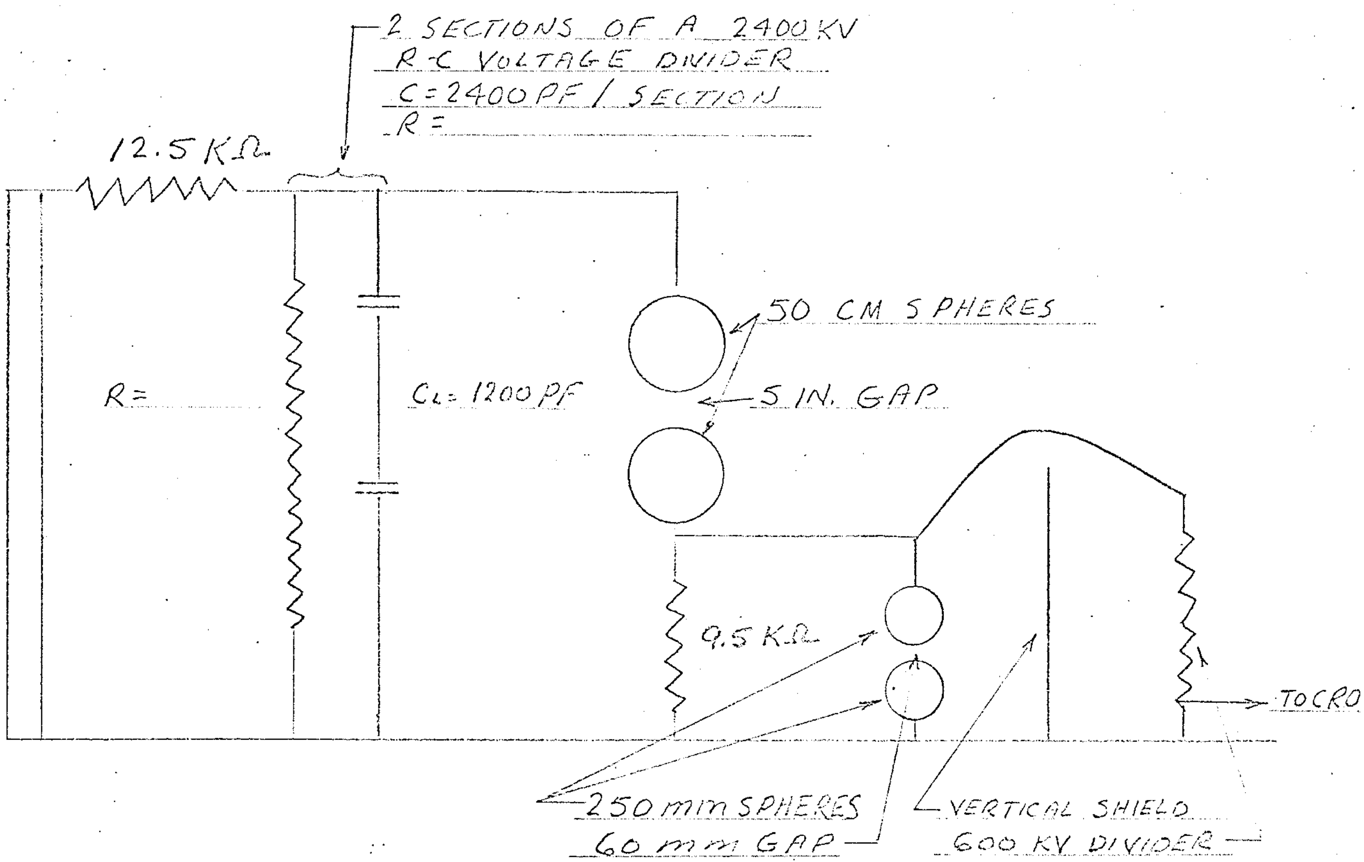

FIGURE 4-20

FINAL CIRCUIT ACHIEVED FOR THE DEVELOPEMENT OF LINEAR FAST RISING VOLTAGE WAVES

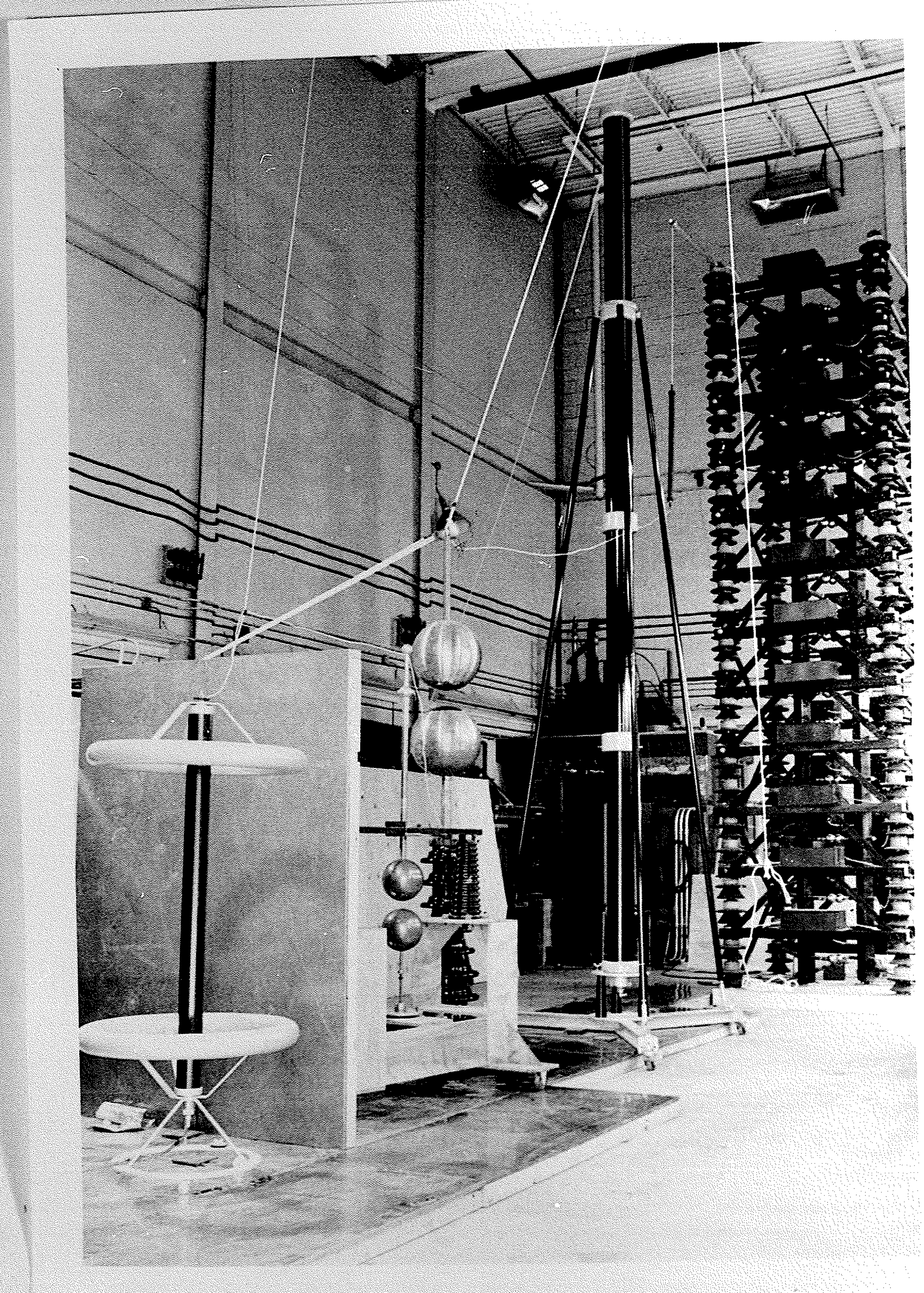

FIGURE 4-21

PHOTOGRAPH OF FINAL CIRCUIT ACHIEVED
FOR THE DEVELOPMENT OF LINEAR FAST RISING WAVES

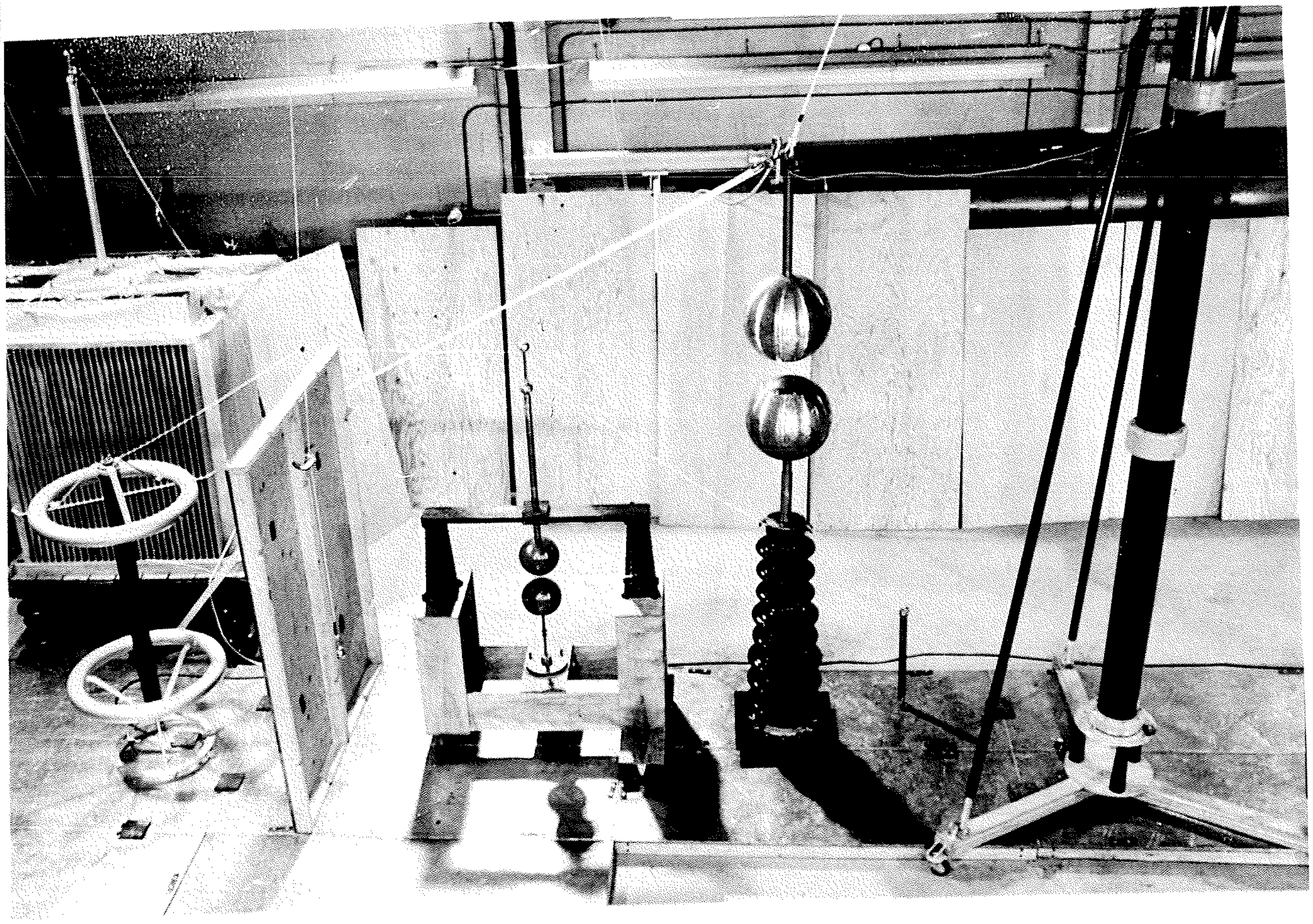

FIGURE 4-22

PHOTOGRAPH OF PART OF FINAL CIRCUIT ACHIEVED FOR THE DEVELOPMENT OF LINEAR FAST RISING WAVES

CHAPTER V

CALIBRATION OF A VOLTAGE DIVIDER USING THE VOLT-TIME CURVE

The response time of a voltage divider may be determined theoretically or experimentally as discussed in Chapter II. Since the theoretical approach is so complex, the experimental method is used in most cases. The experimental method involves the CIGRE volt-time curve shown on figure 2-3. To calibrate a divider by means of this volt-time curve, a linear rate of rise must first be obtained. As can be seen from Chapters III and IV, the development of a wave which has a linear rate of rise is difficult to obtain. Once a linear rate of rise is obtained, a series of oscillograms are taken for various rates of rise. These oscillograms are then analyzed and compared to the volt-time curve. This chapter will deal with the analysis of the oscillograms and the determination of the response time.

Analysis of the Oscillograms

The breakdown characteristics of a test object under an idealized linearly rising voltage can be expressed by the relationship between any two of the three quantities: rate of voltage rise, breakdown voltage and time to breakdown.

The CIGRE working group decided as follows: Two quantities, the peak voltage and the rate of rise of voltage are derived from each oscillogram. The peak voltage is the maximum amplitude recorded on the oscillogram. The rate of rise is the slope of the best fit straight line through that portion of the voltage rise which lies above the peak value of the power frequency breakdown voltage (Upf) of the gap. The best fit line is drawn in such a position that the positive and negative deviations between it and the recorded trace are equal.

The deviation from linearity is defined as the time interval between the two closest parallel lines which enclose the oscillation between Upf and the peak voltage and which have the same slope as the best fit straight line.

It is interesting to note that for most of the oscillograms that will be presented there is no measurable mean deviation. The mean deviation is probably somewhat dependent upon the quality of oscilloscope and camera used for recording the oscillogram. An inferior oscilloscope and camera would not record the high frequency oscillations in as much detail, and consequently, a smaller deviation would result.

For the CIGRE determination of the volt-time curve, it was suggested that an average of a series of tests be taken for each point on the volt-time curve. In this case it was felt that it would be more advantageous to plot the results of each point since many circuit changes and charging voltage changes were made throughout to attempt to achieve a linear rise.

In Chapter IV it was discovered that in order to make a full study of voltage dividers it would be necessary to have much more loading capacitance available. Since such was not the case, the divider could only be calibrated at the fastest rise time that could be achieved with the circuit components available. It is obvious therefore that much further work can be done on determining the response time of the divider used. With this thought in mind, attempts were not made to achieve maximum accuracy by including temperature and pressure corrections. In any event the air density correction factor would not likely exceed 2%.

Determination of the Response Time

Once the time to breakdown and rate of rise of voltage have been determined, it is a simple matter to determine the response time by means of the CIGRE volt-time curve. The experimentally determined time-to-breakdown is compared to that given by the CIGRE curve for the same rate of rise. The difference between these two values is the response time of the divider.

Calibration of a 600 KV Compensated High-Resistance Divider

The divider consists of a 46.2 KΩ resistor approximately 7 ft. long, mounted in an insulation tube. The divider has capacitance grading electrodes at the top and bottom to improve its response time (see figure 5-1-a).

The complete divider and oscillographic circuit is shown in figure 5-1-b. The divider ratio is 628/1. At several times throughout the testing described in chapters III and Iv data were taken for calibration of the divider.

The first set of data labelled A on page 95 and shown on the oscillograms of figures 5-3 and 5-4 were taken using the circuit of figure 5-2-a. If we assume that the response time of a voltage divider is constant for any rate of rise, the volt-time curve for the voltage divider in question will be a constant time increment below the CIGRE volt-time curve, shown on figure 2-2 and replotted on figure 5-5. If the test data are correct, they should form such a curve. In this case since the results as shown on figure 5-5 curve a do not form this curve, the results are therefore unsatisfactory. Even more obvious an indication is that the approximate response time indicated by these results is in the order of 900 nanoseconds. Since a

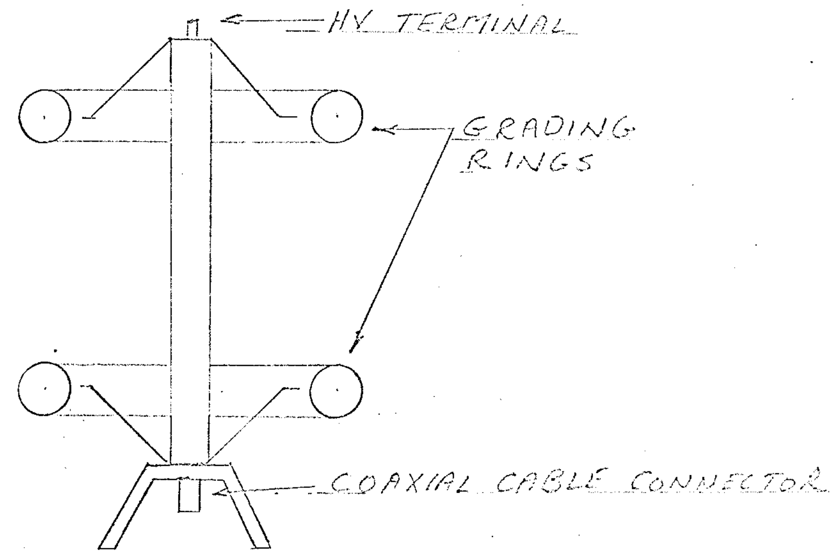

600 KV 46.2 KΩ HAEFLY DIVIDER

FIGURE 5-1-a

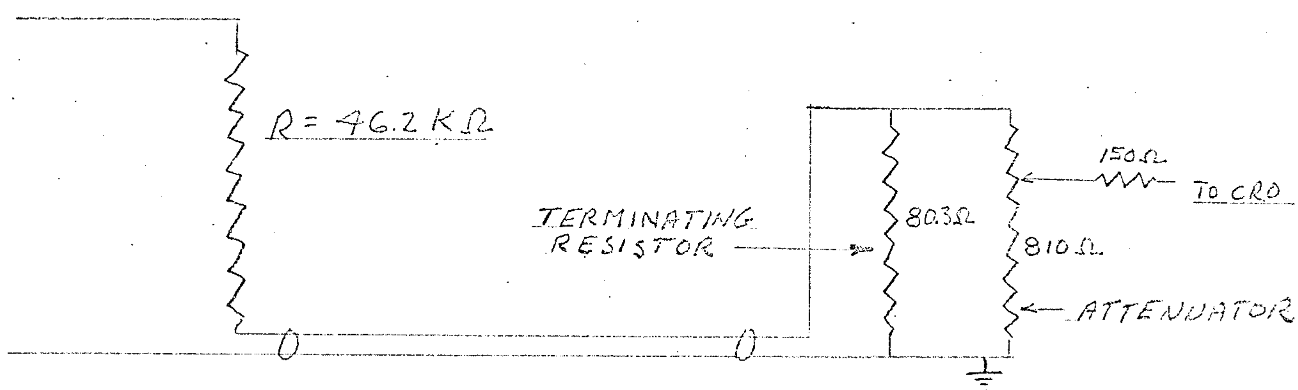

$$RATIO = \frac{46,200}{\frac{80.3 \times 810}{80.3 + 810}} = \frac{628}{1}$$

FIGURE 5-1-b

FIGURE 5-1

CONSTRUCTION DETAILS AND RATIO OF THE 600 KV HAEFLY VOLTAGE DIVIDER

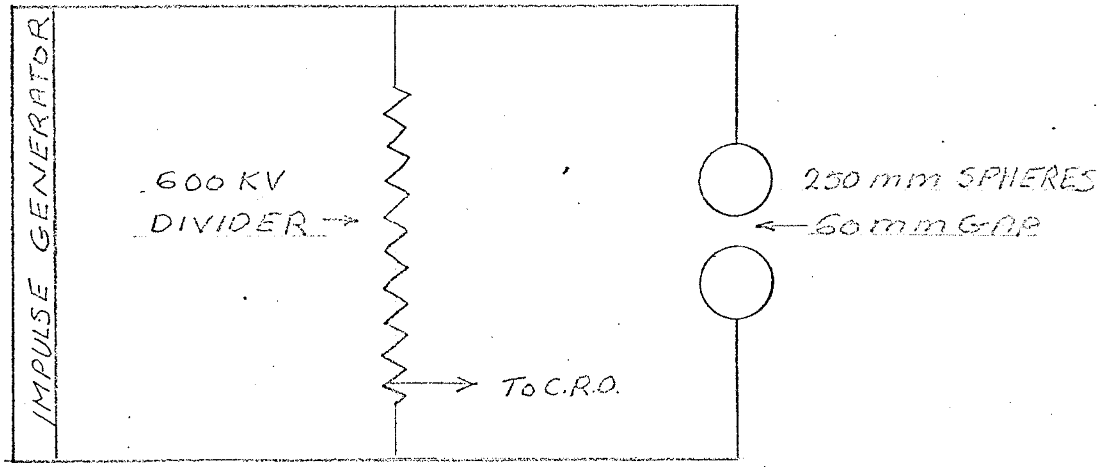

FIGURE 5-2-a

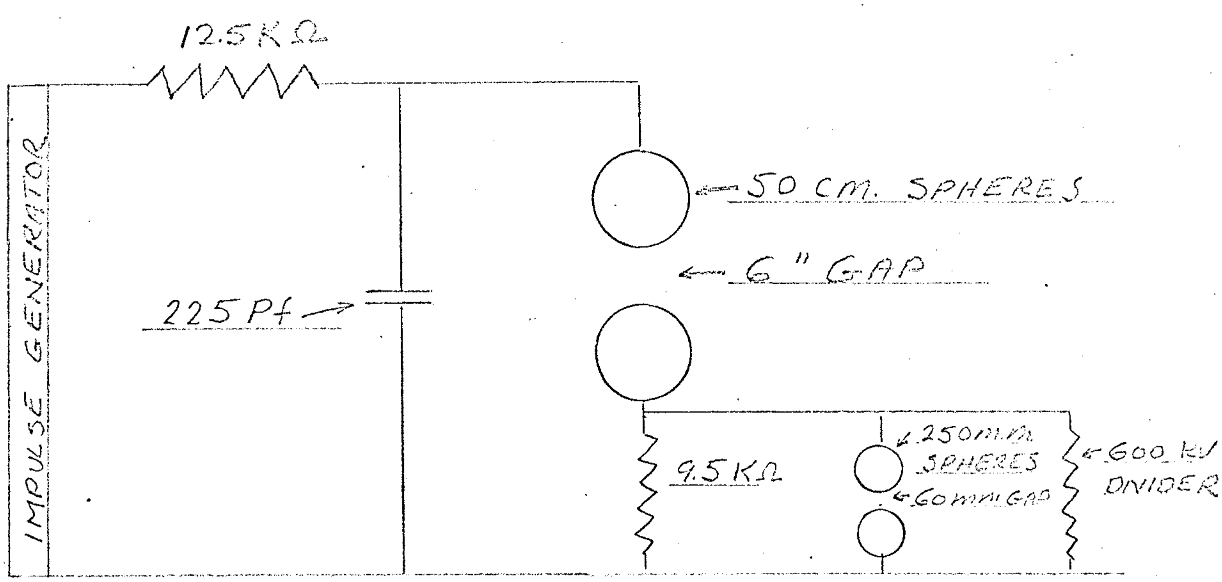

FIGURE 5-2-b

FIGURE 5-2 CIRCUITS USED FOR CALIBRATING THE 600 KV HAEFLY VOLTAGE DIVIDER

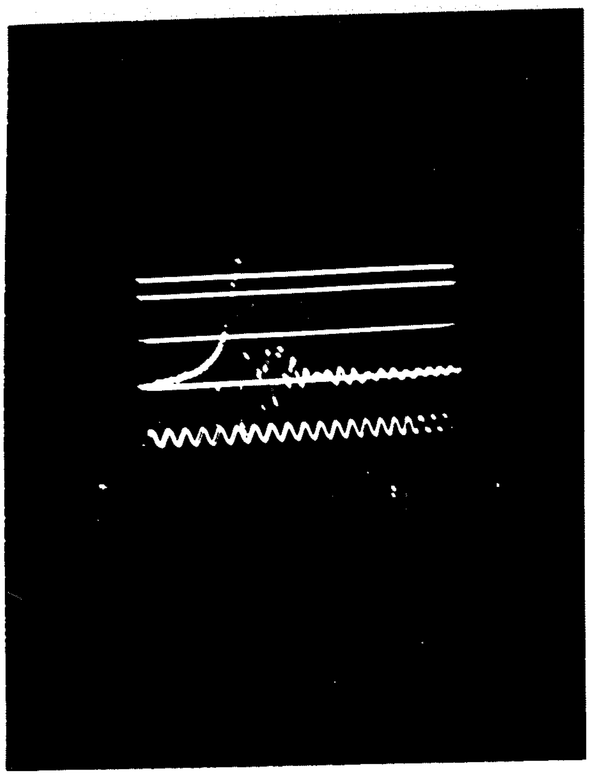

FIG 5-3-a
TIMING WAVE 10 MHz
CAL. 100, 200, 242
CHARGE 15 KV
ATTENUATION 100%

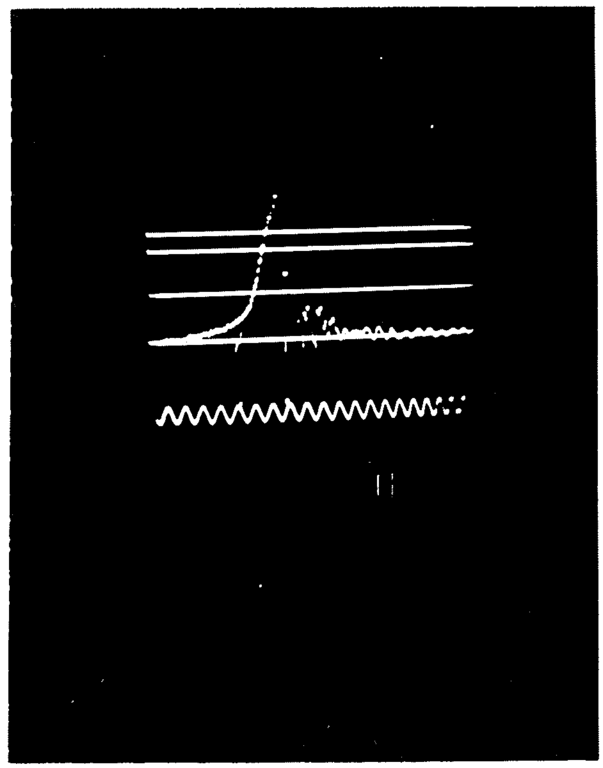

FIG 5-3-b
TIMING WAVE 10 MHz
CAL. 100, 200, 242 V
CHARGE 15 KV
ATTENUATION 100%

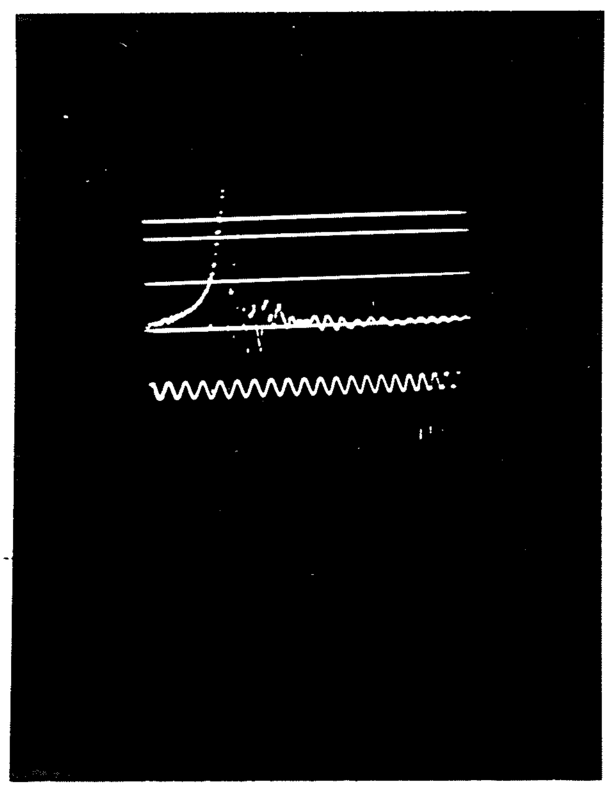

FIG 5-3-c
TIMING WAVE 10 MHz
CAL. 100, 200, 242
CHARGE 15 KV
ATTENUATION 100%

FIGURE 5-3 VOLT-TIME OSCILLOGRAMS

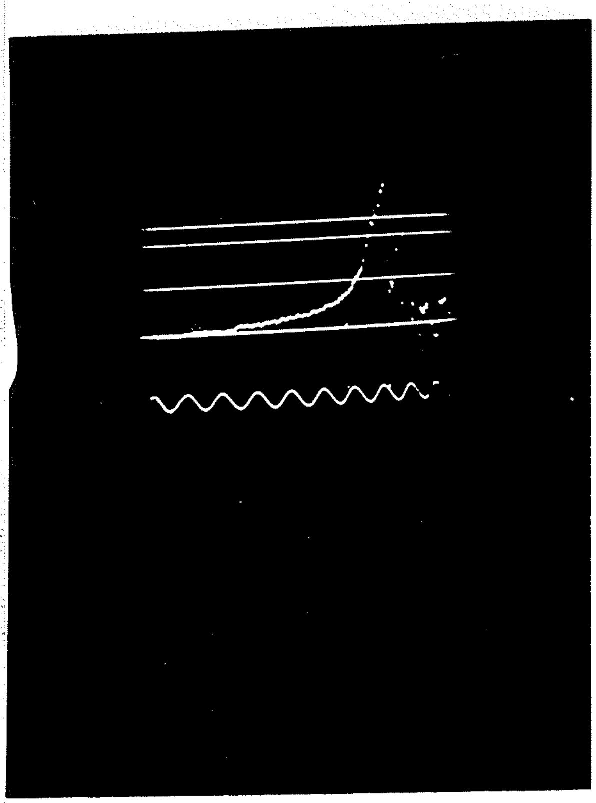

G 5-4-a
MING WAVE 10 MHz
L. 100, 200, 242
ARGE 20 KV
TENUATION 100%

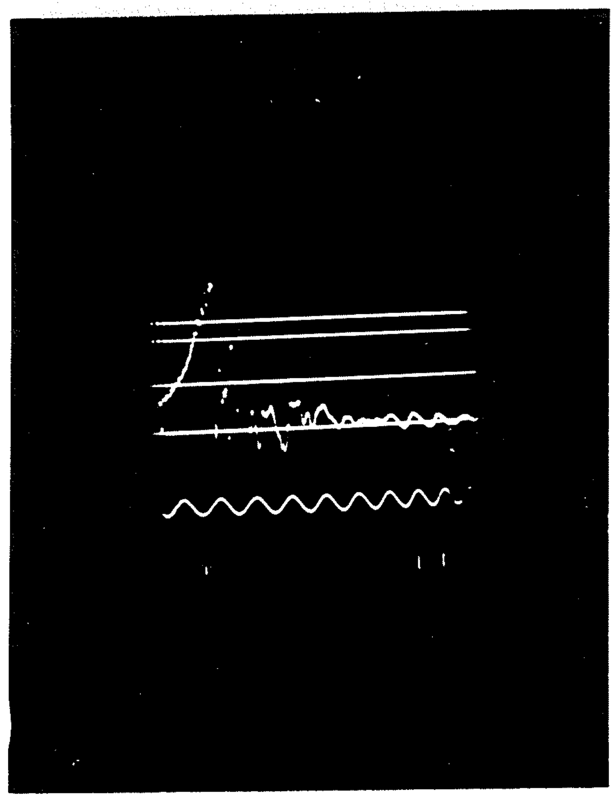

FIG 5-4-b
TIMING WAVE 10 MHz
CAL. 100, 200, 242 V
CHARGE 20 KV
ATTENUATION 100%

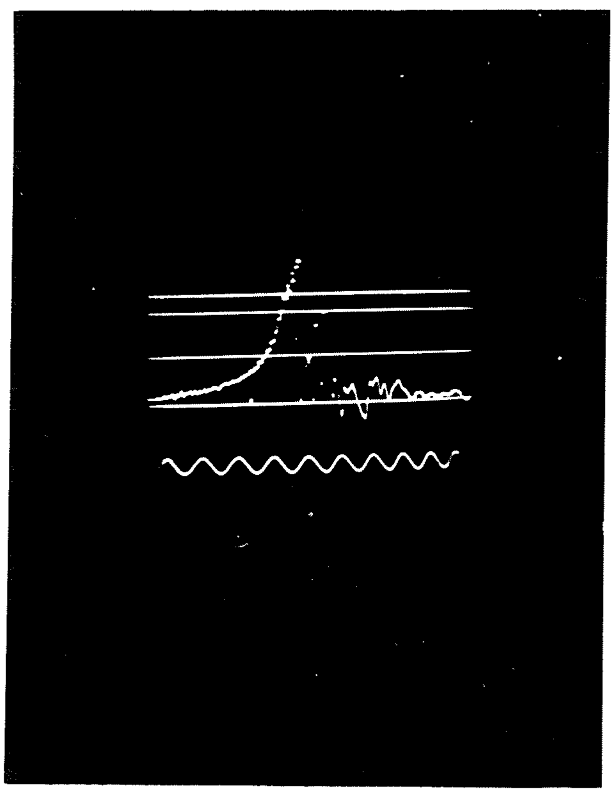

G 5-4-c
MING WAVE 10 MHz
L. 100, 200, 242
ARGE 20 KV
TENUATION 100%

FIGURE 5-4 VOLT-TIME OSCILLOGRAMS

FIGURE 5 - 5

SPHERE GAP VOLT-TIME CURVES

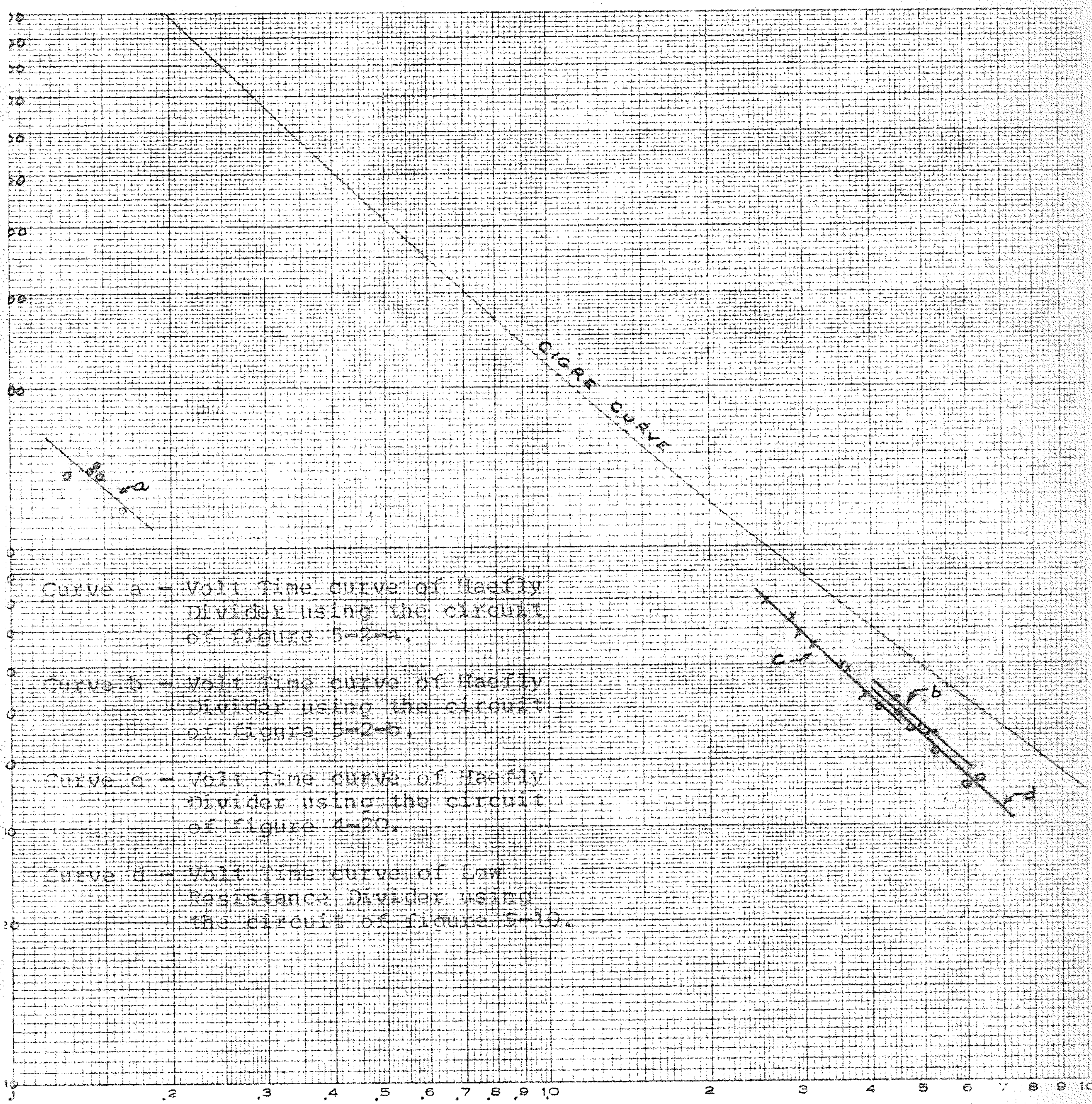

S - Rate of Rise (KV/Nanosecond)

divider of this type is known to have a very low response time (less than 50 nanoseconds) the results are obviously erroneous. This demonstrates the result of testing with a non-linear highly oscillatory rate of rise.

The second set of data labelled B on page 95 determined from oscillograms 5-6-a and 5-6-b were taken with the circuit shown on figure 5-2-b. The data are shown on figure 5-5 curve b. These results are quite consistent and show an extremely small response time of thirteen nanoseconds. Due to capacitive energy limitations combined with inconsistent stray coupling, it was very difficult to get a series of satisfactory traces. In most cases the stray coupling did not result in sufficient initial voltage to result in a linear rate of rise. This phenomenon was described in detail in Chapter III. The energy losses were also not consistent in that the losses due to corona on the various leads affected the output differently for each shot. With these points in mind only those oscillograms that rose to breakdown without a bend in the rise were used for calibration. A larger loading capacitor would be essential for a more detailed study.

The third set of data labelled C on page 95

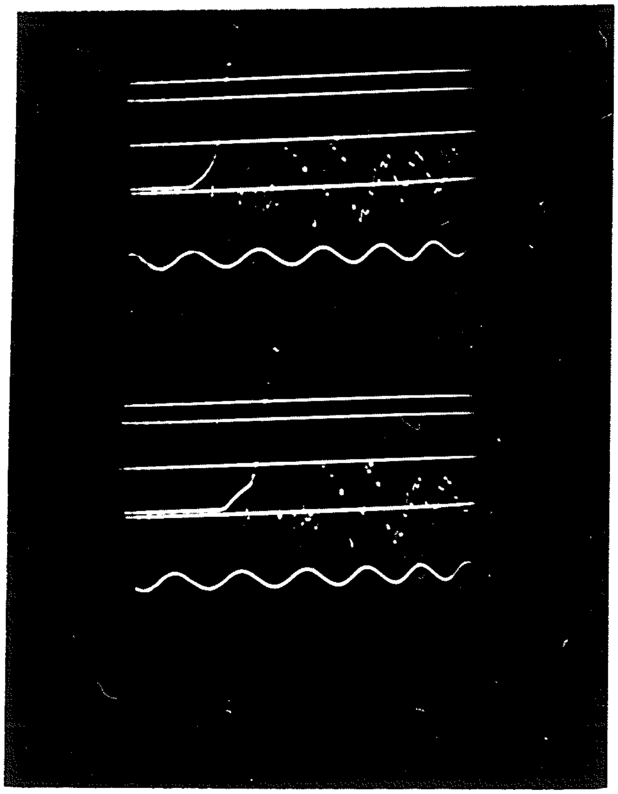

FIG 5-6-a
TIMING WAVE 10 MHz
CAL. 100, 200, 242
CHARGE 30 KV
ATTENUATION 100%

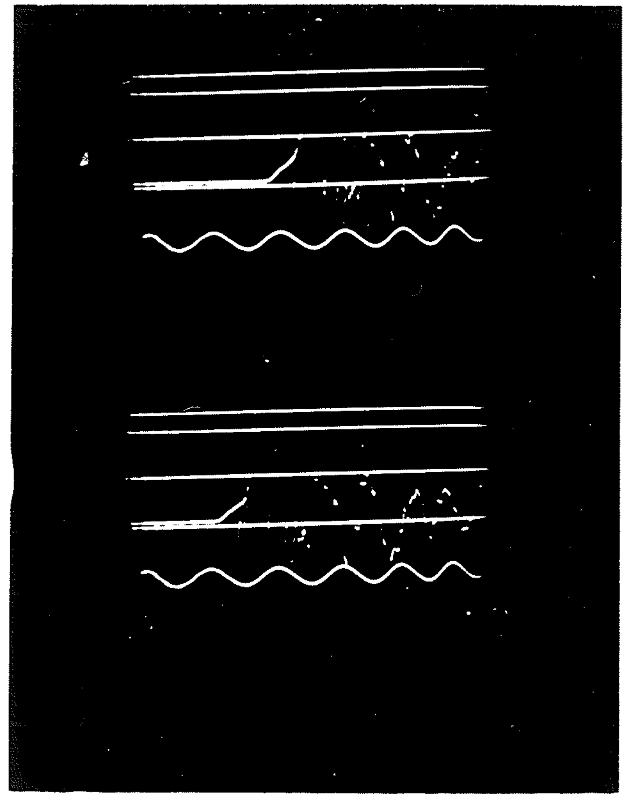

FIG 5-6-b
TIMING WAVE 10 MHz
CAL. 100, 200, 242
CHARGE 30 KV
ATTENUATION 100%

FIGURE 5-6 VOLT-TIME OSCILLOGRAMS

were taken using the circuit of figure 4-20. The oscillograms used in this case are shown on figures 5-7 and 5-8. The shield used in this case increases the response time by approximately three nanoseconds to sixteen nanoseconds as shown on figure 5-5, curve C. This is due to the increased ground capacitance resulting from the shield which bypasses more of the higher frequency components of the wave.

Calibration of a Low Resistance Uncompensated Divider

This divider consisted of four 100 ohm (nominal) non-inductive wire wound resistors. Each resistor was wound from number 30 wire on a 7/8 inch form and was 13½ inches long. The divider was constructed similar to the one described in detail in reference 13. The low resistance section of the divider was constructed using bifilar elements of 1/8 inch Karma ribbon .001 inches thick. "Karma" is the trade name for an alloy (W 1.73% + Cr 20% + AL + Fe) having a high resistivity and a low temperature coefficient of resistance. Sheet mylar insulation was placed between the adjacent sections. The resistance of this low voltage section is 1.06 ohms. Figure 5-9-b shows the dividing ratio to be 392 to 1. (See figure 5-9-a for the divider details.)

Figure 5-10 shows the circuit used for calibrating the divider. Notice that the divider was

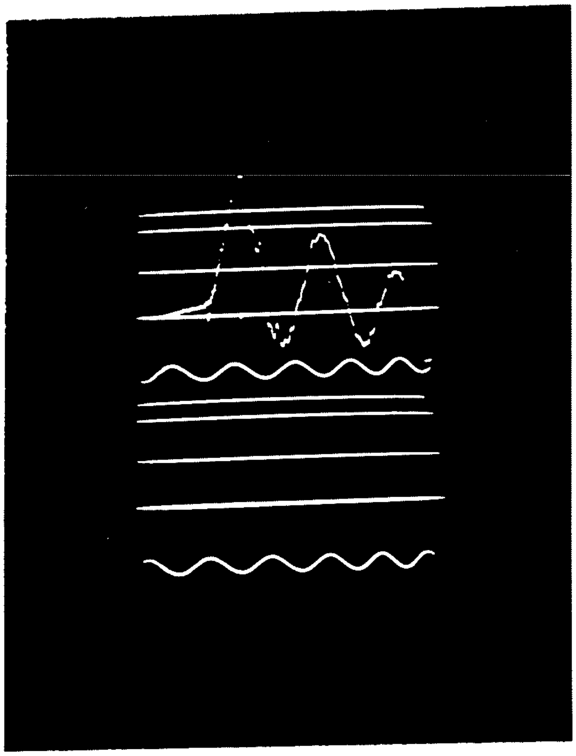

FIG 5-7-a
TIMING WAVE 10 MHz
CAL. 100, 200, 242
CHARGE 26 KV
ATTENUATION 100%

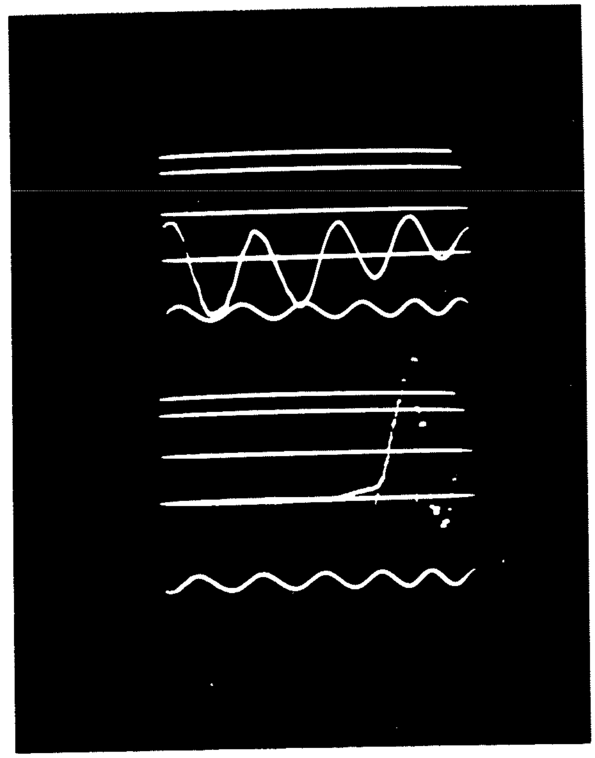

FIG 5-7-b
TIMING WAVE 10 MHz
CAL. 100, 200, 242 V
CHARGE 33 KV
ATTENUATION 100%

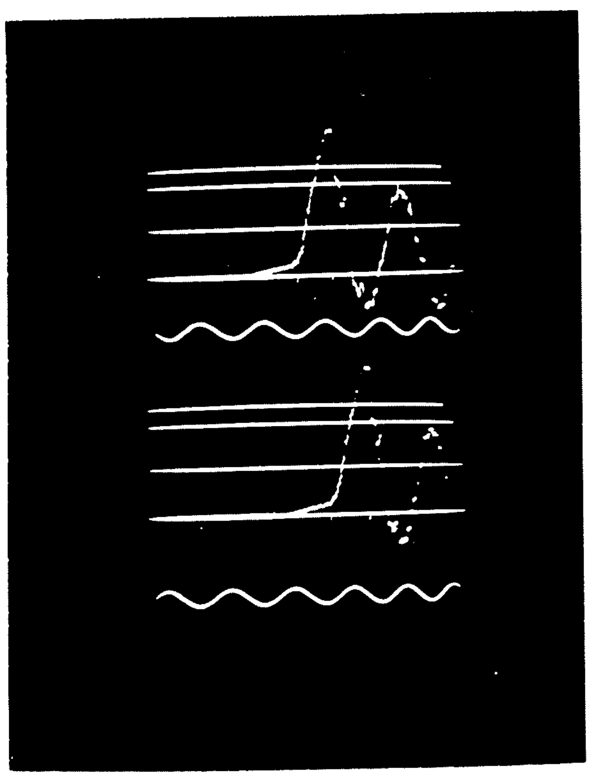

FIG 5-7-c
TIMING WAVE 10 MHz
CAL. 100, 200, 242
CHARGE 33 KV
ATTENUATION

FIGURE 5-7 VOLT-TIME OSCILLOGRAMS

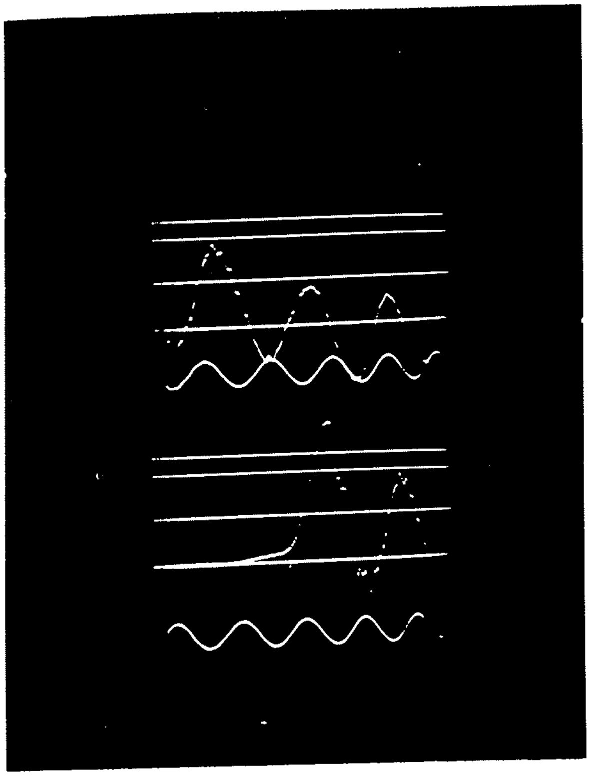

FIG 5-8-a
TIMING WAVE 10 MHz
CAL. 100, 200, 242
CHARGE 31.5 KV
ATTENUATION 100%

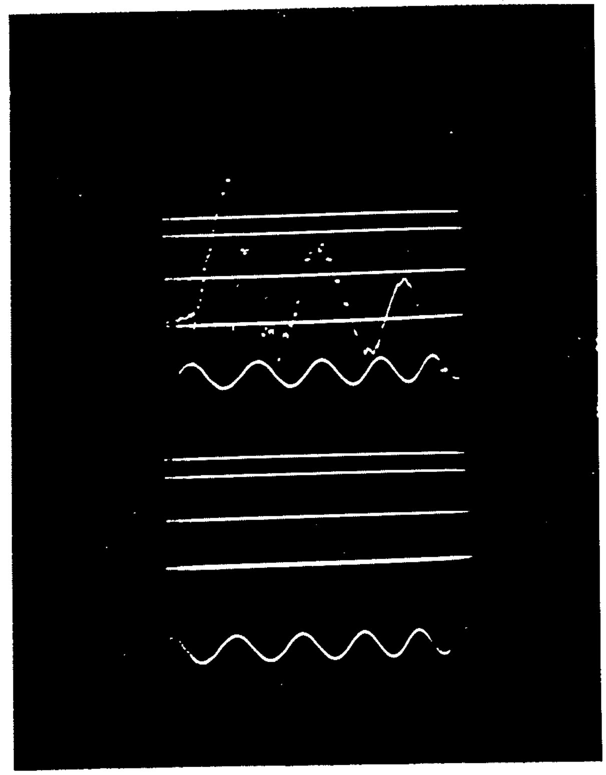

FIG 5-8-b
TIMING WAVE 10 MHz
CAL. 100, 200, 242 V
CHARGE 31.5 KV
ATTENUATION 100%

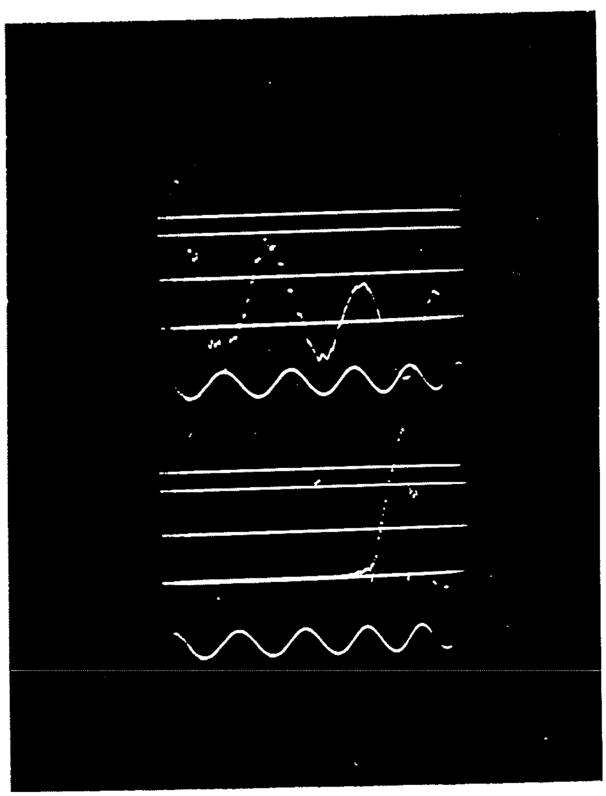

FIG 5-8-c
TIMING WAVE 10 MHz
CAL. 100, 200, 242
CHARGE 31.5 KV
ATTENUATION 100%

FIGURE 5-8 VOLT-TIME OSCILLOGRAMS

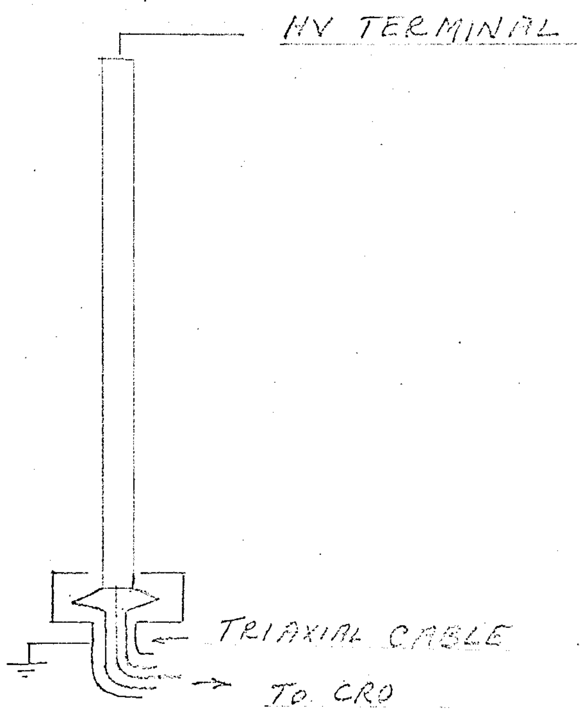

LOW RESISTANCE UNCOMPENSATED DIVIDER
FIGURE 5-9-a

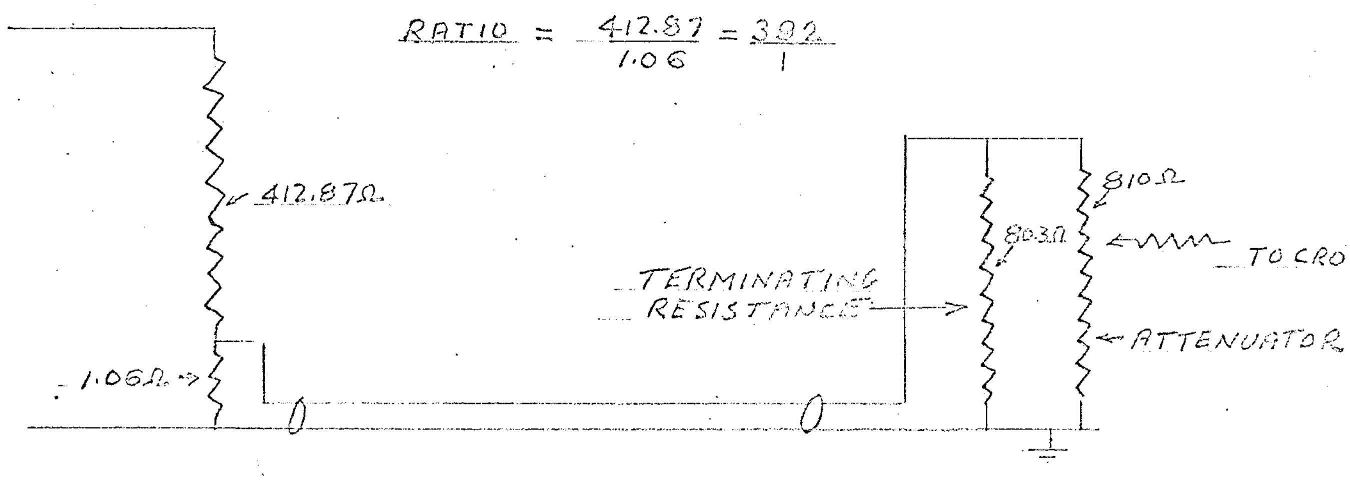

FIGURE 5-9-b

FIGURE 5-9 CONSTRUCTION DETAILS AND RATIO OF LOW RESISTANCE UNCOMPENSATED DIVIDER

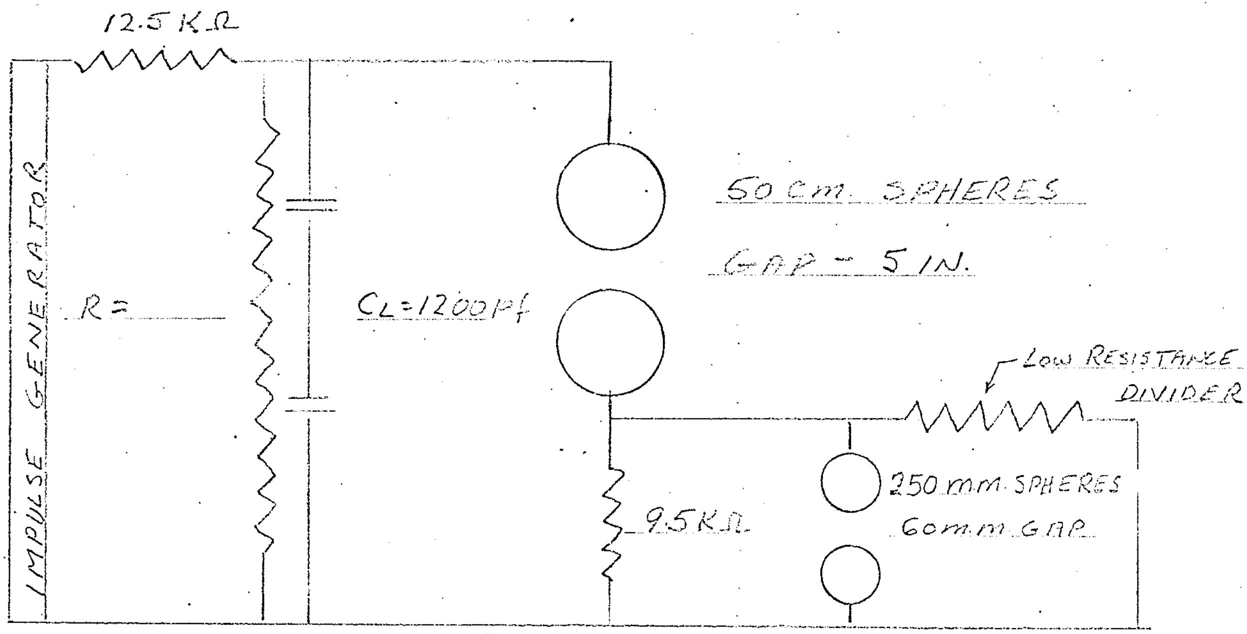

FIGURE 5-10.

CIRCUIT USED FOR CALIBRATING THE LOW RESISTANCE UNCOMPENSATED DIVIDER placed horizontally to the ground plane. This was done to minimize the high frequency capacitance ground currents and thus improve the divider response to the fast rising wave. The data taken on this divider are labelled D on page 95 and are shown on figure 5-5 curve d. The oscillograms used are shown on figures 5-11 and 5-12.

From figure 5-5 curve d it can be seen that the divider has a response time of fifteen nanoseconds. A low response time of this order would be expected for a divider of this type since the low resistance essentially minimizes the effect of any ground capacitance.

Most of the oscillograms used for calibration of the dividers include a 100 volt and a 200 volt calibration line and a 60 Hz breakdown voltage line which is equal to a calibration voltage of 242 volts for the attenuation used. The 100 volt and 200 volt lines were used to calibrate the peak voltage. The 60 Hz breakdown voltage line was to be used to calibrate if the rise was not linear but it was decided that only those waveforms that rose linearly throughout would be used.

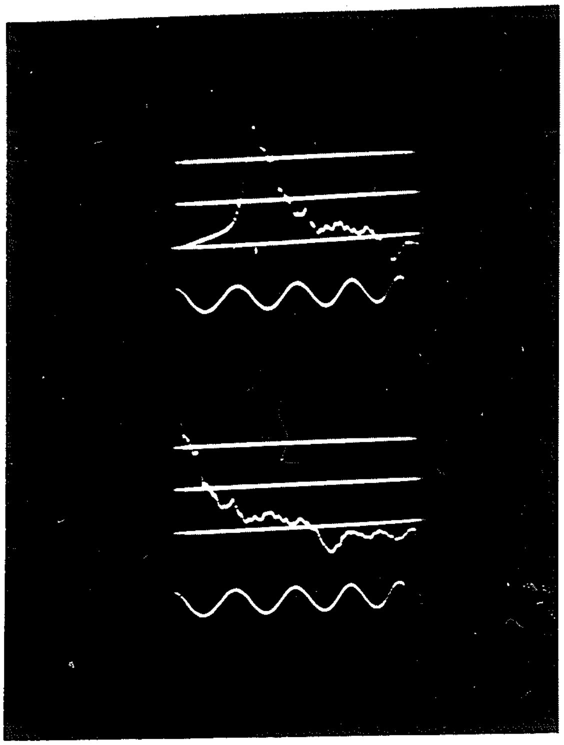

FIG 5-11-a
TIMING WAVE 10 MHz
CAL. 100, 200 V
CHARGE 37 KV
ATTENUATION 50%

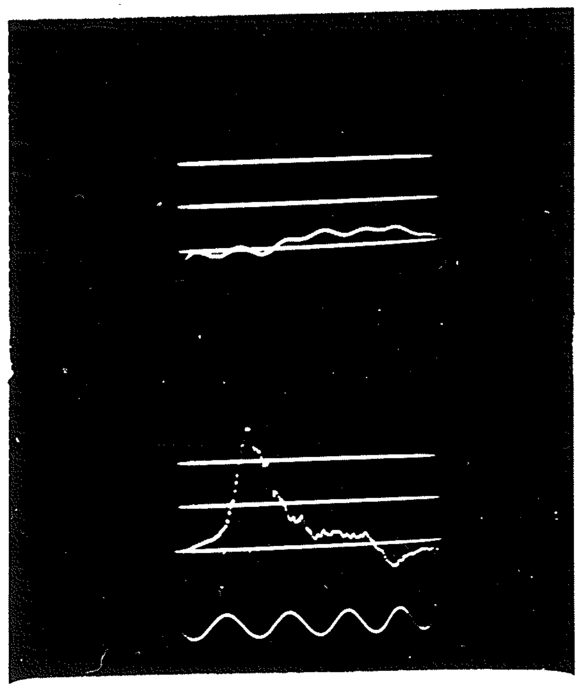

FIG 5-11-b
TIMING WAVE 10 MHz
CAL. 100, 200 V
CHARGE 37 KV
ATTENUATION 50%

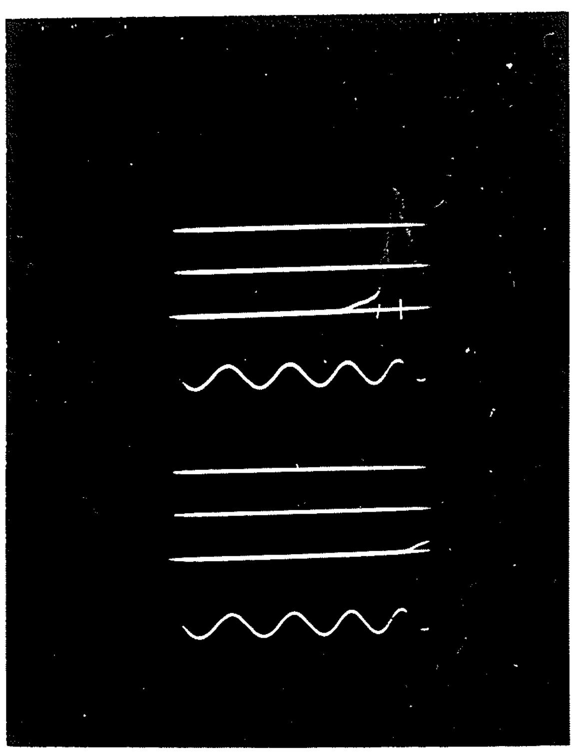

FIG 5-11-c
TIMING WAVE 10 MHz
CAL. 100, 200 V
CHARGE 34.5 KV
ATTENUATION 50%

FIGURE 5-11 VOLT-TIME OSCILLOGRAMS

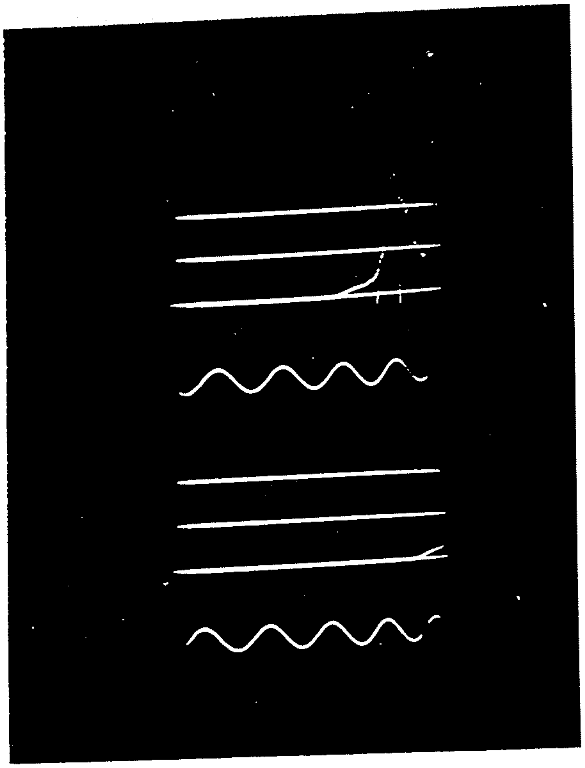

FIG 5-12-a
TIMING WAVE 10 MHz
CAL. 100, 200 V
CHARGE 34.5 KV
ATTENUATION 50%

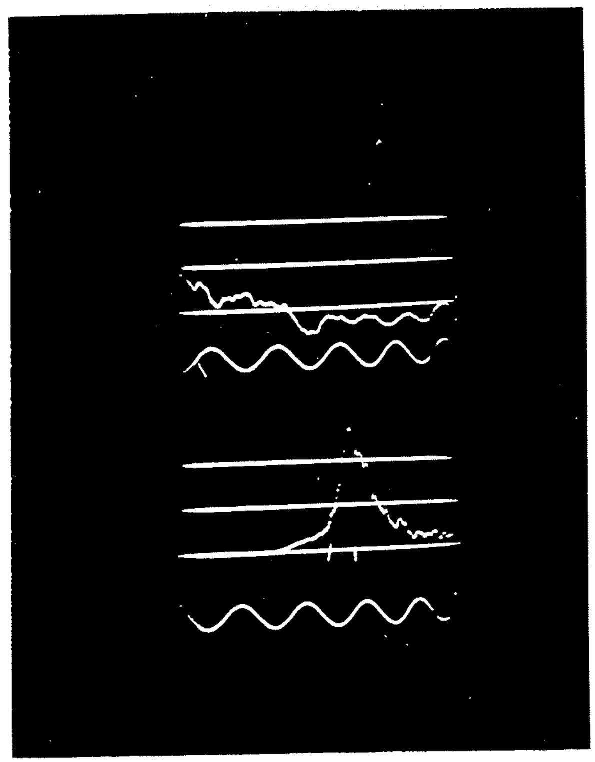

FIG 5-12-b
TIMING WAVE 10 MHz
CAL. 100, 200 V
CHARGE 34.5 KV
ATTENUATION 50%

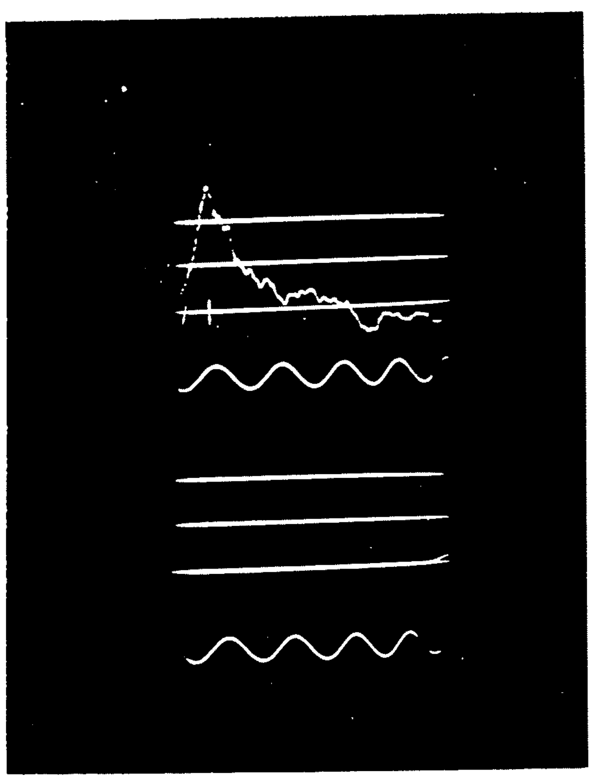

FIG 5-12-c
TIMING WAVE 10 MHz
CAL. 100, 200 V
CHARGE 34.5 KV
ATTENUATION 50%

FIGURE 5-12 VOLT-TIME OSCILLOGRAMS

TABLE I

	OSCILLOGRAM	SLOPE tan Θ	PEAK VOLTAGE (m.m.)	TIME TO BREAKDOWN (m.m.)	PEAK VOLTAGE (VOLTS)	PEAK VOLTAGE (KV)	TIMING OSC. (m.m.)	TIMING OSC. (Nanoseconds)	TIME TO BREAKDOWN (Nanoseconds)	KV/Nanosecond	REMARKS
	5-3-a	.517	15.50	3.00	282.5	177.5	2.15	100	139.5	.127	
	5-3-b	.327	18.95	5.80	345.0	217.0	2.15	100	270.0	.081	
	5-3-c	.668	17.05	2.55	309.0	194.0	2.15	100	118.5	.164	Circuit Fig 5-2-a
A	5-4-a	.328	17.55	5.35	319.0	200.5	3.65	100	146.5	.137	Results Curve A Fig 5-5
	5-4-b	.278	18.05	6.50	328.0	206.0	4.55	100	143.0	.144	
	5-4-c	.278	17.20	6.20	313.0	197.0	4.40	100	141.0	.140	
	5-6-a-1	.586	20.20	3.45	370.0	232.0	7.80	100	44.3	5.24	
	5-6-a-2	.490	19.80	4.05	363.0	228.0	7.90	100	51.3	4.45	Circuit Fig 5-2-b
B	5-6-b-1	.562	19.95	3.55	364.0	228.5	7.75	100	45.8	4.98	Results Curve A Fig 5-5
	5-6-b-2	.563	20.00	3.55	365.0	229.0	7.90	100	45.0	5.09	
	5-7-a	.445	18.05	4.05	327.0	205.5	7.75	100	52.3	3.93	
	5-7-b	.354	17.50	4.95	317.0	199.5	6.30	100	78.6	2.54	
	5-7-c-1	.413	18.15	4.40	330.0	207.5	7.45	100	59.0	3.51	Circuit Fig 4-20
C	5-7-c-2	.373	18.25	4.90	332.0	208.5	6.70	100	73.0	2.86	Results Curve C Fig 5-5
	5-8-a	.346	17.45	5.05	317.0	199.5	7.40	100	68.3	2.92	
	5-8-b	.380	18.25	4.80	337.0	212	8.20	100	58.5	3.62	
	5-8-c	.412	17.90	4.35	325.0	204	6.70	100	65.0	3.14	
	5-11-a	.543	15.20	2.80	276.0	217	7.90	100	35.4	6.14	
	5-11-b	.466	15.40	3.30	280.0	220	8.00	100	41.3	5.33	
D	5-11-c	.498	14.70	2.95	262.0	206	6.00	100	49.3	4.18	Circuit Fig 5-10
	5-12-a	.530	15.10	2.85	277.0	218	6.30	100	45.2	4.84	Results Curve D Fig 5-5
	5-12-b	.489	15.40	3.15	280.0	220	6.50	100	48.5	4.54	
	5-12-c	.506	15.45	3.05	282.0	222	8.40	100	36.3	6.30	

CHAPTER VI

CONCLUSIONS

The two main methods of determining the response time of a voltage divider are the step response method and the volt-time curve method. Since the step response method is a lengthy and difficult method, it is not satisfactory for the normal laboratory.[5]

Utilization of the volt-time curve to determine the response time of a voltage divider is an accurate and comparatively easy procedure. The use of the volt-time curve is based on the fact that a voltage divider can accurately record a rate of rise providing the rate of rise lasts long enough. For the same rate of rise the difference between the experimentally determined time to breakdown and that given by the CIGRE curve is the response time of the voltage divider.

According to the U.S. Bureau of Standards (Park and Cones) the rate of rise need be linear only above the power frequency breakdown voltage of the gap.[13]

Attempts at achieving a linear rate of rise over the complete rise were made here to permit a complete study of the oscillations developed.

The conclusions for this thesis can best be presented in itemized form.

1. The response time of a divider can be considered, in most cases, to be a sufficient criterion of the voltage divider accuracy.
2. The impulse generator itself can be used to achieve a fairly low rate of rise if sufficient loading capacitance is available. For fast rates of rise however, a series gap must be used.
3. When using the series gap method, if only a fairly low value of loading capacitance is available, it is difficult to get good results for any but the highest rates of rise since the energy availability is such that any series resistance will cause a non-linear rise.
4. Increasing the load capacitance will allow for a decreased rate of rise since series resistors can be used, will allow for damping resistors to eliminate oscillation and will allow the use of a filtering circuit.
5. The series gap must be adjusted to provide sufficient overvoltage to the 60 mm gap to ensure that it breaks down on the front of the wave.

6. The series gap must also be adjusted so that the impulse generator output voltage is sufficiently high to cause breakdown on the front of the wave. This is particularly important in synchronizing the waveform with the oscilloscope sweep.
7. A series resistor must be placed between the generator and the loading capacitor to isolate the generator from the main circuit. Its resistance should be high enough to cause a fairly slow voltage rise across the series gap and thereby create a high series gap impedance and accordingly a low voltage across the divider before the gap breaks down.
8. The resistance between the series gap and ground depends on the series resistor from the generator to the loading capacitor. If its resistor is high the resistance from the series gap to ground can be quite high. If the series resistor is low, the resistor from the series gap to ground should be low. The intent is to minimize the voltage appearing across the divider before the series gap breaks down.
9. The approximate frequencies of the oscillations developed in the circuit are calculable as shown in the Appendices.

10. To reduce the frequency of the oscillations the loop inductance and the gap capacitances must be minimized. The loops must therefore be as small as possible. The gap capacitance can be reduced by raising the spheres as high off the ground plane as is practicable without increasing the loop induc ance significantly.
11. Reducing the oscillations by means of damping resistors is impossible for fast rates of rise since the resistors required are too large to maintain a high rate of rise.
12. The 60 mm gap introduces a high frequency oscillation which is impossible to eliminate without seriously altering the circuit characteristics. The series gap introduces a 10 MHz oscillation which is transferred into the divider circuit by the stray coupling mentioned in 13.
13. Stray coupling which exists between the series gap and the voltage divider can be substantially reduced by means of a shield. The shield, however, increases the response time.
14. The high resistance compensated divider has a response time of approximately thirteen nanoseconds.
15. The low resistance divider also has a low

response time (approximately sixteen nanoseconds). It can be used however only for short duration work due to the limited divider size.

CHAPTER VII

FUTURE WORK

An extension of the work carried out in this thesis is possible if adequate capacitors are available. With the circuit conditions essential for a linear rate of rise discovered in the work, a complete calibration of the voltage divider mentioned over a wide range of rates of rise would be possible. This should be done to determine the divider response time more accurately.

The calibration of dividers with a very large response time should also be carried out since this type of divider is the type most often used in industry.

Once the divider response time is accurately determined, a study of fast changing voltages, such as the collapse of the voltage across a rod gap, can be made. This is an essential study in the view of the power transformer designers since the required insulation strength of the power transformer is so completely dependent on the time-of-chop of a rod gap. This study will not be simple but a complete understanding of the voltage divider would greatly simplify the problem.

APPENDIX I

CALCULATION OF LOOP INDUCTANCES AND SPHERE GAP CAPACITANCES

Many of the oscillations measured on the oscillograms of Chapters III and IV are due to loop inductances and sphere gap capacitances. This section shows how these loop inductances and sphere gap capacitances can be estimated.

Calculation of Inductances

(i) Equation for loop inductance.[1]

The inductance of a rectangle of length a and breadth b made of wire of radius r is

$$L = \frac{2303}{10^9}\left[4(a+b)\log_{10}\frac{2a}{r} - 4a\log_{10}\frac{(a+d)}{b} - 4b\log_{10}\frac{(b+d)}{b}\right] + \frac{1}{10^9}\left[8(d+r) - 7(a+b)\right] \text{ hy}$$

Where $d = \sqrt{a^2 + b^2}$

and a,b and r are in centimeters.

(ii) Equation for the inductance of a single line to ground.[2]

$$L = 2 \times 10^{-7} \ln \frac{D}{r_1 e^{-\frac{1}{4}}} \quad \text{hy/metre}$$

1. Standard Handbook for Electrical Engineers. Seventh Edition, p. 53.

2. Elements of Power Systems - William D. Stevenson Jr., McGraw-Hill - P. 25

Where D is the distance from the line to ground in metres and r is the radius of the conductor in metres, now consider circuit A1 which was the circuit used for the set of data labelled C on page 95

In this circuit there are 5 loops labelled A, B, C, D and E and 4 lines labelled a, b, c, d and e. Using the above equations the inductance of the loops and lines are calculated to be:

Loop A	-	$34\frac{1}{2}$ μh
Loop B	-	18 μh
Loop C	-	$10\frac{1}{2}$ μh
Loop D	-	12 μh
Loop E	-	8 μh
Line a	-	$5\frac{1}{2}$ μh
b	-	$3\frac{1}{2}$ μh
c	-	$2\frac{1}{2}$ μh
d	-	$2\frac{1}{2}$ μh
e	-	1 μh

Calculation of Capacitances [1]

i) Equation for the capacitance between spheres.

For 2 equal spheres of radius r (cm) at a distance d (cm) apart the charge per unit

1. Static and Dynamic Electricity - R.W. Smythe (McGraw Hill)

voltage is

$$Q = -4\pi\epsilon r \sinh\beta \sum_{n=1}^{\infty} \operatorname{Csch}(2n\beta)$$

where $\cosh\beta = \frac{d}{2r}$

Therefore, $C = \frac{Q}{V} = \frac{Q}{1} = -4\pi\epsilon r \sinh\beta \sum_{n=1}^{\infty} \operatorname{Csch}(2n\beta)$

ii) Equation for the capacitance of a sphere to ground.

For a sphere of radius r (cm) at a distance d (cm) from the ground plane the charge per unit voltage is

$$Q = 4\pi\epsilon r \sinh\alpha \sum_{n=1}^{\infty} \operatorname{Csch} n\alpha$$

where $d = a \cosh\alpha$

Therefore, $C = \frac{Q}{V} = \frac{Q}{1} = 4\pi\epsilon r \sinh\alpha \sum_{n=1}^{\infty} \operatorname{Csch} n\alpha$

Now consider circuit A1 once again.

Using the above equations

Capacitance between two 50 cm spheres 6 inches apart = 13 pf

Capacitance between two 25 cm spheres 60 mm apart = 7 pf

Capacitance between a 50 cm sphere and ground 8½ feet apart = 28 pf

Capacitance between a 25 cm sphere and ground 3½ feet apart = 14 pf

The values of inductance and capacitance calculated in this section are at best approximations. They are sufficiently accurate however to calculate various resonant frequencies that exist in the circuit.

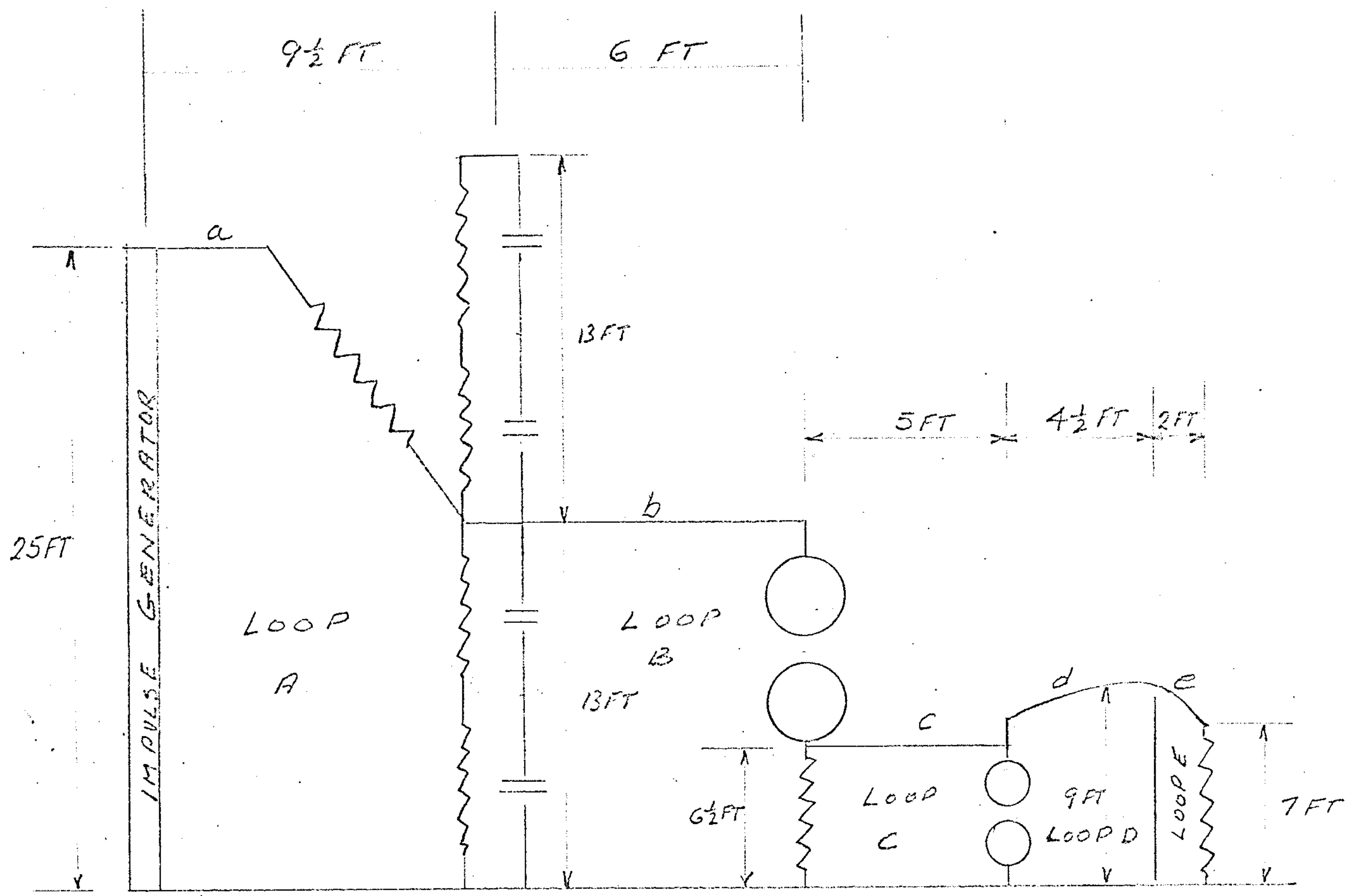

FIGURE A-1

CIRCUIT USED FOR ESTIMATING LOOP INDUCTANCES AND LINE CAPACITANCES

APPENDIX II

CALCULATION OF RESONANT FREQUENCIES
AND CRITICAL DAMPING RESISTANCES

This section shows the calculation of the resonant frequencies resulting from the capacitances and inductances calculated in Appendix I. Also shown is the critical resistance that would be required to damp out each of the oscillations.

The resonant frequency is given by

$$f = \frac{1}{2\pi\sqrt{LC}}$$

The critical damping resistance is given by

$$R = 2\sqrt{\frac{L}{C}}$$

A resonant frequency could result from any of the following combinations:

1. Inductance of loop A and line a with the capacitance of the loading capacitance.
2. Inductance of loop B and line b with the capacitance of the loading capacitance.
3. Inductance of loop B and line b with the capacitance of the series gap and of the series gap to ground.
4. Inductance of loop C and line c with the capacitance of the series gap and of the series gap to ground.

5. Inductance of loop C and line c with the capacitance of the 60 mm gap and of the 60 mm gap to ground.

6. Inductance of loop D and line d with the capacitance of the 60 mm gap and of the 60 mm gap to ground.

Estimation of Parameters

In order to calculate the resonant frequencies it is necessary to estimate the parameters to be used since they are normally combinations of two of the calculated parameters. They are also calculated using idealized conditions. For example, all the loops are not true loops but rather are loops made of circuit components. With this in mind the following estimates are at best approximations but most likely result in fairly representative values.

Inductance of loop A combined with line a (LA-a) equals 30 μh

also LB - b = 15 μh

LC - c = 10 μh

LD - d = 10 μh

The capacitance of the loading capacitance is of course known:

C_1 = 1200 pf

The capacitance of the series gap combined with the capacitance of the series gap to ground.

$C_2 \;=\; 25$ pf

The capacitance of the 60 mm gap combined with the capacitance of the 60 mm gap to ground

$C_3 \;=\; 15$ pf

Calculation of Resonant Frequencies

$$f_1 = \frac{1}{2\pi\sqrt{L_{A-a} C_1}} = 1.2 \text{ Mhz}$$

$$f_2 = \frac{1}{2\pi\sqrt{L_{B-b} C_1}} = 1.7 \text{ Mhz}$$

$$f_3 = \frac{1}{2\pi\sqrt{L_{B-b} C_2}} = 8.3 \text{ Mhz}$$

$$f_4 = \frac{1}{2\pi\sqrt{L_{C-c} C_2}} = 10 \text{ Mhz}$$

$$f_5 = \frac{1}{2\pi\sqrt{L_{C-c} C_3}} = 13 \text{ Mhz}$$

$$f_6 = \frac{1}{2\pi\sqrt{L_{D-d} C_3}} = 13 \text{ Mhz}$$

The above frequencies are basically those estimated before either of the gaps break down. After the series gap breaks down there is still a significant capacitance from the bottom sphere to ground. Hence oscillations may still be developed. When the 60 mm gap breaks down, the capacitance of the gap is essentially eliminated.

Calculation of Critical Damping Resistance

$$R_1 = 2\sqrt{\frac{L_{A-a}}{C_1}} = 306 \text{ ohms}$$

$$R_2 = 2\sqrt{\frac{L_{B-b}}{C_1}} = 224 \text{ ohms}$$

$$R_3 = 2\sqrt{\frac{L_{B-b}}{C_2}} = 1540 \text{ ohms}$$

$$R_4 = 2\sqrt{\frac{L_{C-c}}{C_2}} = 1260 \text{ ohms}$$

$$R_5 = 2\sqrt{\frac{L_{C-c}}{C_3}} = 1640 \text{ ohms}$$

$$R_6 = 2\sqrt{\frac{L_{D-d}}{C_3}} = 1640 \text{ ohms}$$

In order to retain the fast rise which was made necessary by the limited loading capacitance available, these damping resistors are prohibitive. The use of any one of these resistors would decrease the rate of rise substantially and would also result in a non-linear rise.

REFERENCES

1. Creed, F.C. and Collins, M.M.C. "The Measurement of Short-Duration Impulse Voltages". I.E.E.E. Trans. on Communications and Electronics, Vol. 82, 1963 pp. 621-629.

2. Creed, F.C.: "Sphere Gap Volt-Time Curves". Bulletin of the Radio and Electrical Engineering Division, National Research Council of Canada, October-December, 1964, Vol. 14, No. 4, pp. 8-14.

3. Creed, F.C.: "Impulse Measurement in the Time Scale Below 0.5 Microseconds". C.I.G.R.E. Paper No. 328, 1964, Appendix III.

4. Creed, F.C.: "NRC Results for CIGRE Volt-Time Curve Study" - 1965. Unpublished.

5. Creed, F.C., Kawamura, T., and Newi, G.: "The Step Response of Measuring Systems for High Impulse Voltages". I.E.E.E. Paper 67-90, 1967

6. Creed, F.C.: "Step Response of High-Voltage Impulse Measuring Systems". Bulletin of the Radio and Electrical Engineering Division, National Research Council of Canada, October-December, 1966, Vol. 16, No. 4, pp. 46-50.

7. Creed, F.C.: "The Measurement Problem in Impulse Testing". E.H.V. Symposium, Winnipeg, Manitoba, September 1966.

8. Schwab, A.: "Measurement of High Impulse Voltages in the Range of Nanoseconds". Arch. Tech. Messen (A.T.M.), No. 360, pp. 9-12, January, 1966.

9. Tropper, H.: "Recording of Impulse Voltages - Theoretical and Experimental Investigation of Sources of Error Introduced by the Measuring Circuit" E.R.A. Technical Report, L/T 168, 1947.

10. Howard, P.R.: "Errors in Recording Surge Voltages" National Physical Laboratory Measurement Section Report, Paper No. 1367, 1952.

REFERENCES

11. Ouyang, M.: "Sphere-Gap Breakdown Characteristic for Steeply Rising Impulse Voltages" E.R.A. Report 5158, 1966

12. Einenkel, H. and Heinz, W.: "Voltage Dividers for the Detection of High Impulse Voltages in the Microsecond Range", Electrotech, A. (E.T.Z.) A. Vol. 87, pp. 789 to 792, October, 1966.

13. Park, J.H. and Cones, H.N.: "Sphere-Gap Volt-Time Curves - Reference Standards for Steep Front Measurements". A.I.E.E. 57-215.